Melt processing of cellulose nanocrystals : thermal, mechanical and rheological properties of polymer nanocomposites

Malladi Nagalakshmaiah

Communauté
UNIVERSITÉ Grenoble Alpes

THÈSE

Pour obtenir le grade de

DOCTEUR DE LA COMMUNAUTÉ UNIVERSITÉ GRENOBLE ALPES

Spécialité: **Mécanique des fluides, Energétique, Procédés**

Arrêté ministériel: 25 mai 2016

Présentée par

Malladi NAGALAKSHMAIAH

Thèse dirigée par **Nadia EL KISSI**

et codirigée par **Alain DUFRESNE**

Préparée au sein du **Laboratoire Rhéologie et Procédés et du Laboratoire Génie des Procédés Papetiers.**

Dans **l'École Doctorale Ingénierie - Matériaux, Mécanique, Environnement, Energétique, Procédés, Production (I-MEP2)**

Melt processing of Cellulose Nanocrystals: Thermal, mechanical and rheological properties of polymer nanocomposites

Thèse soutenue publiquement le **23rd September 2016**,

Devant le jury composé de:

Madame Claire BARRES
Maître de Conférences, INSA de Lyon, France. (Rapporteur)

Monsieur, Lazhar BENYAHIA
Professeur. Université du Maine, Le Mans, France. (Président)

Monsieur, Bruno VERGNES
Professeur, CEMEF, Nice, France. (Rapporteur)

Madame, Nadia EL KISSI
Dr., directeur de recherche CNRS. Directeur de thèse (Membre)

Monsieur Alain DUFRESNE
Professeur, Grenoble INP, France. Co-directeur de thèse (Membre)

Knowledged person may fail in life but hard worker never fails

(Sai ram)

To my father, wife and son for their unlimited love and support.

Acknowledgements

This dissertation reports the results of the work carried out in 2013-2016 at two research laboratories: Laboratoire Rhéologie et Procédés (LRP) and Laboratoire de Génie des Procédés Papetiers (LGP2) from the Université Grenoble Alpes, France. This dissertation was funded by French Ministry of Higher Education and Research.

First, I am thankful to my PhD supervisors, Dr Nadia El Kissi and Professor Alain Dufresne for the opportunity, support and patience during last three years. They encouraged me to propose any ideas on my study, and were always available when I required their guidance. Without their instruction and involvement, this thesis would not be fruitful. I am really benefitted with their extensive scientific insight. They mould me to develop as a researcher. I am very thankful to the committee members for their time and patience to read my thesis. I am very much grateful to my master's thesis supervisor Dr. Julien Bras, who encouraged and helped me to get knowledge in the field of cellulose nanocrystal based composites. I would like to thank Dr. Frederic Pignon for his guidance and help during SAXS measurements. I would like to extend my sincere thanks to Cécile, Hélène Galliard, Mohamed Karrouch, Didier Blésès, and Bhertine for their technical support.

I would like to take this opportunity to express my greatest gratitude to each one of my friends, colleagues and my family who walked this way with me during these months. I wish to extend my gratitude to my office mates Maxime, Xabel, Fanny, Benjamin and Monica who always cheered for me. My sincere gratitude to Seema, Florian, Raphile, Karima, Lamia and Karthik for their help and support. My dearest friends and mentors Srinivasrao Kota, Suresh, Guru, Ravindra for their encouragement throughout the PhD.

My special thanks to Dr. Gregory Berthome (INPG-SIMaP), and Dr. Theyencheri Narayanan for their help and discussion on experimental characterizations. My earnest thanks to

Professor Dominique Lachenal for giving me the opportunity to pursue postmaster in Pagora. I am grateful to all the professors, PhD students and post-doctors in LRP and LGP2 for their kind help and suggestions, especially to my colleagues and friends.

(Malladi Nagalakshmaiah)

Scientific Publications (2013−2016)

1. Nagalakshmaiah. Malladi, Nadia Elkissi and Alain Dufresne. Ionic compatibilization of cellulose nanocrystals with quaternary ammonium salt and their melt extrusion with polypropylene. (ACS applied materials and interfaces 2016, 8, 8755-8764)

2. Nagalakshmaiah. Malladi, Nadia Elkissi, Frederic Pignon, and Alain Dufresne. Surface adsorption of triblock copolymers (PEO-PPO-PEO) on cellulose nanocrystals and their melt extrusion with polyethylene. (RSCAdvances-2016)

3. Nagalakshmaiah. Malladi, Nadia Elkissi, Gérard Mortha, and Alain Dufresne. "Structural Investigation of cellulose nanocrystals extracted from chili leftover and their reinforcement in cariflex-IR rubber latex." Carbohydrate polymers 136 (2016): 945-954.

4. Nagalakshmaiah. Malladi, Nadia Elkissi, Oleksandr Nechyporchuk, and A. Dufresne. Fabrication of polymer nanocomposites with poly [(styrene)-co-(2-ethylhexyl acrylate)] modified cellulose nanocrystals with poly styrene. (Yet to submit)

Conference proceedings:

1. Nagalakshmaiah Malladi, Nadia Elkissi and Alain Dufresne. Structural morphology, rheology and flow instabilities of commercial grade cellulose nanocrystals. (**Oral talk**, GFR 2014)

2. Nagalakshmaiah Malladi, Nadia Elkissi and Alain Dufresne. Surface modified cellulose nanocrystals in aqueous medium with quaternary salt and reinforced in polypropylene by melt extrusion (**Oral talk**, 1st International EPNOE Junior Scientists Meeting, Netherlands - ISBN 978-961-248-473-6, 2015)

3. Nagalakshmaiah. Malladi, Nadia Elkissi and Alain Dufresne. Surface modified cellulose nanocrystals with quaternary salt and their melt extrusion with PP. (**Invited oral talk**, ICNP 2015)

4. Nagalakshmaiah Malladi, Nadia Elkissi and Alain Dufresne. Surface adsorption of triblock copolymers (PPO-PEO-PPO) on cellulose nanocrystals and their melt extrusion with polycaprolactone. (**Oral talk**, EPNOE-2015)

5. Nagalakshmaiah Malladi, Nadia Elkissi and Alain Dufresne. Fabrication of polymer nanocomposites with poly [(styrene)-co-(2-ethylhexyl acrylate)] modified cellulose nanocrystals with poly styrene (**Oral talk**, 3rd Biopolymers conference-2015)

6. Nagalakshmaiah Malladi, Nadia Elkissi and Alain Dufresne. Melt extrusion of adsorbed Cellulose nanocrystals with polyethylene: A Small angle x-ray Scattering Characterization. (**Oral talk**, TAPPI Nano 2016)

Poster presentations:

1. Nagalakshmaiah Malladi, Nadia Elkissi and Alain Dufresne. Preparation of polymer nanocomposites by melt extrusion (JDD-2014, 2nd best poster)

2. Nagalakshmaiah Malladi, Nadia Elkissi and Alain Dufresne. Structural morphology of cellulose nanocrystals extracted from chili leftover and their reinforcement in cariflex-IR rubber latex (JSMD-2014)

3. Nagalakshmaiah Malladi, Nadia Elkissi and Alain Dufresne. Surface modified cellulose nanocrystals in aqueous medium with quaternary salt and reinforced in polypropylene by melt extrusion(JSMD-2014)

4. Nagalakshmaiah Malladi, Nadia Elkissi and Alain Dufresne. Blends of triblock copolymers (PPO-PEO-PPO) adsorbed cellulose nanocrystal melt extrusion with polycaprolactone. (3rd Biopolymer conference-2015)

5. Nagalakshmaiah Malladi, Nadia Elkissi and Alain Dufresne. Fabrication of polymer nanocomposites with poly [(styrene)-co-(2-ethylhexyl acrylate)] modified cellulose nanocrystals with poly styrene. (EPNOE-2015)

6. Nagalakshmaiah Malladi, Nadia Elkissi and Alain Dufresne. Melt rheology of modified CNC/PP composites. (JDD-2015)

Symbols and abbreviations

AFM	Atomic force microscopy
BNC	Bacterial nanocellulose
CNC	Cellulose nanocrystals
DLS	Dynamic light scattering
DP	Degree of polymerization
DSC	Differential scanning calorimetry
DMA	Dynamic mechanical analysis
EHA	Ethyl hexyl acrylate
FEG-SEM	Field emission gun scanning electron microscopy
SEM	Scanning electron microscopy
FTIR	Fourier transform infrared spectroscopy
γ	Shear rate
η	Viscosity
G'	Storage modulus
G''	Loss modulus
I (q)	Scattered intensity
QS	Quaternary salt
MFC	Micro fibrillated cellulose
Mw	Weight-average molar mass
NFC	Nanofibrillated cellulose
PEO	Polyethylene oxide
PPO	Polypropylene oxide
PCL	Polycaprolactone
PDI	Polydispersity index
LLDPE	Linear low density polyethylene
PP	Polypropylene
PS	Polystyrene

Table of Contents

Abstract:

Due to environmental concerns the development towards the bio-based composite materials for different industrial applications is nowadays a frequent research subject. Many studies are performed on the use of natural fibres in composites as an alternative to conventional synthetic fillers, which are traditionally used to reinforce thermoplastic matrices. This dissertation focuses on the development of such composite materials using the bio-based and biodegradable reinforcing agent- Cellulose nanocrystals (CNC).

Cellulose nanocrystals are rod like structured nanomaterials which can be extracted from the plant biomass by acid hydrolysis. They carry negative electric charges due to the surface sulphate groups and are endorsed for better dispersion in aqueous medium. Recently, CNC has gained a lot of attention to adopt their distinctive mechanical properties to polymer matrices in order to be sustainable, ecologically friendly nanocomposites. In addition to their mechanical and reinforcing properties, CNC are remarkable in optical and surface properties. It enlarged the interest of the industries to produce commercial grade CNC.

In the present study, commercial grade CNC procured from university of Maine was used. In order to understand the size, surface morphological, thermal, functional properties of CNC different techniques like atomic force microscopy, zeta sizer, X-ray diffraction, FT-IR and thermogravimetric analysis were used.

However, the recent industrial-scale production of CNC justifies the use of industrially scalable processes such as melt extrusion, to produce thermoplastic polymer composites. It is a highly viable and solvent-free process but relatively infrequent for the processing of polymer nanocomposites using CNC as the reinforcing phase, mainly due to the irreversible agglomeration up on drying. CNCs are classically prepared by a sulfuric acid hydrolysis treatment resulting in the formation of surface sulfate groups that are well-known to lower the thermal stability of the nanoparticles. These two factors limit the use of melt processing for the preparation of CNC reinforced nanocomposites.

This thesis was introduced to overcome the above mentioned issues by using simple and green process (aqueous methods) like surface modification and physical adsorption. Initially surface modified CNC was used to reinforce PP. In this study we profitably used these negatively charged sulphated groups, and quaternary ammonium salt was ionically adsorbed on CNC by a simple aqueous method. Fourier transform infrared spectroscopy, thermogravimetric analysis, and X-ray diffraction were used to characterize adsorbed CNC, and changes in polarity were investigated by contact angle measurements. Modified CNC was extruded with polypropylene at 190°C, and the ensuing composites were characterized in terms of mechanical (by dynamic mechanical analysis and tensile tests), thermal (by DSC), and morphological (SEM) properties. The melt rheology of PP-based nanocomposites was also reported.

Physical adsorption of CNC using triblock copolymer was used to reinforce into polyethylene. In this work, pluronic grade triblock copolymer was adsorbed on the surface of CNC in order to improve the thermal stability and also its dispersion from the dried state. The adsorbed cellulose nanocrystals (A-CNCs) were characterized to check their thermal, functional and structural properties by thermogravimetric analysis (TGA), Fourier transform infrared spectroscopy (FTIR), X-ray diffraction (XRD) and atomic force microscopy (AFM). Interestingly, improved thermal stability was observed and also the dispersion of A-CNC in aqueous medium was much better than for unmodified CNC. The aqueous A-CNC suspensions were characterized by small angle X-ray scattering (SAXS) to evaluate the dispersion of the nanoparticles. The flow properties of A-CNC dispersions were also analysed. Further, A-CNC was used to prepare nanocomposites by melt extrusion using linear low density polyethylene (LLDPE) as matrix. The thermo-mechanical and morphological properties of the ensuing nanocomposites were characterized by dynamic mechanical analysis (DMA), differential scanning calorimetry (DSC) and scanning electron microscopy (SEM). The dispersion state of A-CNC within the polymeric matrix was also characterized by SAXS.

In order to enhance thermal stability of CNC, they were modified with laboratory prepared statistical copolymer, *viz.*, poly [(styrene)-*co*-(2-ethylhexyl acrylate)], by ionic interactions and these modified CNC were characterized to

determine their thermal, functional and structural properties by means of thermogravimetric analysis (TGA), Fourier transform infrared spectroscopy (FTIR), X-ray diffraction (XRD) and atomic force microscopy (AFM). The hydrophobic nature was investigated by using contact angle. In order to get good compatibility between CNC and polystyrene matrix, and with the anticipation of high mechanical properties, the modified and adsorbed CNC were incorporated into polystyrene by melt extrusion. The thermomechanical performance of the ensuing composites was examined by means of differential scanning calorimetry and dynamic mechanical analyser (DMA). The non-linear mechanical properties and morphology were also studied using tensile test and scanning electron microscopy (SEM).

It was observed that the polymer nanocomposites prepared by surface modification and adsorption had a positive impact on the storage modulus, tensile strength and Young's modulus. Importantly, no evidence of micro aggregates in the matrix was observed in the scanning electron microscopy images contrary to non-treated CNC. Both the surface modification and adsorption are water based methods that are industrially viable solutions.

RÉSUMÉ:

En raison des préoccupations environnementales le développement de matériaux composites bio-sourcés pour diverses applications industrielles est un sujet de recherche très dynamique et en plein essor. De nombreuses études sont en effet menées sur la capacité des fibres naturelles à représenter une alternative possible aux fibres synthétiques traditionnellement utilisées comme renfort dans les composites. Cette thèse porte sur le développement de matériaux composites à matrice thermoplastique et à renfort biosourcé et biodégradable, en privilégiant les nanocristaux de cellulose (CNC).

Les nanocristaux de cellulose sont des nanomatériaux structurés, en forme de bâtonnets, qui peuvent être extraits à partir de la biomasse végétale par hydrolyse acide. Ils portent des charges électriques négatives en raison des groupes sulfate de surface et sont donc facile à disperser en milieu aqueux. Du fait de leurs propriétés mécaniques importantes, l'étude des CNC connaît ces dernières années un regain d'intérêt, visant à intégrer ces charges nanométriques dans des matrices polymères pour élaborer des nanocomposites biosourcés, durables et écologiques. Les propriétés mécaniques et la capacité de renfort ne sont pas le seul atout des CNC qui présentent en plus des propriétés optiques remarquables. De ce fait, l'intérêt de l'industrie pour ces matériaux, dans des domaines de plus en plus variés, est croissant, justifiant le développement d'une production de CNC de qualité commerciale à grande échelle.

Dans cette étude, nous utiliserons des CNC commercialisés par l'université du Maine. Ils seront caractérisés, en termes de morphologies, propriétés de surface, thermiques, fonctionnelles par différentes techniques et notamment par microscopie à force atomique, zetamétrie, diffraction des rayons X et analyse thermogravimétrique.

Pour rester dans l'esprit de l'élaboration de nanocomposites biosourcés compatibles avec un développement industriel, outre l'utilisation de CNC commerciaux, le procédé d'élaboration du composite doit également être viable à l'échelle industrielle. L'extrusion, couramment utilisée pour la mise en forme des thermoplastiques, et de plus ne nécessitant pas l'utilisation de solvants en contradiction avec l'éco-compatibilité du processus, paraît tout à fait indiquée en ce sens. Ce procédé pose cependant un certain nombre de difficultés du fait des spécificités des CNC. En effet, le traitement par hydrolyse acide pour la préparation des CNC résulte en la formation de groupes sulfates à la surface des nanocharges, qui du fait de leur faible stabilité thermique, limitent l'utilisation des CNC dans des procédés haute température. Par ailleurs, la phase de séchage des suspensions cellulosiques, nécessaire avant leur incorporation à chaud dans la matrice polymère, peut provoquer l'agglomération irréversible des CNC, affectant de fait leur intérêt en tant que charge de renfort. Ces deux facteurs représentent donc un verrou, qu'il faut pouvoir lever, pour envisage une mise en forme à l'état fondu, par extrusion par exemple, pour la préparation de composites thermoplastiques à renfort cellulosique.

C’est l’un des objectifs de cette thèse. Nous développerons pour cela des procédés éco-compatibles, notamment en milieu aqueux, pour compatibiliser les interactions CNC/polymère, en privilégiant notamment la modification ou l’adsorption physique à la surface des CNC.

Nous avons dans un premier temps utilisé la modification de surface pour élaborer des nanocomposites à matrice polypropylene (PP). Pour cela, nous avons mis à profit les groupes sulfates chargés négativement qui résultent de l’hydrolyse acide en les faisant réagir, par adsorption ionique en milieu aqueux, avec un sel d'ammonium quaternaire. La spectroscopie infrarouge par transformée de Fourier (FT-IR), l’analyse thermogravimétrique (TGA) et la diffraction des rayons X (XRD) ont permis de caractériser les CNC modifiés. Les changements de polarité ont été étudiés par des mesures d'angle de contact. Un mélangeur bi-vis a été utilisé pour incorporer les CNC modifiés au PP à 190° C, et les composites ainsi élaborés ont été caractérisés en termes de propriétés mécaniques, thermiques et morphologiques, par analyse mécanique dynamique (DMA), par des essais de traction, par calorimétrie différentielle à balayage (DSC) et par microscopie électronique (SEM). Le comportement rhéologique à l'état fondu des nanocomposites PP/CNC a également été étudié.

Dans un second temps, nous avons testé la modification des CNC par adsorption physique en utilisant un copolymère tribloc, pluronic, la réaction ayant lieu encore une fois en milieu aqueux. L’objectif est d’améliorer la stabilité thermique des CNC ainsi que leur capacité de dispersion une fois

séchés. Les CNC adsorbés (A-CNCs) ont été caractérisées par leurs propriétés thermiques, fonctionnelles et structurelles par TGA, FT-IR, XRD et par microscopie à force atomique (AFM). Les suspensions aqueuses de A-CNC ont été caractérisées par diffusion de rayons X aux petits angles (SAXS) pour évaluer la qualité de la dispersion. Leurs propriétés en écoulement ont également été analysées par rhéométrie. De même que pour les CNC modifiés, les A-CNC ont été incorporés dans une matrice polymère, un polyéthylène basse densité linéaire (LLDPE). Le nanocomposite obtenu par extrusion à chaud a été caractérisé par ses propriétés mécaniques, thermiques et morphologiques, par DMA, DSC et SEM. L'état de dispersion des A-CNC dans la matrice polymère a également été caractérisé par SAXS.

Dans un troisième volet de ce travail, nous avons cherché à améliorer la stabilité thermique des CNC. Nous avons développé pour cela, au laboratoire, un copolymère statistique : le poly [(styrène) -co- (acrylate de 2-éthylhexyle)]. La modification des CNC a été obtenue selon voies interactions ioniques. Les CNC modifiés ont été caractérisés pour déterminer leurs propriétés thermiques, structurales et fonctionnelles par TGA, FT-IR, XRD et AFM. Leur nature hydrophobe a été étudiée par des mesures d'angles de contact. Les CNC modifiés et adsorbés ont été incorporés dans un polystyrène (PS) par extrusion à l'état fondu. Là encore, les performances thermo-mécanique des composites ainsi élaborés ont été étudiées par DSC et par DMA. Leurs propriétés mécaniques non linéaires sont analysées au moyen de test de traction et leurs

morphologies observées par SEM. Les résultats montrent un impact positif sur le module de conservation, la résistance à la traction et le module d'Young. Les images de microscopie ne révèlent en outre la présence d'aucun agrégat, contrairement aux observations réalisées avec les CNC.

Il apparaît en conclusion que, tant la modification que l'adsorption en surface, toutes deux réalisées en milieu aqueux, sont des solutions industriellement viables, qui méritent d'être développées à plus grande échelle.

General introduction:

From the last four decades most of the industries replaced the petroleum derived polymers with bio-based materials (1). Because the widely used plastic materials are based on fossil raw materials and also in modern world their production is very high and these materials eventually discarded once used. This leads to the growing landfills and creates environmental issues (2).

Due to the limited fossil fuel resources and the impact of petroleum-based materials on the environment, there is a large effort put by scientists and engineers nowadays to replace those materials by bio-based alternatives. Bio-based polymers have the potential to reduce the carbon dioxide released into the atmosphere and therefore hinder greenhouse effect and global warming while alleviating the concern about recycling (2). Biodegradable plastics and biocompatible composites generated from renewable biomass are considered promising materials that could replace synthetic polymers and reduce global dependence on fossil fuel sources.

In this context most of the researchers and industries are mainly focussed on cellulose based composites in order to replace or decrease the influence of the plastic usage. In general cellulose based composites are called biocomposites. These biocomposites are categorised as follows for better understanding in figure-1.

The first generation of biocomposites was mainly developed on single concept like mixing of wood fibre with plastics in equal proportion whereas mechanical performance was not major concern. Second generation was started using all kinds of natural fibres from agricultural biomass like flax, jute fibres and so on. Comparatively the natural fibre content was slightly lesser than the 1st generation composites. The third generation biocomposites has attracted the modern world. The plastic based materials were replaced by bioplastics which are generally

prepared from renewable resources, as for example poly lactic acid (PLA), and production was main concern.

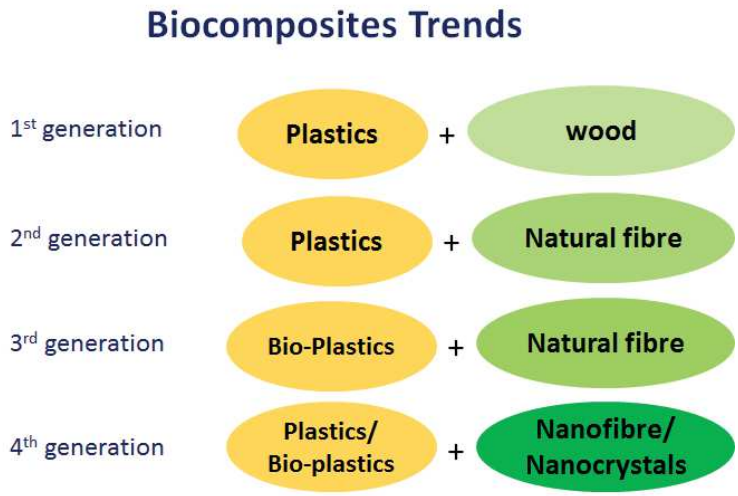

Figure-1 biocomposites generations based on filler

Reinforcing bioplastics with natural fibre is increasing nowadays. The most recent trend is fourth generation bio-composites. They are frequently based on cellulose nanofibers (CNF) and cellulose nanocrystals (CNC). In this framework the filler content used in the preparation of biocomposites is significantly less and the mechanical performance will be improved.From last two decades the patent activity in the field of biocomposites is increasing as can be seen in figure-2. The patent trends for nanocomposites mentioned in the graph are from first to fourth generations. The statistics shows that the ultimate interest of the industries as well as research institutes is in the field of nanocomposites.

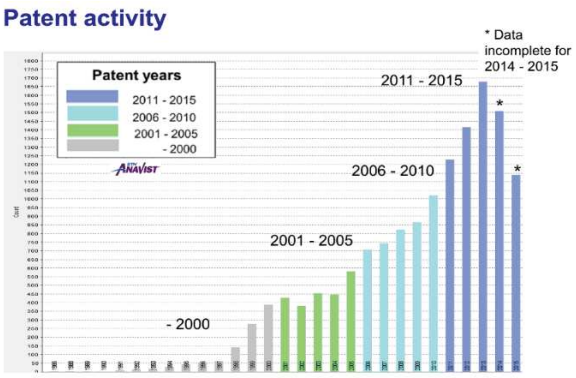

Figure-2 Patent activities from last two decades (source: VTT)

In the present thesis only fourth generation composites were discussed, that means only polymer composites related to cellulose nanocrystals. The definitive interest has come from the ultimate mechanical properties of the rod like cellulose nanocrystals (CNC) or nano crystalline cellulose (NCC).

CNC are the primary structural building blocks of the plant. They can be obtained by sulfuric acid hydrolysis, in the form of aqueous colloidal suspensions stabilized by sulphate groups. The acid degrades the amorphous regions of the cellulose fibres, leaving smaller rod-like cellulose crystallites, with a cross section between 3 and 20 nm and a length of few hundred nanometres depending on the source. The development of scalable technologies for the isolation and application of cellulose nanocrystals has been actively pursued by various groups, notably in USA, Canada, and Europe (3).

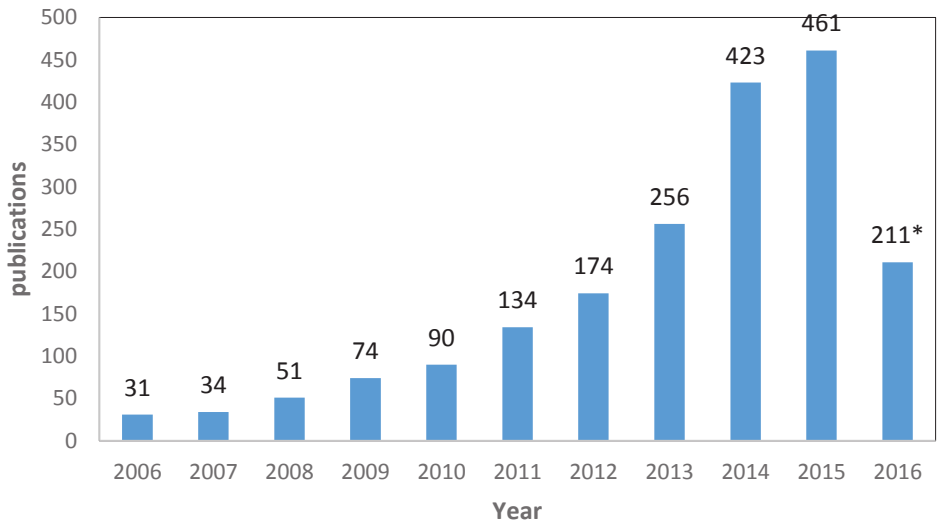

Figure-3 Evolution of the number of research publications on cellulose nanocrystals during last ten years (2006 − May-2016) according to Web of sciences (*= in complete)

Figure-3 shows the number of research articles published on CNC during last ten years and results were obtained from Web of Sciences. Generally, gradient increase of number of publications on cellulose nanocrystals can be found from 2006 to 2015, which induced the sharp change from few articles in 2006 to more than 460 articles in 2015. During 2016 the

results were incomplete as it is still going. Specifically, the continuous rise of number of articles on the study of cellulose nanocrystals appeared since 2008. The vast interest on CNC is due to their high elastic modulus (150 Gpa), high aspect ratio (10-70), high surface area (150 m2/g) and crystallinity up to 95% (4-7). The number of patents reported on CNC based research topics until 2015 was more interesting because of their studies in the field of paper and composites (almost 68%). From figure-4, it is evident that the CNC based composites are of much interest.

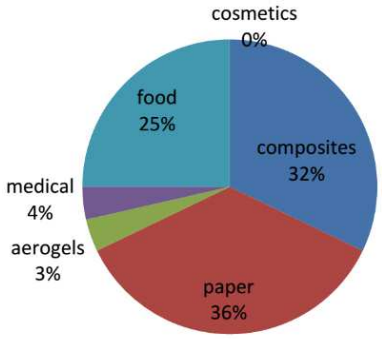

Figure-4 Number of patents reported on cellulose nanocrystals application in 2015.

Nanocomposites can be prepared by the reinforcement of CNC in polymers by different processes and in particular solvent casting, thermopressing, melt spinning and extrusion. But the most promising, green and most viable process is melt extrusion. In order to prepare CNC based nanocomposites by melt extrusion there are however major challenges like irreversible aggregation up on drying of CNC and low thermal stability due to sulphated groups endorsed from sulfuric acid hydrolysis (8). This thesis work is mainly focussed to overcome the above mentioned challenges by modifying the cellulose surface, using green process, based on aqueous methods.

This dissertation is the summarization of my research during last three years on this ageless bio-nanomaterial and the structure of dissertation is shown in Figure 5. Chapter 1 is the literature review or state of the art on cellulose nanocrystals. In this chapter, four areas of the research on cellulose nanocrystals (preparation, properties, surface modification, and composites) are introduced in detail through the analysis and comparison of selected publications.

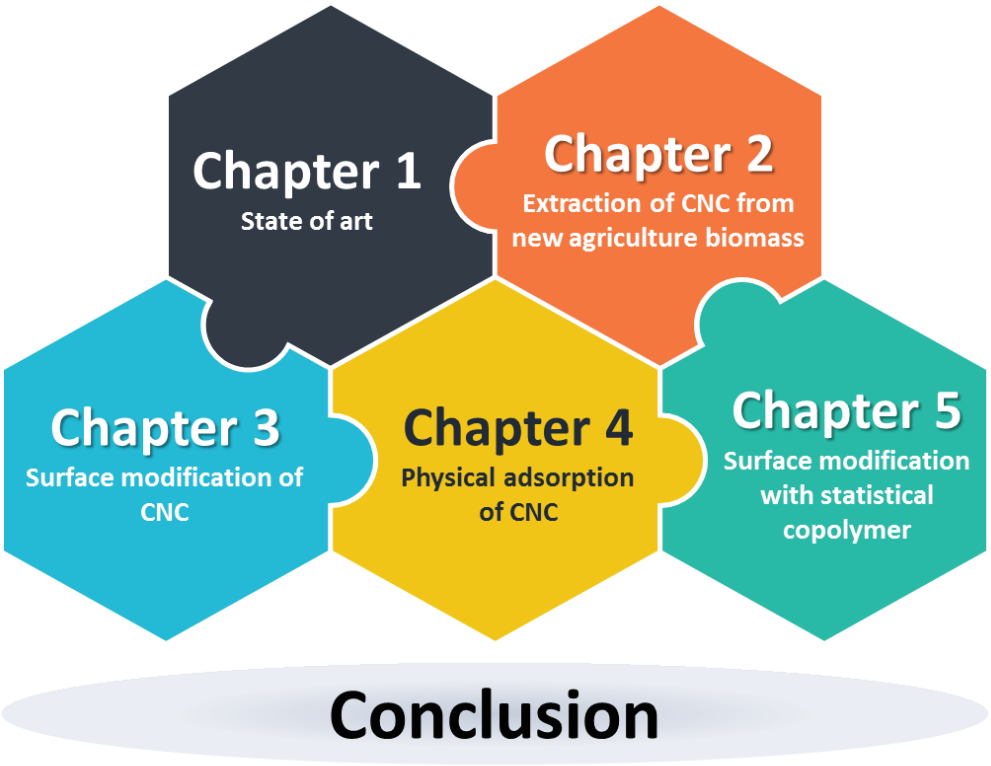

Figure-5 structural organization of the reported dissertation

Chapter 2 is a research work on the preparation of cellulose nanocrystals from alternative sources like agriculture biomass and their reinforcement in latex was studied. Chapter 3 is mainly focussed on surface modification of CNC by quaternary salt using water based method and their melt processing with PP. Chapter 4 deals with physical adsorption of triblock copolymers on surface of CNC and their reinforcement in polyethylene was reported. Chapter 5 is about the surface modification of the CNC by using statistical copolymer and

their melt extrusion with polystyrene was reported. The dissertation ends up with a brief conclusion.

References:

1. Weber C.J., Biobased Packaging Materials for the Food Industry: Status and Perspectives, Food Bio pack Project, EU (2000)10-84, ISBN 87-90504-07-0.
2. Gröndahl M., Eriksson L., Gatenholm P., Material Properties of Plasticized Hardwood Xylans for Potential Application as Oxygen Barrier Films, Biomacromolecules, 5(2004)1528-1535.
3. Leung, A. C. W.; Lam, E.; Chong, J.; Hrapovic, S.; Luong, J. H. T. Reinforced plastics and aerogels by nanocrystalline cellulose. J. Nanopart. Res. 2013, 15, 1636
4. Cavaille, J.Y., Ruiz, M.M., Dufresne, A., Gerard, J.F., Graillat, C., 2000. Processing and Characterization of new thermoset nanocomposites based on cellulose whiskers. Compos. Interfaces 7 (2), 117–131.
5. Klemm, D.; Kramer, F.; Moritz, S.; Lindström, T.; Ankerfors, M.; Gray, D.; Dorris, A. Angew. Chem., Int. Ed.2011, 50, 5438−5466.
6. Habibi, Y.; Lucia, L. A.; Rojas, O. J.Chem. Rev.2010, 110, 3479− 3500.
7. Moon, R. J.; Martini, A.; Nairn, J.; Simonsen, J.; Youngblood, J.Chem. Soc. Rev.2011, 40, 3941−3994.
8. Lin, N.; Dufresne, A. Physical and/or Chemical Compatibilization of Extruded Cellulose Nanocrystal Reinforced Polystyrene Nanocomposites.Macromolecules2013, 46, 5570−5583.

Chapter-1
State of the art

Chapter-1 state of the art

1. Literature review

1.1 Cellulose

Cellulose is the most abundant material on the Earth, among polysaccharides. Cellulose occurs in vivo in plant cell walls in the form of slender micro fibrils. Cellulose possesses outstanding physical and mechanical properties such as high modulus, low density and high surface area. In the last decade the interest on nanocellulose is increasing due to those remarkable physical and mechanical properties.

1.1.1 Feed stocks

Cellulose can be derived from various sources such as: wood (hard and softwood), seed based fibres like cotton, coir etc. Agricultural biomass is also a potential source like cotton, chili and rice leftover (1) , bast fibres (flax, hemp, jute, ramie etc.), grasses (bagasse, bamboo etc.), marine animals (tunicate), algae, fungi, invertebrates and bacteria (2). Currently wood is the major source for the production of cellulose (3, 4). Cellulose is the one of the constituents present in the wood along with the hemicelluloses and lignin, comparatively less to cellulose content. Wood species can be distinguished as hard-and softwoods based on their anatomical features. Hardwood is more complex and heterogeneous in structure than softwood (5). Generally, softwood fibres are 3 - 4 times longer than hardwood (6). However, it is known that hardwoods have more rigid structure than softwoods due to their high Runkel ratio (cell wall thickness divided by lumen radius) (7). At the same time, non-wood that is agriculture biomass (after harvesting crops) is of increasing interest as a source of cellulose since it commonly comprises less lignin. According to OECD–FAO (Organization for Economic Cooperation and Development and the Food and Agriculture Organization) agriculture outlook, every year farmers are harvesting 35 million tonnes of natural fibres from animals and plants (1). Subsequently, the isolation and purification of fibres are easier and

less harmful for cellulose in terms of size and morphology (3). Moreover, the further fibrillation of such cellulose is less energy-consuming especially for the preparation of nanofibrillated cellulose (8).

1.1.2 Structure and chemistry

Cellulose is the most abundant natural biopolymer on earth that is renewable, biodegradable, as well as non-toxic. It is a carbohydrate polymer made up of repeating units of D-glucopyranose and consists of three hydroxyl groups per anhydroglucose unit (AGU) giving the cellulose molecule a high degree of functionality.

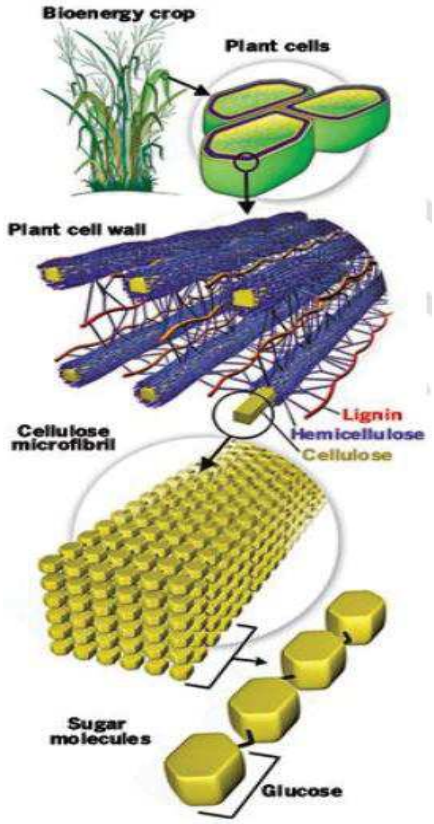

Figure-1 cellulose in plant cell wall and its basic structure [Source: C&EN]

The basic structure of cellulose is shown in Figure-1. The knowledge of the molecular structure of cellulose is of prime importance as it explains the characteristic properties of

cellulose, such as hydrophilicity, chirality, biodegradability and high functionality. As a renewable material, cellulose and its derivatives have been widely studied, focusing on their biological, chemical, as well as mechanical properties.

The materials based on cellulose and its derivatives have been used for more than 150 years in a wide variety of applications, such as food, paper production, biomaterials, pharmaceuticals and textile industry. More recently a strong interest increased regarding cellulose at nanoscale. As shown in Figure-1, two types of nanocellulose can be considered .i.e. cellulose nanocrystals (CNC) or micro fibrillated cellulose or nanofibrillated cellulose (NFC).

1.2 Nanocellulose

The individual cellulose elements with either a diameter or length in nanometre range (<100 nm) is referred to nanocellulose. Depending on the production conditions, which influence the dimensions, composition, and properties, the nanocellulose can be divided into three main categories (9) as follows. 1) Cellulose nanocrystals (CNC) 2) Nanofibrillated cellulose (NFC) or micro fibrillated cellulose (MFC) or cellulose nanofibrils (CNF) 3) Bacterial nanocellulose (BNC). However, the terminology of cellulose nanomaterials has not been standardized yet. CNC and NFC are produced by disintegration of cellulose fibres to the nano sized material (see Figure 2). On the contrary, BNC is generated by a build up from low molecular weight sugars by aerobic bacteria. Regardless of its type, the nanocellulose exhibits hydrophilic character, relatively large specific surface area, broad potential of surface chemical modification etc.

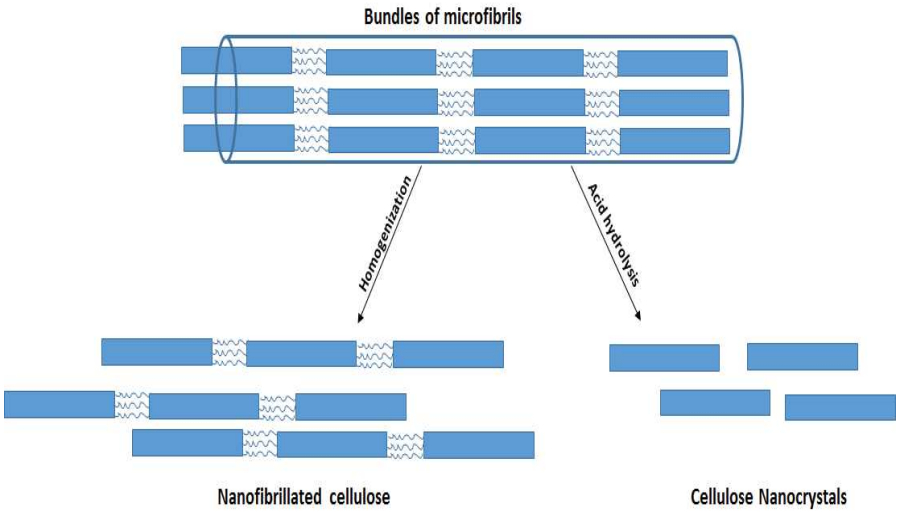

Figure-2 Schematic representation of nanofibrillated cellulose and cellulose nanocrystals individualization from cellulose microfibrils

1.2.1 Cellulose nanocrystals

Cellulose nanocrystals, generally known as cellulose whiskers, were first produced by Rånby (1949) using acid hydrolysis of cellulose fibres in aqueous suspensions. In this method, the concentrated sulfuric acid (H_2SO_4) is commonly used, which degrades amorphous regions of cellulose and leaves crystalline ones. By such a treatment, rod-like CNC with sulphate groups at their surface are produced. Their morphology generally depends on the source of cellulose. Typically, nanocrystals with diameters of 3−35 nm and length between 100 nm and several micrometres depending on the biological origin were produced (10). The deep review on CNC production is shown in section 1.3.

1.2.2 Nanofibrillated cellulose

NFC as a new cellulosic material was introduced by Turbak et al. (11, 12) who produced cellulose with the lateral dimensions in nanometre range by passing softwood pulp aqueous suspension through a high-pressure homogenizer. During such treatment, strongly entangled networks of nanofibrils, having both crystalline and amorphous domains, are produced due to high shearing forces. They possess high aspect ratio and gel-like behaviour in water with pseudo plastic and thixotropic properties (9). Depending on the processing conditions,

cellulose fibres can be disintegrated to NFC with the lateral dimensions from ~3 nm, representing elementary fibrils, to tens of nanometres, which corresponds to microfibrils. Typically, NFC has a diameter of 5−50 nm and a length of few micrometres (13, 14).

1.2.3 Bacterial nanocellulose

Bacterial nanocellulose (BNC) is high-purity cellulose generated by Gluconacetobacter bacterial strains in aqueous culture media containing sugar source. The time of such process ranges from days up to two weeks (15). BNC has the same chemical composition as plant cellulose; however, it is free of functional groups other than hydroxyl, e.g., carboxyl or carbonyl, which are usually introduced to wood or plant-derived cellulose during the purification process. BNC is also free from the other polymers, e.g., lignin, hemicelluloses or pectin. BNC is assembled into hierarchical structures of nanofibrils with a width of 10 nm and a length of more than 2 μm (16). It has a degree of polymerisation (DP) in the range of 3000-9000 and a crystallinity index of 80−90 %.

1.3 Cellulose nanocrystals

Cellulose Nanocrystals (CNC) are obtained by sulfuric acid hydrolysis, which form aqueous colloidal suspensions stabilized by sulphate groups. The acid degrades the amorphous regions of microfibrils, leaving smaller rod-like cellulose crystallites, with a cross section between 3 and 20 nm and a length of few hundred of nanometres.

1.3.1 Laboratory scale production

Every research start at a laboratory table and in the same manner, the extraction of cellulose nanocrystals has started journey almost seven decades ago. That method is acid hydrolysis of cellulose fibres by sulfuric acid which yield rod like nanoparticles. This process is widely used, it is the most established laboratory process and it has been applied to a wide variety of raw materials. It is interesting to note that many attempts with diverse hydrolysing agents

were made to produce cellulose nanocrystals with different surface groups as shown in Figure 3. As shown in the scheme-1 (see figure-3) sulfuric acid is used as the hydrolysing agent, the non-crystalline regions of cellulose fibres being preferentially hydrolysed, whether the highly resistant crystalline regions remain intact. It is worth to note that during the hydrolysis, sulfuric acid can react with hydroxyl groups of cellulose, which yields charged sulphate esters on the surface of nanocrystals and promotes the dispersion of nanoparticles in water (17). The low toxicity oxidation was also reported with ammonium persulfate [$(NH4)_2S_2O_8$] (scheme 2) which yields the isolation of carboxylate cellulose nanocrystals (18). The combination of (2, 2, 6, 6-Tetramethylpiperidin-1-yl) oxyl (TEMPO) and sodium hypochlorite, surface hydroxyl groups of cellulose nanocrystals can be selectively transformed into carboxyl groups (scheme-3), which may be useful for subsequent surface modification (19). Hydrolysis with hydrochloric acid preserves the hydroxyl groups (scheme 4) of native cellulose but leads to less stable aqueous suspensions (20). Moreover, an acid mixture composed of hydrochloric and an organic acid (acetic acid) can be used to hydrolyse cellulose fibres inducing the hydrolysis and modification in one single-step process, (21) which offers the hydrophobic acetyl groups (scheme 5) on the surface of cellulose nanocrystals. Recently, some novel systems have been developed for the isolation of cellulose nanocrystals, such as enzymatic hydrolysis (22), ionic liquid hydrolysis (23) and gaseous acid hydrolysis (24). However, most of the researchers extensively use sulfuric acid hydrolysis for the preparation of CNC. Because the rest of the methods are not so easy to scale up and also the toxicity and recovery of the chemicals are difficult. Importantly the yield is comparatively less than that of the sulfuric acid hydrolysis. Hence in this study, the sulfuric acid hydrolysed CNCs were used.

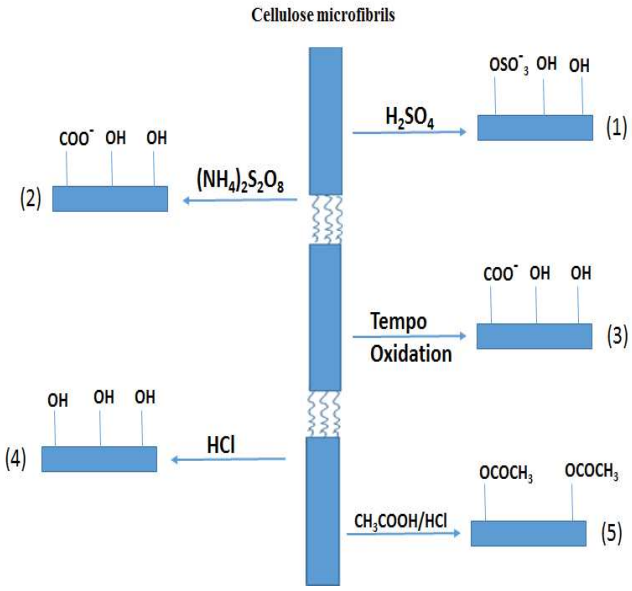

Figure 3 The different extraction methods of cellulose nanocrystals (1) Sulfuric acid hydrolysis (2) ammonium persulfate oxidation (3) TEMPO oxidation (4) hydrochloric acid hydrolysis (5) HCl/CH3COOH (hydrochloric acid treatment provides hydroxyl, acetic acid provides acetyl groups).

Recently, high energy ball milling (HEBM) mechanical process was reported (25) for the preparation of CNC. Microcrystalline cellulose (MCC) was used as starting material, and was micronized through a HEBM process. This process was optimised by varying the concentration of CNC (0.5–2 wt. %) and time (15–60 min) parameters, in order to obtain a high yield (50-75%) of well-separated CNC. The schematic diagram of process was shown in figure 4. The centrifugal force (fig 4 a) generated in the mill provides an impact effect to micronize the MCC in between the beads. Furthermore, upon ultra-sonication (fig 4 b), high-speed liquid jets are created. These liquid jets pressurize the liquid locally between the particles at high speed (1000 km/h) to separate or fibrillate them and to promote additional particle collisions, so as to result in very small particles.

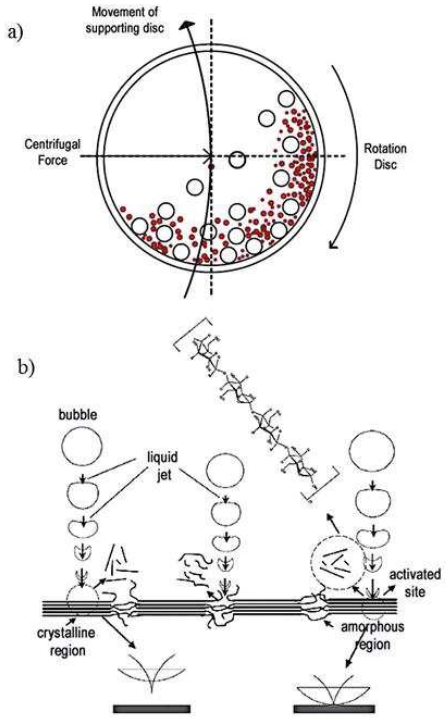

Figure 4 (a) High energy bead milling[25, 26] and (b) ultra-sonication working mechanism[27].

1.3.2 Industrial production

The scale-up or production of nanocellulose from industries is increasing rapidly. All over the world the manufacturing facilities have started the production from kg to multiple tons. The worldwide production units of nanocellulose (CNC, CNF AND MFC) are shown in figure 5. Alberta Innovates-Technology Futures has constructed the world's first pilot plant to produce cellulose nanocrystals, with the production capacity of 100 kg per week. Domtar Corp. and FP Innovations have created a joint venture (new organization named CelluForce) to build a commercial-scale plant for the production of cellulose nanocrystals, in a $40.8 million project. In January 2012, CelluForce officially announced to open a plant for the production of cellulose nanocrystals with a target production rate of 1 ton/day. For the industrial production of cellulose nanocrystals, two issues should be emphasized. One is the standardization for the procedure and conditions of cellulose nanocrystals production, which is being constituted by TAPPI standard recommendation (28). Another issue is the further

development of practical end-uses for cellulose nanocrystal-based materials, despite the fact that a large and growing body of information on potential applications of cellulose nanocrystals has been

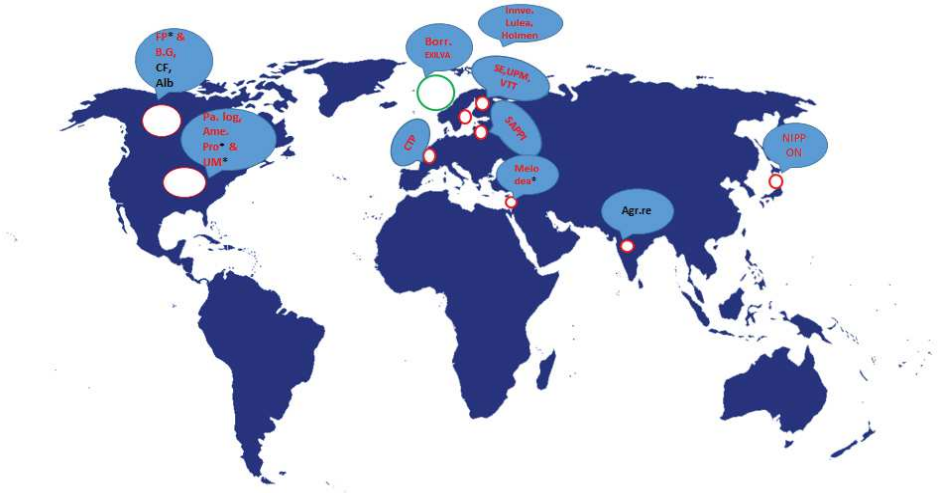

Figure 5 nanocellulose production all over the world (* cellulose nanocrystals)

identified and demonstrated in the lab. It seems that many companies are interested by the potential of cellulose nanocrystals to improve the quality of their products but are unaware of the cost and sustainability of supply.

Name and place of the production unit	Production capacity per day (Kg)	Product type	Possible applications
CelluForce-CANADA	1000	CNC	Commercial sales
Paper logic -USA	2000	NFC, CNF and CNC	unknown
University of Maine-USA	1000	NFC, CNF and CNC (dry &wet)	Commercial sales
Borregaard-NORWAY	1000	NFC, CNF	Rheology modifier eg: cosmetics
American process-USA	500 to 1000	NFC, CNC	Commercial sales
Nippon paper-JAPAN	150-500	Tempo- CNC, NFC and CNC	Health sector
Innventia-SWEDEN	100	CNF	Composites

CTP/ FCBA - FRANCE	100	Enzi. NFC, T-CNF	Commercial sales
OHI paper- JAPAN	100	CNF	Unknown
Stora Enso-FINLAND	unknown	CNF	Unknown
UPM- FINLAND	unknown	CNF	Unknown
SAPPI- NETHERLANDS	unknown	CNF	Unknown
Lulea university- SWEDEN	unknown	CNF	Unknown
Holmen - SWEDEN	100	CNC	Unknown
Alberta innovates - CANADA	20	CNC	Unknown
India council for Ag. research	10	CNC	Unknown
Melodea - Israel	unknown	CNC	Health sector
FP-Innovations - CANADA	unknown	CNC, CNF	Unknown
Blue goose refineries- CANADA	10	CNC	Unknown

Table-1 production of nanocellulose all over the world (Based on TAPPI Nano outlook)

1.4 Nanocomposites

It is well-known that nanocomposites are composites containing fillers that have at least one nano-sized dimension. Bio-sourced nanocomposites can be prepared by the reinforcement of CNC in matrix, and in particular polymeric matrices, by different processes such as casting, thermopressing, melt spun and extrusion. The reason behind huge market of bio sourced CNC based nanocomposites is their exceptional mechanical and thermal properties.

The use of cellulose nanocrystals as nanofiller or reinforcing phase is their most widely studied application. They have the potential to significantly enhance the mechanical properties of plastic composites. The recent reviews published in the composites field presented in Table 2, show that all the publications on cellulose nanocrystals from last two years were focused on composites.

Title	Year	Reference
A Review on Grafting of Biofibers for Biocomposites	2016	29
Rheological properties of cellulose nanocrystal-embedded polymer composites: a review	2016	30
Recent advances and migration issues in biodegradable polymers from renewable sources for food packaging	2015	31
A Review of Natural Fiber Reinforced Poly(Vinyl Alcohol) Based Composites: Application and Opportunity	2015	32
Self-healing polymer nanocomposite materials: A review	2015	33
Extraction of cellulose nanocrystals from plant sources for application as reinforcing agent in polymers	2015	34
Review of Nanocellulose for Sustainable Future Materials	2015	35
Different preparation methods and properties of nanostructured cellulose from various natural resources and residues: a review	2015	36

Table-2 Recent review publications on cellulose nanocrystals composites from last two years (2015 & 2016).

1.4.1 Processing techniques

The major processing techniques for polymer nanocomposites based on cellulose nanocrystals are casting-evaporation, melt-compounding and electrospinning. These techniques have been reported in the literature to homogeneously mix cellulose nanocrystals with a polymeric matrix, as shown in Figure 6. The first study on the effect of processing approach on the properties of cellulose nanocrystals-based composites was reported by Hajji et al (36).

Composites generally prepared by casting-evaporation proved good mechanical behaviour that is better than the one obtained using the melt extrusion process method. This can probably be attributed to less structural damage and preservation of nanocrystals' orientation in the matrix during casting-evaporation. A good dispersion level is obtained in water for

sulphated cellulose nanocrystals. Thus, it is simple to process nanocomposites by casting and water evaporation using either water-soluble polymers or polymer aqueous dispersions (latex) as the matrix. The casting evaporation is very tedious for water-insoluble polymers. Because the aqueous suspension of cellulose nanocrystals should be exchanged with the solvent medium that is appropriate for the polymer dissolution. The dispersion of cellulose nanocrystals is also a big issue due to the hydrophilic nature of CNC in hydrophobic solvent medium to avoid the aggregation. For the solvent exchange, several successive centrifugations are needed. Importantly, this process needs a lot of organic solvents, it is lengthy and more energy consuming (37).

The casting-evaporation process allows each nanocrystal to preserve its individualization state resulting from its colloidal dispersion in solvents, and consequently, such a process keeps the maximum reinforcing effect for the composites. Indeed, during slow liquid evaporation, strong interactions between nanoparticles can settle and promote the formation of a rigid percolating network. During slow solvent evaporation, because of Brownian motions in the suspension or solution (whose viscosity remains low, up to the end of the process when the latex particle or polymer concentration becomes very high), the rearrangement of the nanoparticles is possible. There is enough time for the interaction and connection among cellulose nanocrystals to form a percolating network, which is the basis of their reinforcing effect for composites (38, 39).

The wet processing approach, such as casting-evaporation, has been extensively used in various reports for the preparation of cellulose nanocrystal-based composites. However, this technique is both non-industrial and non-economic, and also limits the number of polymer matrices that can be used in association with cellulose nanocrystals. As explained in section 1.3.2 the large-scale production of cellulose nanocrystals is required for the more industrial composite processing techniques to be able to produce cellulose nanocrystal-based

composites, e.g. melt-compounding techniques, such as extrusion. This process is well-known as solvent free process (green) and importantly this process is industrially viable procedure since it is largely used in the polymer industry. However, due to the issues of inherent incompatibility between the cellulose and the polymer, and thermal stability associated to the presence of sulphate groups on the cellulose surface, this processing method is infrequently employed for the preparation of cellulose nanocrystal-based composites, because of the irreversible agglomeration of CNC upon drying process. The sulphate groups resulting from H_2SO_4 hydrolysis seriously induce the reduction of the thermal stability of nanocrystals (40).

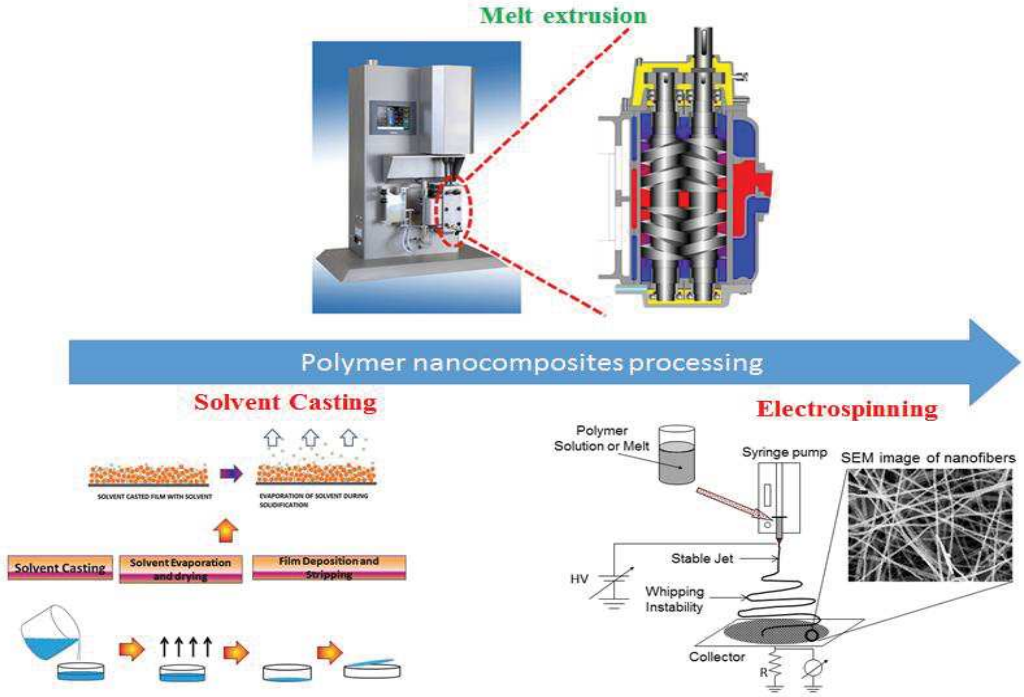

Figure-6 Common processing techniques for polymer nanocomposites based on CNC.

Electrospinning is another process to prepare the nanocomposites by mixing CNC with polymer matrix, which yields the elaboration of thin polymer fibres with few nanometres. In this process, a polymer solution is positively charged to high voltage to produce the submicron scale fibres from a slit to a collector. Therefore, to find suitable solvents to

dissolve cellulose and to process it in the melt state are the key points for this processing technique (41). Unfortunately, very few studies have been reported for the preparation of cellulose nanocrystal-based electrospinning composite fibres, which shows the remaining challenge of this processing approach.

1.4.2 Nanocomposites by melt extrusion

Towards the development of the nanocomposites by melt extrusion, few interesting results were reported in the literature like surface modification of CNC (64, 58) (coating with surfactant), physical adsorption (65, 67) (with macromolecules), chemical grafting (42, 43) (derivatization and grafting with new molecules) and blending or premix (66) (with polymer) to prepare the capsules. The main aim of the above mentioned methods is to promote the dispersion and compatibility of CNC with hydrophobic matrices. The recent processes used in the melt compounding of the CNC were shown in the figure-7. In the surface modification process the quaternary salt was used to create electrostatic interaction with CNC in aqueous medium, which improved thermal stability and the dispersion in hydrophobic medium. These modified CNC were successfully reinforced into PP matrices and their impact on the mechanical properties was reported. In another study a simple physical adsorption of triblock copolymer on CNC and their reinforcement in LLDPE was reported. The grafted CNC was also used to reinforce in the PLA matrices was reported. In the recent study the capsulation of CNC by using polycarbonate (PC) precipitation and their reinforcement in the PC matrix was studied. Basically the four processes shown and discussed in figure 7 overcome the main issues like thermal stability and aggregation up on drying process. Despite of having intensive studies the chemical grafting, premix processes are not applicable at industrial level as they require lot of orgonic solvents. Interestingly the physical adsorption surface modification is evolved as most promising to work at industrial scale.

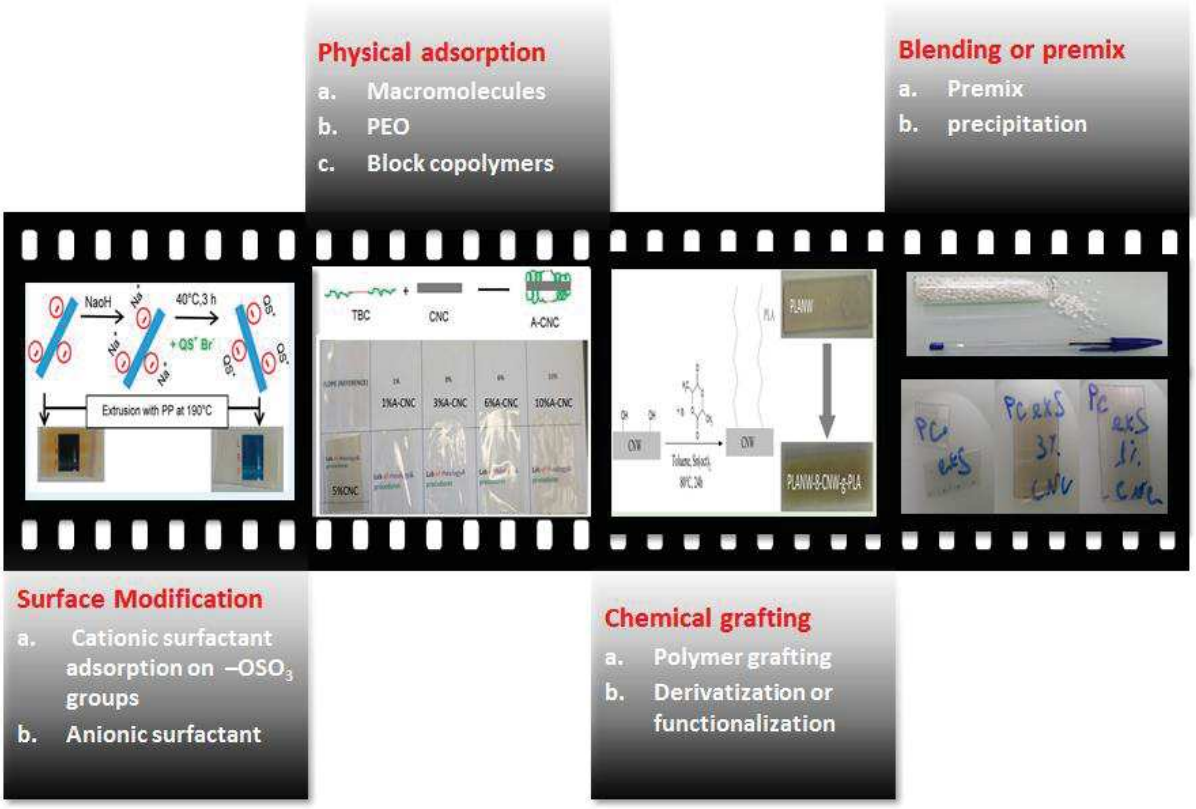

Figure-7 Different strategies reported in the literature for elaboration of nanocomposites by extrusion

Table-3 summarized the systems reported on the melt extrusion of CNC with various polymers from last five years. It is clear that from last two years the researchers are more focussed on polymer nanocomposites obtained by melt processing, resulting in a number of publications almost twice that of articles published in 2014 and 2015. This is due in particular to the high demand of industries. It is worth noting that most of the research articles published is based on the chemical grafting, which helps to improve the CNC dispersion and also thermal stability. However, the molecules grafted on CNC notably limits the inter particle interactions which leads to poor mechanical behaviour. In the same time, grafting will improve the compatibility between the filler and the matrices which obviously will improve the mechanical properties of the composites. Chemical grafting of polymers on the

surface of the CNC by ring opening polymerization came to focus between 2010-2013, which was used to improve the compatibility between the grafted polymer and the matrix (42, 43). However, these methods are highly impossible to use at industrial level as it requires more organic solvents and also this is highly exhausting (solvent exchange) process. In order to overcome these issues, researchers focussed on development of new methods that are compatible with industrialisation. A simple approach is derivatization of CNC by introducing small groups like acetylation, esterification, silylation etc. The derivatization process can improve the dispersion in the polymers. Importantly, surface properties of CNC such as hydrophilicity, surface energy, surface charge and density will change compared to that of neat CNC. CNC were successfully encapsulated by using dispersed nano-objects protective encapsulation (DOPE) process (63). However, this process was unsuccessful in improving the thermal stability of nanocrystals and the dispersion state of CNC in the matrix was poor. The compatibility between the alginate and the polymer was a big concern.

One more process is physical modification of cellulose nanocrystals by using the Beycostat surfactant was reported in the literature (64). In this study an increased amount of surfactant improves the dispersion of the CNC in the PLA matrix but the surfactant has also a negative effect, such as polymer chain degradation of the PLA. Also, the surfactant was not completely miscible in the PLA matrix as reported.

Surface modification of CNC	Filler content (wt. %)	Polymer matrices	Reference	Year
Grafting	1-8	PCL	42	2011
Grafting	2-8	PLA	43	2011
Neat	3-30	PEO	44	2011
Neat	3-30	PVAc	45	2011
Physical Adsorption	1-9	LDPE	46	2012

Neat	1-5	PLA	47	2012
Neat	1-15	PEVA	48	2013
Adsorption/Grafting	1-20	PS	49	2013
Premix or Blends	1-5	PLA	50,51	2013
Adsorption	1-9	LDPE	52	2014
Modified	1-5	PLA	53	2014
Grafting	1-5	LDPE/HDPE	54	2014
Grafting	1	PLA	55	2015
Adsorption	6	PBS	57	2016
Grafting	5	PLLA	56	2016
Modification	1-10	PP	58	2016
Neat	1-3.5	PA	59	2016
Neat	1-10	PA	60	2015
Adsorbed	1-30	LDPE	61	2016
Neat	1-7	PLA	62	2016

Table-3 Melt extrusion of modified, grafted and neat CNC with various polymers from last five years.

By considering the issues mentioned earlier, for the first time the physical adsorption of PEO chains on the surface of the CNC was reported (46), which improved the thermal stability as well as dispersion in hydrophobic matrices (with LDPE). Although, this process cannot be applied for other high melting polymers as these adsorbed CNC are not stable at high temperature. Physical and chemical compatibilization with PS proved that PEO adsorbed CNC did not improve the thermal stability (49).

The physical modification and adsorption are simpler approach compared to the grafting and chemical modification to commercialise the process. The optimization of this process is vital to improve the mechanical behaviour of the composites. In addition, the interfacial interactions between i) the adsorbed macromolecules to CNC filler ii) polymer and adsorbed

CNC filler and iii) the mechanism between cellulose nanocrystals has to be established. Although there have been many studies on surface modification of cellulose nanocrystals to reinforce all kinds of polymeric matrices (as shown in Table 3), no proper industrial modification process is available for the commercialization use. Irrespective of physical or chemical modification, each modification method has its own limitations as discussed above. In the future, for the purpose of developing cellulose nanocrystal-based composites to replace petrochemical plastics, novel surface modification is required, with simple treatment or procedure, high-efficiency property regulation, optimized performance of composites and industrial production.

1.5 Conclusion

The substantial interest in renewable biopolymers in the field of polymer composites is increasing in recent years. More precisely, cellulose is the most considerable interest in the advantage of renewable biopolymer for the advancement of the polymer composites field. The acid hydrolysis of the cellulose fibres yields the CNC which is stronger than Kevlar. From last twenty years, researcher's interest on CNC is significantly increased especially in the field of the nanocomposites. The recent years production of CNC was highly increased. Moreover this material is available to the industries in huge quantities in order to develop the new functional materials. The unique properties of CNC made industries to concentrate on CNC as their best choice of filler to replace the regular petroleum based materials.

Solvent casting was the mostly used process to prepare polymer composites based on CNC but this can be applied only at the lab scale and it seems less realistic for industries considering high amount of the organic solvents and time. Recently, melt processing methods gained a lot of interest because they can be utilised at industrial level. In order to process polymer nanocomposites based on CNC at industrial level, extrusion is most considerable process. However, CNC are limiting the melt processing because of the low thermal stability and irreversible aggregation up on drying. In order to overcome these issues researchers developed many methods like physical modification, chemical grafting and blend or premix capsules. However, all these methods are not possible to use at industrial level. Certainly, the production of CNC and their applications for the betterment of the new materials is emerging area in the nanotechnology. However, it is very clear that there are still many challenges to overcome for the development of the nanocomposites by melt extrusion process.

1.6 References:

1. Nagalakshmaiah, M., Mortha, G., & Dufresne, A. (2016). Structural investigation of cellulose nanocrystals extracted from chili leftover and their reinforcement in cariflex-IR rubber latex. Carbohydrate polymers, 136, 945-954.
2. Varshney VK, Naithani S (2011) Chemical Functionalization of Cellulose Derived from Nonconventional Sources. In: Kalia S, Kaith BS, Kaur I (eds) Cellulose Fibers: Bio- and Nano-Polymer Composites. Springer Berlin Heidelberg, pp 43–60.
3. Siró I, Plackett D (2010) Microfibrillated cellulose and new nanocomposite materials: a review. Cellulose 17:459–494. DOI: 10.1007/s10570-010-9405-y.
4. Stelte W, Sanadi AR (2009) Preparation and Characterization of Cellulose Nanofibers from Two Commercial Hardwood and Softwood Pulps. Ind Eng Chem Res 48:11211–11219. DOI: 10.1021/ie9011672.
5. Wiedenhoeft AC, Miller RB (2005) Structure and function of wood. In Rowell RM (ed) Handbook of wood chemistry and wood composites. CRC Press, pp 9–33.
6. Shackford LD (2003) A Comparison of Pulping and Bleaching of Kraft Softwood and Eucalyptus Pulps. 36th International pulp and paper congress and exhibition. São Paulo, Brazil.
7. Wang QQ, Zhu JY, Gleisner R, Kuster TA, Baxa U, McNeil SE (2012) Morphological development of cellulose fibrils of a bleached eucalyptus pulp by mechanical fibrillation. Cellulose 19:1631–1643. doi: 10.1007/s10570-012-9745-x.
8. Nechyporchuk, O., Belgacem, M. N., & Bras, J. (2016). Production of cellulose nanofibrils: A review of recent advances. Industrial Crops and Products.
9. Klemm D, Kramer F, Moritz S, et al. (2011) Nanocelluloses: A New Family of Nature-Based Materials. Angew Chem Int Ed 50:5438–5466. doi: 10.1002/anie.201001273.
10. Moon RJ, Martini A, Nairn J, et al (2011) Cellulose nanomaterials review: structure, properties and nanocomposites. Chem Soc Rev 40:3941–3994.doi: 10.1039/C0CS00108B.
11. Turbak AF, Snyder FW, Sandberg KR (1983a) Microfibrillated Cellulose, a New Cellulose Product: Properties, Uses, and Commercial Potential. In Sarko A (ed) Proceedings of the Ninth Cellulose Conference. Applied Polymer Symposia 37. N.Y.: Wiley. pp. 815–827.
12. Turbak AF, Snyder FW, Sandberg KR (1983b) Microfibrillated cellulose. Patent U.S. 4374702.

13. Isogai A (2013) Wood nanocelluloses: fundamentals and applications as new bio-based nanomaterials. J Wood Sci 59:449–459. doi: 10.1007/s10086-013-1365-z.
14. Lavoine N, Desloges I, Dufresne A, Bras J (2012) Microfibrillated cellulose-Its barrier properties and applications in cellulosic materials: A review. Carbohydrate Polymers 90:735–764. doi: 10.1016/j.carbpol.2012.05.026.
15. Gatenholm P, Klemm D (2010) Bacterial Nanocellulose as a Renewable Material for Biomedical Applications. MRS Bulletin 35:208–213. doi: 10.1557/mrs2010.653.
16. Stevanic JS, Joly C, Mikkonen KS, Pirkkalainen K, Serimaa R, Rémond C, Toriz G, Gatenholm P, Tenkanen M, Salmén L (2011) Bacterial nanocellulose-reinforced arabinoxylan films. J Appl Polym Sci 122:1030–1039. doi: 10.1002/app.34217.
17. Dong, X. M.; Revol, J.-F.; Gray, D. G. Effect of micro crystallite preparation conditions on the formation of colloid crystals of cellulose. Cellulose 1998, 5, 19–32
18. Leung, A. C. W.; Hrapovic, S.; Lam, E.; Liu, Y.; Male, K. B.; Mahmoud, K. A.; Luong, J. H. T. Characteristics and properties of carboxylated cellulose nanocrystals prepared from a novel one-step procedure. Small 2011, 7, 302–305.
19. Hirota, M.; Tamura, N.; Saito,T.; Isogai, A. Water dispersion of cellulose II nanocrystals prepared by TEMPO-mediated oxidation of mercerized cellulose at pH 4.8. Cellulose 2010, 17, 279–288. 16
20. Beck-Candanedo, S.; Roman, M.; Gray, D. G. Effect of reaction conditions on the properties and behavior of wood cellulose nanocrystal suspensions. Biomacromolecules 2005, 6, 1048-1054.
21. Braun, B.; Dorgan, J. R. Single-step method for the isolation and surface functionalization of cellulosic nanowhiskers. Biomacromolecules 2009, 10, 334–341.
22. Filson, P. B.; Dawson-Andoha, B. E.; Schwegler-Berry, D. Enzymatic-mediated production of cellulose nanocrystals from recycled pulp. Green Chem. 2009, 11, 1808–1814.
23. Man, Z.; Muhammad, N.; Bustam, A. S. M. A.; Kumar, M. V.; Rafiq, S. Preparation of cellulose nanocrystals using an ionic liquid. J. Polym. Environ. 2011, 19, 726–731.
24. Kontturi, E.; Meriluoto, A.; Nuopponen, M. Processing for preparing micro- and nanocrystalline cellulose. 2011, Patent WO2011/114005.
25. Amin, K. N. M., Annamalai, P. K., Morrow, I. C., & Martin, D. (2015). Production of cellulose nanocrystals via a scalable mechanical method. RSC Advances, 5(70), 57133-57140.
26. V. K. Baheti, R. Abbasi and J. Militky, World J. Eng., 2012, 9,45–50.

27. W. Li, J. Yue and S. Liu, Ultrason. Sonochem. 2012, 19, 479 - 485.
28. TAPPI, Workshop on international standards for nanocellulose. Arlington, USA, June 9th, 2011.
29. Wei, L., & McDonald, A. G. (2016). A Review on Grafting of Biofibers for Biocomposites. Materials, 9(4), 303.
30. Ching, Yern Chee, et al. "Rheological properties of cellulose nanocrystal-embedded polymer composites: a review." Cellulose 23.2 (2016): 1011-1030.
31. Scarfato, P., Di Maio, L., & Incarnato, L. (2015). Recent advances and migration issues in biodegradable polymers from renewable sources for food packaging. Journal of Applied Polymer Science, 132(48).
32. Tan, B. K., Ching, Y. C., Poh, S. C., Abdullah, L. C., & Gan, S. N. (2015). A review of natural fiber reinforced poly (vinyl alcohol) based composites: Application and opportunity. Polymers, 7(11), 2205-2222.
33. Thakur, V. K., & Kessler, M. R. (2015). Self-healing polymer nanocomposite materials: A review. Polymer, 69, 369-383.
34. Ng, H. M., Sin, L. T., Tee, T. T., Bee, S. T., Hui, D., Low, C. Y., & Rahmat, A. R. (2015). Extraction of cellulose nanocrystals from plant sources for application as reinforcing agent in polymers. Composites Part B: Engineering, 75, 176-200.
35. Kim, J. H., Shim, B. S., Kim, H. S., Lee, Y. J., Min, S. K., Jang, D., ... & Kim, J. (2015). Review of nanocellulose for sustainable future materials. International Journal of Precision Engineering and Manufacturing-Green Technology, 2(2), 197-213.
36. Hajji, P.; Cavaille, J. Y.; Favier, V.; Gauthier, C.; Vigier, G. Tensile behavior of nanocomposites from latex and cellulose whiskers. Polym. Compos. 1996, 17, 612–619.
37. Dufresne, A. Processing of polymer nanocomposites reinforced with cellulose nanocrystals: a challenge. Int. Polym. Proc. 2012, 27, 557–564.
38. Dufresne, A. comparing the mechanical properties of high performances polymer nanocomposites from biological sources. J Nanosci. Nanotechnol. 2006, 6, 322–330.
39. Dufresne, A. Polysaccharide nanocrystal reinforced nanocomposites. Can. J. Chem. 2008, 86, 484–494.
40. Dufresne, A. Nanocellulose: a new ageless bio nanomaterial. Mater. Today 2013, 16, 220–227.
41. Dufresne, A. Nanocellulose. From nature to high performance tailored materials. Walter de Gruyter GmbH, Berlin/Boston, 2012, pp. 261−262.

42. Goffin, A. L., Raquez, J. M., Duquesne, E., Siqueira, G., Habibi, Y., Dufresne, A., & Dubois, P. (2011). Poly (ε-caprolactone) based nanocomposites reinforced by surface-grafted cellulose nanowhiskers via extrusion processing: Morphology, rheology, and thermo-mechanical properties. Polymer, 52(7), 1532-1538.
43. Goffin, A. L., Raquez, J. M., Duquesne, E., Siqueira, G., Habibi, Y., Dufresne, A., & Dubois, P. (2011). From interfacial ring-opening polymerization to melt processing of cellulose nano whisker-filled polylactide-based nanocomposites. Biomacromolecules, 12(7), 2456-2465.
44. Alloin, F., D'Aprea, A., Dufresne, A., El Kissi, N., & Bossard, F. (2011). Poly (oxyethylene) and ramie whiskers based nanocomposites: influence of processing: extrusion and casting/evaporation. Cellulose, 18(4), 957-973.
45. Mathew, A. P., Gong, G., Bjorngrim, N., Wixe, D., & Oksman, K. (2011). Moisture absorption behavior and its impact on the mechanical properties of cellulose whiskers-based polyvinyl acetate nanocomposites. Polymer Engineering & Science, 51(11), 2136-2142.
46. Ben Azouz, K., Ramires, E. C., Van den Fonteyne, W., El Kissi, N., & Dufresne, A. (2011). Simple method for the melt extrusion of a cellulose nanocrystal reinforced hydrophobic polymer. ACS Macro Letters, 1(1), 236-240.
47. Fortunati, E., Armentano, I., Zhou, Q., Iannoni, A., Saino, E., Visai, L., & Kenny, J. M. (2012). Multifunctional bio-nanocomposite films of poly (lactic acid), cellulose nanocrystals and silver nanoparticles. Carbohydrate Polymers, 87(2), 1596-1605.
48. Sonia, A., Dasan, K. P., & Alex, R. (2013). Celluloses microfibres (CMF) reinforced poly (ethylene-co-vinyl acetate) (EVA) composites: Dynamic mechanical, gamma and thermal ageing studies. Chemical engineering journal, 228, 1214-1222.
49. Lin, N., & Dufresne, A. (2013). Physical and/or chemical compatibilization of extruded cellulose nanocrystal reinforced polystyrene nanocomposites. Macromolecules, 46(14), 5570-5583.
50. Bitinis, N., Verdejo, R., Bras, J., Fortunati, E., Kenny, J. M., Torre, L., & López-Manchado, M. A. (2013). Poly (lactic acid)/natural rubber/cellulose nanocrystal bionanocomposites Part I. Processing and morphology. Carbohydrate polymers, 96(2), 611-620.
51. Bitinis, N., Fortunati, E., Verdejo, R., Bras, J., Kenny, J. M., Torre, L., & López-Manchado, M. A. (2013). Poly (lactic acid)/natural rubber/cellulose nanocrystal

bionanocomposites. Part II: Properties evaluation. Carbohydrate polymers, 96(2), 621-627.

52. Pereda, M., Kissi, N. E., & Dufresne, A. (2014). Extrusion of polysaccharide nanocrystal reinforced polymer nanocomposites through compatibilization with poly (ethylene oxide). ACS applied materials & interfaces, 6(12), 9365-9375.
53. Arrieta, M. P., Fortunati, E., Dominici, F., Rayón, E., López, J., & Kenny, J. M. (2014). PLA-PHB/cellulose based films: Mechanical, barrier and disintegration properties. Polymer Degradation and Stability, 107, 139-149.
54. Mokhena, T. C., & Luyt, A. S. (2014). Investigation of polyethylene/sisal whiskers nanocomposites prepared under different conditions. Polymer Composites, 35(11), 2221-2233.
55. Yang, W., Dominici, F., Fortunati, E., Kenny, J. M., & Puglia, D. (2015). Melt free radical grafting of glycidyl methacrylate (GMA) onto fully biodegradable poly (lactic) acid films: effect of cellulose nanocrystals and a masterbatch process. RSC Advances, 5(41), 32350-32357.
56. Spinella, S., Samuel, C., Raquez, J. M., McCallum, S. A., Gross, R., & Dubois, P. (2016). Green and Efficient Synthesis of Dispersible Cellulose Nanocrystals in Biobased Polyesters for Engineering Applications. ACS Sustainable Chemistry & Engineering, 4(5), 2517-2527.
57. Ludueña, L. N., Fortunati, E., Morán, J. I., Alvarez, V. A., Cyras, V. P., Puglia, D., ... & Pracella, M. (2015). Preparation and characterization of polybutylene-succinate/poly (ethylene-glycol)/cellulose nanocrystals ternary composites. Journal of Applied Polymer Science.
58. Nagalakshmaiah, M., El Kissi, N., & Dufresne, A. (2016). Ionic compatibilization of cellulose nanocrystals with quaternary ammonium salt and their melt extrusion with polypropylene. ACS applied materials & interfaces, 8(13), 8755-8764.
59. Peng, J., Walsh, P. J., Sabo, R. C., Turng, L. S., & Clemons, C. M. (2016). Water-assisted compounding of cellulose nanocrystals into polyamide 6 for use as a nucleating agent for microcellular foaming. Polymer, 84, 158-166.
60. Nicharat, A., Sapkota, J., Weder, C., & Foster, E. J. (2015). Melt processing of polyamide 12 and cellulose nanocrystals nanocomposites. Journal of Applied Polymer Science, 132(45).
61. Volk, N., He, R., & Magniez, K. (2015). Enhanced homogeneity and interfacial compatibility in melt-extruded cellulose nano-fibers reinforced polyethylene via surface

adsorption of poly (ethylene glycol)-block-poly (ethylene) amphiphiles. European Polymer Journal, 72, 270-281.

62. Kamal, M. R., & Khoshkava, V. (2015). Effect of cellulose nanocrystals (CNC) on rheological and mechanical properties and crystallization behavior of PLA/CNC nanocomposites. Carbohydrate polymers, 123, 105-114.
63. Lemahieu, L., Bras, J., Tiquet, P., Augier, S., & Dufresne, A. (2011). Extrusion of Nanocellulose-Reinforced Nanocomposites Using the Dispersed Nano-Objects Protective Encapsulation (DOPE) Process. Macromolecular Materials and Engineering, 296(11), 984-991.
64. Bondeson, D.; Oksman, K. Dispersion and Characteristics of Surfactant Modified Cellulose Whiskers Nanocomposites. Compos.Interfaces2007, 14, 617−630.
65. Pereda, M.; El Kissi, N.; Dufresne, A. Extrusion of Polysaccharide Nanocrystal Reinforced Polymer Nanocomposites through Compatibilization with Poly(ethylene oxide). *ACS Appl. Mater. Interfaces* 2014, *6*, 9365-9375.
66. Mariano, M.; El Kissi, N.; Dufresne, A. Melt Processing of Cellulose Nanocrystal Reinforced Polycarbonate from a Masterbatch Process. *Eur. Polym. J.* 2015, *69*, 208-223.
67. Nagalakshmaiah, Malladi, Nadia El Kissi, and Alain Dufresne. Surface adsorption of triblock copolymer (PEO-PPO-PEO) on cellulose nanocrystals and their melt extrusion with polyethylene. RSC advances (2016) in press.

Chapter-2

Extraction of cellulose nanocrystals from agriculture biomass

Structural investigation of cellulose nanocrystals extracted from chili leftover and their reinforcement in cariflex-IR rubber latex

(Carbohydrate polymers 136 (2016): 945-954)

Chapter-2: Structural investigation of cellulose nanocrystals extracted from chili leftover and their reinforcement in cariflex-IR rubber latex

ENGLISH ABSTRACT

The morphology and chemical composition of chili fibres were investigated. Unusual low lignin content was found when compared to other annual plants. High aspect ratio cellulose nanocrystals (CNCs) were prepared from these fibres by an acid hydrolysis treatment. CNCs extracted from chili leftover were characterized using FT-IR, AFM, TGA and XRD to access their functional, structural, thermal and crystallinity properties, respectively. The length and diameter of the chili leftover CNC were 90-180 nm and 4-6 nm, respectively, resulting in an average aspect ratio of 26. This high aspect ratio ensures percolation at low filler content which in turn results in high thermal and mechanical properties of the nanocomposites. These CNCs were used to prepare nanocomposite films using the highly marketing commercial latex called Cariflex-Isoprene (IR) by casting/evaporation in order to investigate their reinforcing effect. The mechanical properties of nanocomposite films were investigated in both the linear and nonlinear range by DMA and tensile test, respectively, and their morphology was studied using scanning electron microscopy.

RESUME FRANÇAIS

La morphologie et la composition chimique de fibres de chili ont été étudiées. La teneur en lignine déterminée est inhabituellement faible par rapport à celle d'autres plantes annuelles. Des nanocristaux de cellulose (CNCs) avec un facteur de forme élevé ont été préparés à partir de ces fibres par un traitement d'hydrolyse acide. Ils ont été caractérisés par FT-IR, AFM, TGA et XRD pour accéder à leurs propriétés fonctionnelles, structurales, thermiques et de cristallinité. La longueur et le diamètre des CNC obtenus sont de l'ordre de 90 à 180 nm et de 4 à 6 nm, respectivement. Le facteur de forme moyen qui en résulte est de 26. Ce ratio élevé assure une percolation du réseau cellulosique à basse teneur en charge. C'est ce réseau qui contrôle les propriétés thermiques et mécaniques élevées des nanocomposites élaborés à partir de ces CNC. De tels composites ont été élaborés par coulée-évaporation avec une matrice de latex commercial, le Cariflex-isoprène (IR). Les propriétés mécaniques linéaires et non linéaires des films nanocomposites ont été étudiées par de DMA et par des essais de traction. Leur morphologie a quant à elle été observée par microscopie électronique à balayage.

2.1 INTRODUCTION

New lignocellulosic materials are of great interest for industry as they have the potential to replace regular sources of materials. Enormous amounts of lignocellulosic materials are available all over the world in different forms according to their application. Lignocellulosic materials used for pulp and paper production are mostly woody plants, although in some developing countries annual crop residues are also extensively used (*Shrinath, Tschirner& Ramaswamy,2003*) and by-products of agriculture and forestry such as harvesting residues, e.g. vegetal straw, maize stover, sugar cane bagasse and wood residues are used by pulp and paper industries.

According to OECD-FAO (Organisation for Economic Co-operation and Development and the Food and Agriculture Organization) agriculture outlook, every year farmers are harvesting 35 million tons of natural fibres from animals and plants. They are used in various applications like fabrics, ropes and twines. They also play an important role in modern civilization through paper and packaging (Bledzki and Gassan, 1999). Hence this work is focused on annual plants, more precisely the chili plant leftover.

The chili pepper is the fruit of plants from the genus *Capsicum* and it belongs to the nightshade family, *Solanaceae*. The word in British English and in Australia, New Zealand, India, Malaysia and other Asian countries is just chili without "pepper"(McLeod, Eshbaugh & Guttman, 1979). It grows in many countries all over the world but the world's largest production is in India. In particular, Guntur, Andrapradesh produces 30% which contributes 75% of India's whole chili exports, according to Government of India ministry of Agriculture. The fibres used in this study are from Guntur, Adigoppula region. This chili plant has single straight and small branches of stalks composed of an inner wooded core walled by the single layer non fibrous bark.

According to the authors knowledge no study has been done to characterize the fibres of chili plant. Henceforth chili leftover will be termed as CLO. A better understanding of its microstructure and chemical composition could offer new opportunities for non-food applications of this renewable resource. The chemical composition depends on several factors, such as plant origin, weather conditions, soil nature, etc.

As evident from the impending commercialization of cellulose nanocrystals (CNCs), most of the industries and researchers are paying more attention towards commercial applications. In this study the nanocrystals from CLO were characterized and nanocomposite films were prepared by casting aqueous mixtures of these CNCs with polymer latex in different ratios. Natural rubber (NR) is a perfect matrix to be used as a model system to study the effect of filler reinforcement, due its high flexibility and low stiffness. NR has been used as matrix for different reinforcing polysaccharide nanofillers such as CNC (Abraham et al., 2013; Bendahou, Habibi, Kaddami, & Dufresne, 2009; Bendahou, Kaddami, & Dufresne, 2010; Bendahou, Kaddami, Espuche, Gouanvé, & Dufresne, 2011; Bras et al., 2010; Chen, Gu, & Xu, 2014; Gu, Li, Jia, Luo, & Cheng, 2009; Gu, Lin, Luo, & Jia, 2012; Pasquini, Teixeira, Curvelo, Belgacem, & Dufresne, 2010; Siqueira, Abdillahi, Bras, & Dufresne, 2010; Siqueira, Tapin-Lingua, Bras, da Silva Perez, & Dufresne, 2011; Visakh, Thomas, Oksman, & Mathew, 2012; Xu, Gu, Luo, & Jia, 2012; Xu, Gu, Luo, Jia, & Yan, 2015; Zhang et al., 2014).

Cariflex-Isoprene latex which has similar or exceeding properties compared to NR without impurities was chosen as the polymeric matrix. The choice of the latex purely depends on the commercial applications. This highly commercially marketable latex from Kraton polymers is pure and transparent. This latex product is clean, high-performance and pure alternative to natural rubber for medical supplies, consumer products and a numerous of other industrial applications such as surgical gloves, catheters, tube connectors, needle shields, medical

bottle stoppers, cohesive bandages electronics, condoms, footwear, food packaging, adhesives, paint additives and resins, according to Kraton polymers *(Blackley, 1997).* In the present study, the morphology and chemical composition of CLO fibres were investigated. CNCs were prepared from these fibres by an acid hydrolysis treatment and characterized by FT-IR, AFM, TGA and XRD. Nanocomposites were prepared by casting a mixture of CNC extracted from CLO and cariflex-isoprene latex. The prepared nanocomposites were investigated in terms of thermal, morphological and mechanical properties.

2.2 EXPERIMENTAL SECTION

2.2.1 Materials

The chili leftover used as raw material was obtained from Adigoppula, India. Sodium hydroxide (99% purity) and anthraquinone were used for alkaline treatment. Sodium chlorite, acetic acid, and sodium hydroxide were used as bleaching agents and sulphuric acid was used for hydrolysis. All chemicals were purchased from Sigma-Aldrich and were used without further purification. Cariflex-isoprene latex was procured from Kraton polymers, Netherlands. It contained spherical particles with an average diameter around 1.5 μm and its solid content was about 65 wt%. The molecular weight and density were 2×10^6 $g.mol^{-1}$ and 0.96 $g.cm^{-3}$, respectively, and the ammonia content was 0.

2.2.2 Preparation of cellulose nanocrystals from chili leftover

Alkali treatment

The alkali treatment was performed to purify cellulose by removing lignin and hemicellulose from plant chips. The cut plant pieces were cooked in an autoclave with an alkali solution (17 wt% NaOH) and 1 wt% anthraquinone at 170°C for 60 min and then it was cooled to room temperature. The resultant pulp was filtered and washed with distilled water until neutral P^H.

Bleaching process

Following alkali treatment, the pulp was bleached by adding a buffer solution of acetic acid, aqueous chlorite (4 wt%) and heated in water bath at 80°C for 90 min. Then the mixture was allowed to cool and was filtered using excess distilled water. The bleaching process was repeated twice.

Acid hydrolysis

CNC was prepared by H_2SO_4 hydrolysis of CLO fibres, according to the procedure described in previous literature for softwood sulfite pulp (Roman & Gray, 2005). The bleached fibres were hydrolysed at a temperature of 45˚C by using 64 wt% sulphuric acid (pre-heated) for 45 min under continuous stirring. The fibre content was 4 wt%. The hydrolysed material was washed by centrifugation at 10,000 rpm at 10°C for 15 min. This centrifugation step was repeated several times. The suspension was dialyzed against distilled water for several days until constant pH of 5-6 was reached. The resulting suspension was then sonicated for 30 min before being refrigerated for further use.

2.2.3 Preparation of nanocomposites

CNC extracted from CLO fibres was used as filler in IR latex. Nanocomposite films were prepared by reinforcing cariflex-IR with various percentages of CNC ranging from 1 to 6 wt%. The IR latex and the CNC aqueous suspension were first mixed in various proportions to obtain final dry films around 1 mm thick. The mixture was stirred using a magnetic stirrer for 3 h. The films were dried at room temperature in a ventilated fuming hood until the nanocomposites were completely dried.

2.3 Characterization of CLO fibres and cellulose nanocrystals

2.3.1 Chemical composition

The chemical composition of CLO at each stage of treatment was determined according to the methods reported by the Technical Association of Pulp and Paper Industry (TAPPI). The cellulose, hemicellulose and lignin contents were accessed according to TAPPI standards.

2.4 Methods

Optical microscopy

Optical microscopy was used to observe the morphology of the CLO fibres after bleaching by using ZEISS AX10 image M1m which was connected to the AXIOCAM MRC5 by AXIO Vision, Germany.

Scanning electron microscopy (SEM)

Scanning electron microscopy (SEM) was used to characterize the CLO fibres before and after bleaching. The morphology of prepared nanocomposites was also observed. The samples were fractured in liquid nitrogen and coated with gold in order to prevent the charring of the sample due to the electron bombardment. The SEM images were captured by using FEI (MED) Quanta200.

Atomic Force Microscope (AFM)

Atomic Force Microscopy was used to study the length and width of the individual nanocrystals using a Nanoscope III (Veeco, Canada). CNC samples were previously diluted at 10^{-4} wt% and a drop of 0.2 mL was deposited onto freshly cleaved mica substrates and dried overnight under room conditions. Each sample was characterized in tapping mode with a silicon cantilever (OTESPA®, Bruker, USA) at different locations and scanning areas:

10x10 μm² and 3x3μm². Both topographical and phase images were captured and images were subjected to 1st order polynomial flattening to reduce the effects of bowing and tilting.

X-ray diffraction (XRD)

Wide angle X-ray diffraction (XRD) analysis was performed on air-dried CNC suspensions stored at ambient temperature (23°C) and controlled relative humidity (50% RH). The samples were placed in a 2.5 mm deep cell and measurements were performed with a diffractometer (X'Pert PRO MPD ®, PAN analytical, Netherlands) equipped with a detector. The operating conditions of the refractometer were: copper Kα radiation (λ = 1.5418 Å), 2θ (Bragg angle) between 2 and 56°, step size 0.067°, counting time 90 s. Each sample was measured once. The crystallinity index, I_c, was evaluated using the Buschle-Diller and Zeronian Equation (Buschle-Diller and Zeronian, 1992).

$$I_c = 1 - \frac{I_1}{I_2}$$

Where I_1 is the intensity at the minimum (2θ = 18.5°) and I_2 is the intensity associated with the crystalline region of cellulose (2θ = 22°).

Fourier Transform infrared (FT-IR) spectrometry

Fourier Transform infrared (FT-IR) spectrometry analysis was done on the raw, unbleached, bleached fibres and air-dried CNC, in order to know the functional groups present in the material in terms of wave number (cm^{-1}). The samples were analysed by ATR (attenuated total reflectance) in which the sample was placed on the evanescent wave on the ATR crystal through which infrared beam will give the data to the detector. The instrument was Perkin Elmer spectrum 65, FT-IR Spectrometer. Each sample was measured twice.

Thermogravimetric analysis (TGA)

The thermal degradation of the samples was monitored by thermogravimetric analysis (TGA) with a thermo-gravimetric analyzer-STA6000 (Perkin Elmer Instruments, England). The weight loss curves were recorded for a 15-30 mg sample at a heating rate of 10°C/min in the temperature range of 30-900°C under oxidizing atmosphere (air).

Dynamic mechanical analysis (DMA)

Dynamic mechanical analysis (DMA) was used to study the viscoelastic behaviour of the materials. DMA experiments were carried out using RSA3 (TA Instruments, USA) equipment working in the tensile mode. The storage modulus E′ (elastic response) and loss modulus E″ (viscous response) of the material were measured as a function of temperature as the polymer was deformed under an oscillatory stress at a controlled temperature in a specified atmosphere. The storage modulus is related to stiffness, and the loss modulus to damping and energy dissipation. Before analysis the samples were stored overnight in desiccators containing silica gel. Varying stress with a frequency of 1 Hz was applied when heating the material from -100°C to 200°C with a ramp rate equal to 3°C.min^{-1}. The length of the sample was 10 mm. Each sample was measured six times in order to check the reproducibility.

Tensile Tests

The tensile high-strain mechanical tests were performed using a RSA3 (TA Instruments, USA) with a load cell of 100 N. Sample dimensions were 4-5 mm and 20 mm for width and length, respectively, and the gap between pneumatic jaws at the start of each test was adjusted to 10 mm. Before analysis the samples were stored overnight in desiccators containing silica gel. All experiments were carried out at room temperature (25°C) with a cross head speed of 3 mm.min^{-1}. The results were averaged on two measurements.

2.5 RESULTS AND DISCUSSION

2.5.1 Chemical composition

The chemical composition of CLO fibres, i.e. the lignin, cellulose and hemicellulose contents, was determined and results are reported in Table 1. These values cannot be compared with data reported in the literature since the chemical composition of these fibres was never published. The lignin content of CLO fibres was rather low (around 7 wt%) whereas high lignin content was expected since other annual plants such as sugarcane bagasse (around 25 wt %) (Satyanarayana and Wypych, 2007; Filho and Badr, 2004) and jute (around 16 wt %) (Razera and Frollini, 2004) have high lignin contents as shown in Table 1. On the other hand, during the preparation of the holocellulose, the bleaching treatment of CLO fibres has lasted a relatively short time and it is most probably not necessary to repeat four times the treatment. After two bleaching treatments the yield was around 91.3 wt%, among which cellulose represents 67.3 wt% of the dried fibres. The chemical composition of CLO fibres has been compared to that of other annual plants in Table 1. CLO fibres appear as a good source to prepare CNC since it presents high cellulose content.

Table 1. Chemical composition of various lignocellulosic fibres in comparison with CLO fibres.

Source	Cellulose (wt%)	Hemicellulose (wt%)	Lignin (wt%)	Reference
Sugarcane bagasse	54.3-55.2	16.8-29.7	24.3-25.3	(Satyanarayana and Wypych, 2007; Filho and Badr, 2004)
Jute	60	22.1	15.9	(Razera and Frollini, 2004)
Chili leftover	67.3±0.5	20.8±0.2	7.3±0.3	This work

2.5.2 Morphological investigation of CLO fibres and CLO-CNC

Scanning electron micrographs of the CLO fibres after different stages of treatment are shown in Figure 1. After the high-temperature alkali treatment and before the bleaching treatment the material was composed of bundles consisting of individual fibres linked together (Fig. 1a). Most of the hemicellulose was hydrolysed and became water soluble and the lignin was partially depolymerized. Most impurities around the fibres were removed, which induced the separation of fibre bundles into individual fibres. Figures 1b and 1c show the morphology of the bleached fibres. The bleaching process helped to remove most of the lignin present in the CLO fibres, leading to further defibrillation. Figure 1d shows the optical microscopy image of individual bleached fibres which length and width were 413 ± 72 µm and 21-28 µm, respectively.

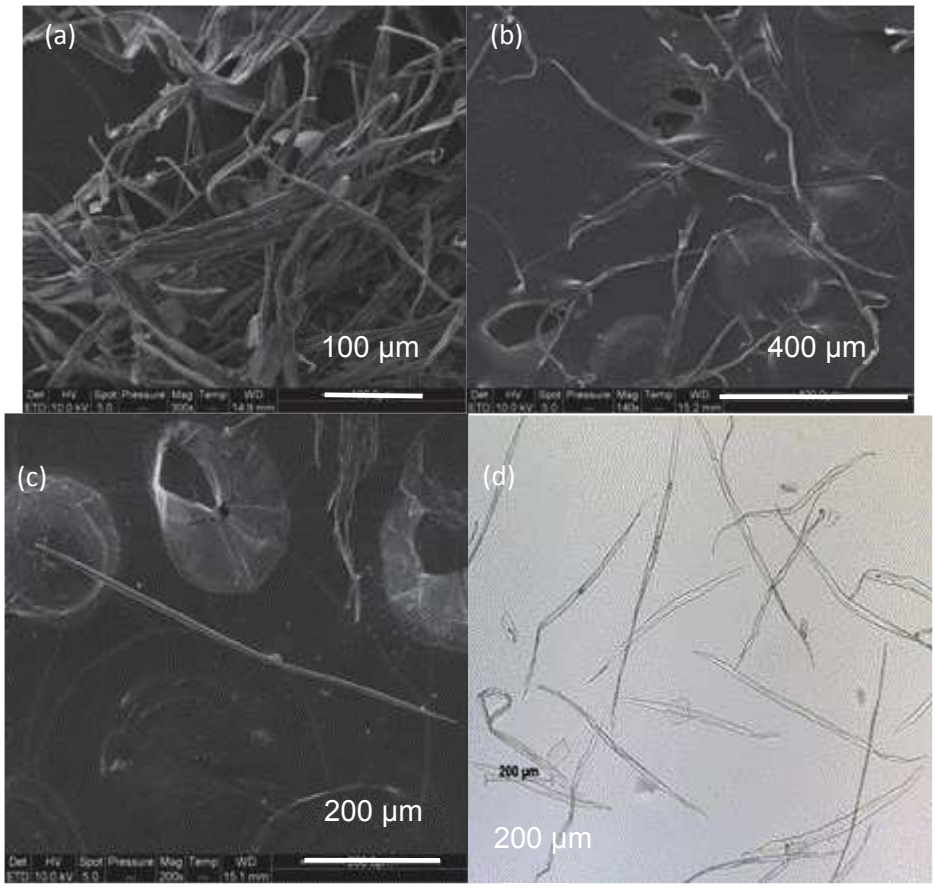

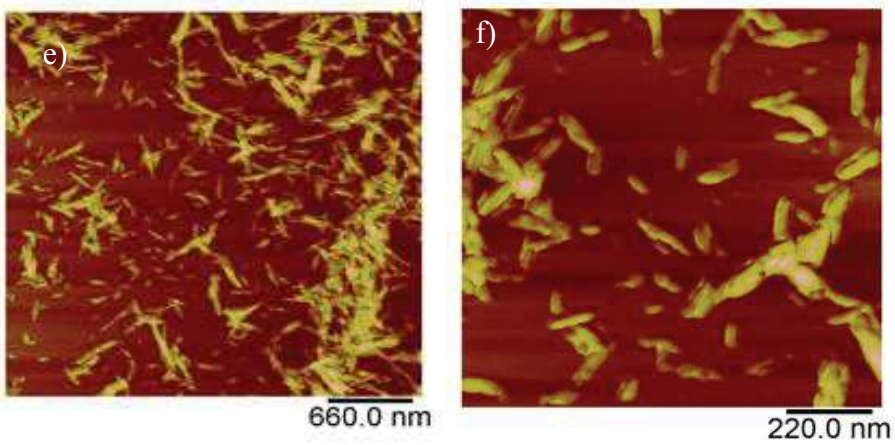

Figure 1. SEM image of (a) unbleached chili fibres and (b, c) individual bleached chili fibres, and (d) optical microscopy image of individual bleached chili fibres. Atomic force microscopy image of CLO-CNC e) 660 nm f) 220 nm.

To produce CNC, cellulose has generally to be treated with H_2SO_4. This acid hydrolysis treatment not only helps to further disintegrate the fibres but also facilitates defibrillation of the fibres to the nanoscale level. It is well known that the amorphous part of cellulose undergoes preferential acidic hydrolysis when compared to crystalline domains. To confirm the separation of individual crystallites and to measure the size of the individual crystals, diluted suspensions were observed by AFM (Fig. 1 e,f). In the micrographs, some aggregation of the nanocrystals can be seen, probably as a result of the water evaporation step during sample preparation. The rod-like or needle-shaped acid-hydrolysed cellulosic nanoparticles were characterized to measure their length (L), width (D), and aspect ratio (L/D) and it was in the range of 90-180 nm, 4-6 nm and 26, respectively, over a minimum of 50 measurements. These values are close to those reported for eucalyptus wood pulp (L = 145 nm; D= 6 nm; L/D = 24) (de Mesquita, Donnici & Pereira, 2010).

2.5.3 FTIR characterization

The FTIR spectra presented in Figure 2 a show the changes in chemical composition that occurred in response to the pre-acid hydrolysis treatment of raw fibres, as well as the H_2SO_4 treatment. The absorbance peaks in the 3,400-3,300 cm^{-1} and 1,634-1,640 cm^{-1} regions were attributed to the stretching and bending vibrations, respectively, of the OH groups of

cellulose. The signals around 2,900-2,800 cm^{-1} correspond to C–H stretching (Sain and Panthapulakkal, 2006). The prominent band at 1,731 cm^{-1} in the spectrum obtained for the raw fibre was assigned to the C=O stretching of the acetyl group and uranic ester groups of the hemicellulose or to the ester linkage of the carboxylic group in the ferulic and p-coumaric acids of lignin and/or hemicellulose (Ahmad, Mosadeghzad, Daik &Ramli, 2008; Zuluaga, Putaux, Velez, Mondragon & Ganan, 2009). The peak at 1,250 cm^{-1} corresponds to the C–O stretching of the aryl group in lignin. These last two peaks were completely absent from the spectra of the alkali-treated fibres and bleached fibres. Taken together, these findings indicate that most of the hemicellulose and lignin were removed before the acid hydrolysis treatment (Troedec, Sedan, Peyratout, Bonnet, Smith, Guinebretiere, Gloaguen & Krausz, 2008).The signals observed in the range of 1,420-1,430cm^{-1} and 1,330-1,380 cm^{-1} in all spectra were attributed to the symmetric bending of CH_2 and the bending vibrations of the C–H and C–O groups of the aromatic rings in polysaccharides, respectively (Jonoobi, Harun, Shakeri , Misra & Oksman, 2009). Finally, the absorbance peaks observed in the 1,028-1,161 cm^{-1} range were attributed to C–O stretching and C–H rocking vibrations of the pyranose ring skeleton (Alemdar and Sain, 2008). The differences between the FTIR spectrum of raw chili fibre and that of CNC clearly indicate that CNC was successfully extracted from chili fibre by the hydrolysis treatment.

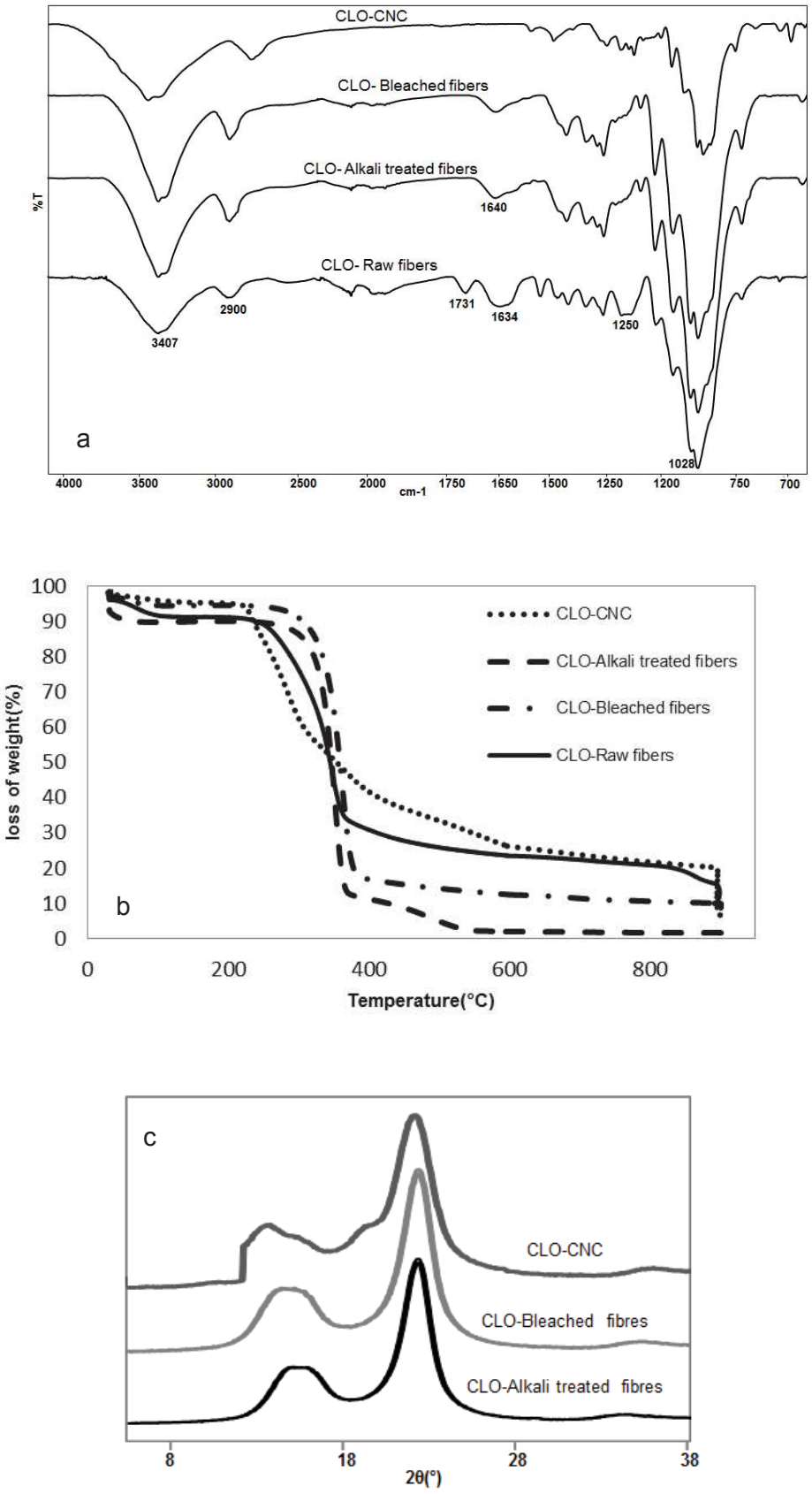

Figure 2. Structural and thermal characterization of raw, unbleached, bleached and acid hydrolysed cellulose from CLO: a) FT-IR, b) TGA, and c) XRD.

2.5.4 Thermogravimetric analysis

The thermal stability of both untreated and chemically treated CLO fibres was characterized using thermogravimetric analysis (TGA). TGA curves corresponding to the weight loss for untreated, alkali treated, bleached, and acid hydrolysed CLO fibres upon continuous heating to 900°C are shown in Figure 2b. Regardless of their treatment an initial weight loss of the fibres is observed below 100°C. It is ascribed to the vaporisation of water associated to the hydrophilic character of lignocellulosic fibres, and this weight drop depends obviously on the initial moisture content of the analysed fibre.

At higher temperatures, a stronger weight drop is observed. When comparing the untreated and alkali treated fibres, it can be concluded that the bleaching treatment results in an increase in the thermal stability. The presence of hemicellulose, lignin, and pectin in the chemical composition of the untreated and alkali treated CLO fibres is responsible for this observation. Indeed, these non-cellulosic materials display a lower decomposition temperature compared to cellulose (Moran, Alvarez, Cyras & Vazquez, 2008) and their progressive removal improves the thermal stability of CLO fibres.

The char residue corresponding the residual weight in the 360-700°C temperature range is around 20-30% for raw fibres, a value significantly higher compared to the alkali treated and bleached fibres. This residual weight is representative of the carbon content in the fibres (Hornsby, Hinrichsen & Tarverdi, 1997). The presence of ash and lignin in the raw fibres results in an increased residue amount at higher temperatures, or char fraction (Ashori, Jalaluddin, Raverty & Mohd Nor, 2006). Indeed, ash doesn't degrade at high temperatures and the pyrolysis of lignin produces more residual char than does the pyrolysis of cellulose (Fahma, Iwamoto, Hori, Iwata & Takemura, 2011).

A significant decrease of the thermal stability is reported after the acid hydrolysis treatment of the fibres. This is ascribed to the surface sulphation resulting from the sulphuric acid treatment (Lin & Dufresne, 2014). A broad range of thermal degradation temperature has been reported for CNC (Dufresne, 2012). It obviously depends on the acid hydrolysis conditions, but also on the specific surface area of the CNC that change the density of sulfate groups (Bettaieb, Khiari, Dufresne, Mhenni & Belgacem, 2015). Moreover, compared to the bleached fibres an increase in the char fraction for CNC compared to the bleached fibres is observed, which is due to the introduction of sulphated groups acting as a flame retardant (Roman & Winter, 2004). The thermal stability of natural fibres is an important parameter to consider for their potential use in the processing of biocomposites.

2.5.5 X-ray diffraction (XRD)

Cellulose has a semi crystalline structure whereas hemicellulose and lignin are fully amorphous materials. X-ray diffraction (XRD) analysis was performed for CLO fibres after the different chemical treatment stages since the crystallinity of cellulose can be affected. The diffraction patterns obtained for alkali treated, bleached, and acid hydrolysed CLO fibres are reported in Figure 2c. Classical patterns for cellulose I with three well-defined crystalline peaks around $2\theta = 16°$, 22°, and 35° and no doublet at $2\theta = 22°$ (Klemm, Heublein, Fink & Bohn, 2005) are obtained.

The crystallinity index was determined using the procedure presented in the Experimental Section. By this method, the crystallinity index was found to be about 52.0%, 68.0% and 78.5 % for alkali treated, bleached and hydrolysed fibres, respectively. The hydrolysis treatment with H_2SO_4 applied to prepare CNC allows removal of amorphous cellulosic domains. Actually, this step consists of the disruption of amorphous regions surrounding and embedding cellulose microfibrils while leaving the microcrystalline segments intact

(Dufresne, 2008; Siqueira, Abdillahi, Bras & Dufresne, 2010). This phenomenon could explain the narrowing of the diffraction peaks. The crystallinity index for CNC prepared from different cellulosic sources ranges between 46 and 96% (Dufresne, 2012). Therefore, the crystallinity index measured for CNC extracted from CLO fibres is within the upper range of values.

2.6. Mechanical properties of nanocomposite films

The appearance of prepared nanocomposites can be seen in Figure 3. A similar visual appearance is reported for both neat and filler containing films. It is a good indication of the homogeneous dispersion of CNC within the polymeric matrix.

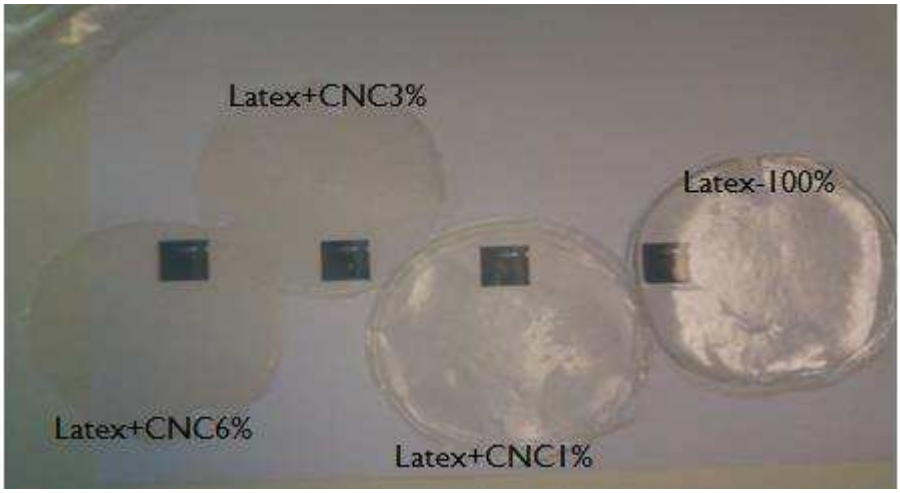

Figure 3. Appearance of the nanocomposite films.

The mechanical properties of nanocomposite films reinforced with CNC extracted from CLO fibres were studied by dynamic mechanical analysis (DMA). Figure 4a shows the evolution of the logarithm of the storage tensile modulus versus temperature in isochronal conditions at a frequency of 1 Hz. The experimental data correspond to the neat matrix and nanocomposite films reinforced with 1, 3 and 6 wt% CLO CNC. The evolution of log (E') corresponding to the unfilled IR matrix was typical of fully amorphous high molecular weight thermoplastic polymers. At low temperatures, the modulus remained roughly constant and it did not

increase with the addition of such low amount of CNC. This may be due to the fact that in this temperature range IR was in the glassy state and the difference between the modulus of the host matrix and the reinforcing phase was not high enough to generate a significant reinforcing effect. Moreover, the sample was soft at room temperature and it was difficult to accurately determine its dimensions. Therefore, the modulus at low temperatures for nanocomposites was normalized to the glassy modulus of the neat matrix.

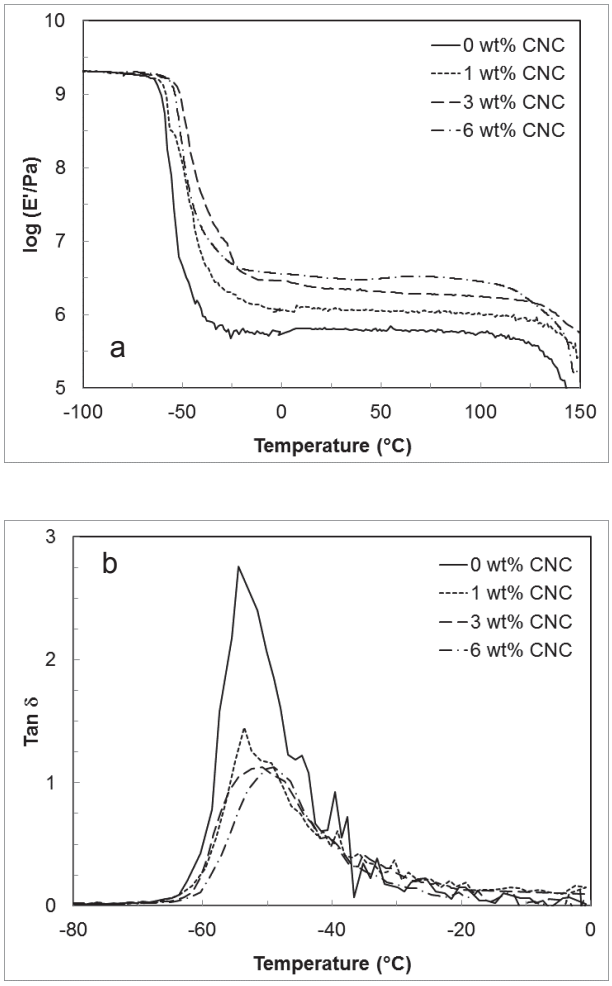

Figure 4. a) Evolution of the logarithm of the storage modulus and b) evolution of the tangent of the loss angle tan δ as a function of temperature for CNC reinforced cariflex-IR rubber nanocomposites.

Then a sharp decrease of log (E') was observed around -55°C. It obviously corresponds to the main relaxation process associated to the glass transition of the polymeric matrix. This

modulus drop is followed by a stabilization over a broad temperature range for which the cohesion of the material is provided by entanglements between the macromolecules (rubbery state). The complete disentanglement of the macromolecules at higher temperatures results in an irreversible modulus drop. It is observed that the rubbery modulus continuously increases as the CNC content increases. This increase is attributed to the reinforcing effect of CNC in the soft rubbery matrix.

Figure 4 b shows the variation of the tangent of the loss angle, tan δ, as a function of temperature for composites with various CNC contents. Tan δ exhibits a maximum around -54.4°C for NR matrix and this peak shifts to higher temperatures with increasing CNC content being , -53°C, -50°C and -49°C, respectively, for CNC1%, CNC3% and CNC6% nanocomposites. This effect could be ascribed to favourable interactions between the cellulose nanofiller and the matrix. Also, the intensity of the relaxation process is lower for composites when compared to neat matrix and it is directly linked to the drop of the elastic tensile modulus during the relaxation process. This can also be ascribed to the decrease of matrix material amount, which is responsible for damping properties, which is possibly an outcome of restriction of molecular mobility of IR polymer chains in the vicinity of CNC.

The nonlinear mechanical behaviour of CLO CNC reinforced nanocomposites was characterized at room temperature. Typical stress-strain curves are shown in Figure 5. These curves clearly show the influence of CNC on the mechanical behaviour of the nanocomposite film. The neat IR matrix and low filler content nanocomposite films exhibit an elastic nonlinear behaviour typical for amorphous polymers at temperature higher than their Tg. The stress shows regular slight increase and remained more or less constant up to the fracture of the film. At higher filler contents, the mechanical behaviour became significantly different. The samples exhibited a stiffer and more brittle behaviour.

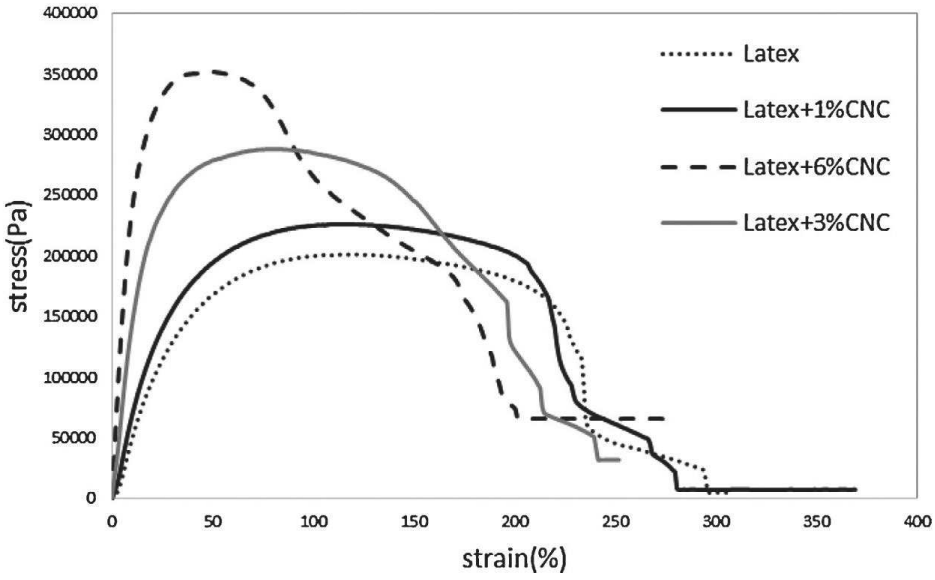

Figure 5. Typical stress-strain curves for CNC reinforced cariflex-IR rubber nanocomposites.

The Young's modulus value was determined from the initial slope of the tensile curves. The mechanical properties derived from these experiments are reported in Table 2. Both the Young's modulus and yield stress value markedly increased when increasing the CNC content whereas the strain at break decreased.

This high reinforcing effect could be assigned as already reported to a mechanical percolation phenomenon of CNC which form a stiff continuous network of cellulosic nanoparticles linked through hydrogen bonding (Azizi Samir, Alloin & Dufresne, 2005; Bras, Hassan, Bruzesse, Hassan, El-Wakil & Dufresne, 2010). This effect was reported to be well predicted from the adaptation of the percolation concept to the classical series-parallel model. Comparison between experimental data and predicted values calculated from the percolation approach can be used to ensure that good dispersion and effective percolation occur. In this model and at sufficiently high temperatures, i.e., when the modulus of the matrix is much lower than the one of the percolating network, the elastic modulus of the composite is simply

Table 2. Yield stress, Young's modulus and yield strain for CNC reinforced cariflex-IR rubber nanocomposites.

Sample	Yield stress (MPa)	Young's modulus (MPa)	Yield strain (%)
IR latex	0.202 ± 0.010	4.8 ± 1.1	113.8 ± 16
IR latex + CNC1%	0.226 ± 0.004	5.7 ± 0.9	108.8 ± 12
IR latex + CNC3%	0.288 ± 0.015	13.4 ± 3.2	62.10 ± 11
IR latex + CNC6%	0.359 ± 0.040	24.6 ± 3.0	46.2 ± 4

the product of the volume fraction and modulus of the rigid percolating network (Dufresne, 2012).

The percolation approach has been used to predict the mechanical performance of CNC reinforced cariflex-IR rubber nanocomposites. The volume fraction of the percolating phase can be calculated from the CNC volume fraction, percolation threshold and critical percolation exponent (0.4 for a 3D network). The percolation threshold was determined from the aspect ratio of CNC and the CNC volume fraction was calculated assuming a density of 0.96 and 1.5 $g.cm^{-3}$ for the polymeric matrix and cellulose, respectively. The calculated percolation threshold for CNC extracted from chili leftover fibres was 2.7 vol%, i.e. around 4.2 wt%. Therefore, only the 6 wt% CNC reinforced nanocomposite film should show a percolation phenomenon. It was also shown that the stiffness of the CNC percolating network increases when increasing the aspect ratio of the nanoparticles (Bras, Viet, Bruzzese & Dufresne., 2011). Similar observation was reported when comparing the mechanical properties of poly(vinyl acetate) reinforced with CNC extracted from cotton (aspect ratio around 10) and tunicin (aspect ratio around 67) (Shanmuganathan, Capadona, Rowan& Weder., 2010). From this earlier report (Bras et al., 2011) that showed the evolution of the stiffness of the network as a function of the constitutive CNC and from the aspect ratio of CNC extracted from chili leftover fibres, it can be assumed that the modulus of the

percolating network should be around 3 GPa. Figure 6 shows the evolution of the modulus for the nanocomposite films as a function of the CNC volume content. Both predicted data and experimental rubbery moduli estimated derived from tensile tests are reported. Below the percolation threshold, the modulus cannot be estimated from the model and the value corresponding to the neat matrix was adopted. It can be clearly observed from this figure that CNC percolation is effectively achieved for the 6 wt% CNC reinforced nanocomposite film.

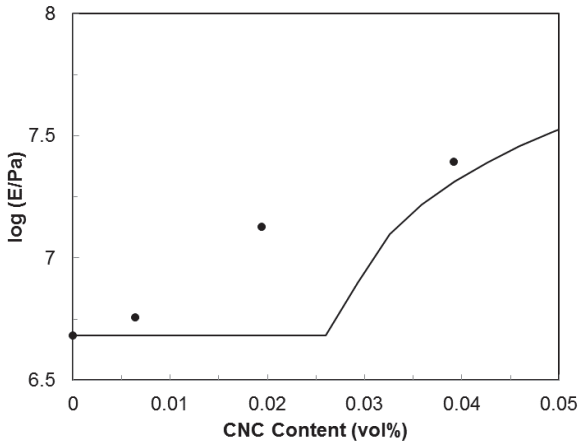

Figure 6. Evolution of the logarithm of the tensile modulus versus CNC content: experimental data (●), and predicted data from the percolation approach (solid line).

2.7 Morphological investigation of nanocomposite films

Chili CNCs were used with IR latex to prepare nanocomposites by casting/evaporation. The prepared films were homogeneous in visual appearance (Figure 1). The cross-section of the current composites did not show any evidence of gradient formation or aggregate (Fig. 6a-d). The cast nanocomposites usually showed a tendency to develop a gradient of CNC concentration between the upper and lower faces of the film resulting in less homogeneous materials with CNCs randomly oriented in horizontal planes. The CNCs in the nanocomposites prepared during this study seem to be randomly oriented and distributed homogeneously throughout the matrix which can be attributed to the processing method used.

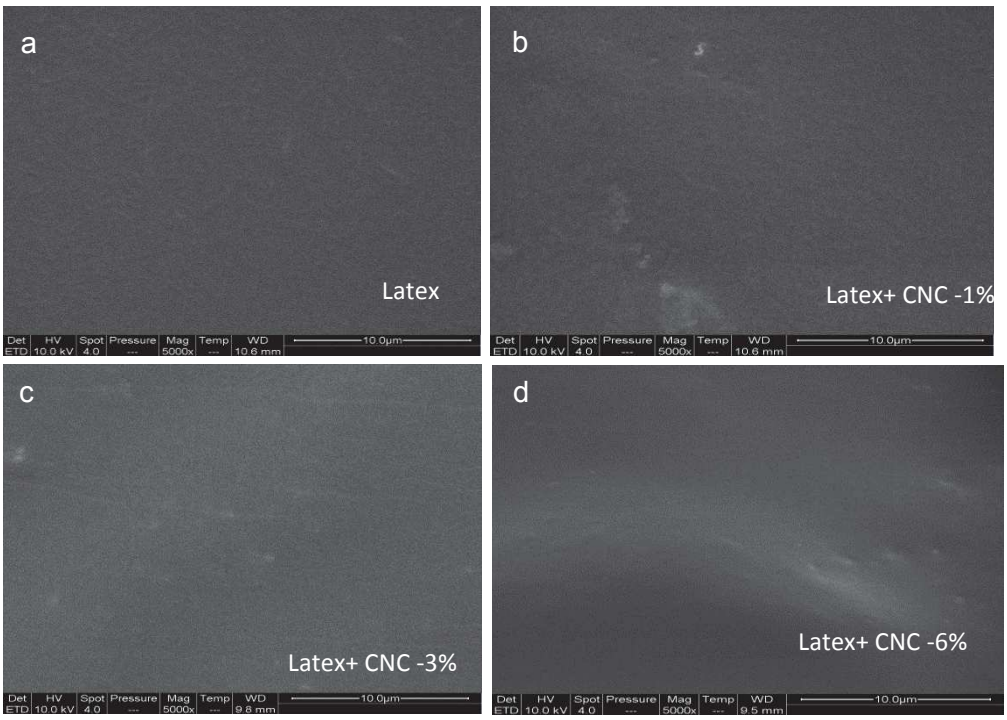

Figure 6. SEM images of the cross section for CNC reinforced cariflex-IR rubber nanocomposites.

2.8 CONCLUSION

Cellulose nanocrystals (CNCs) were successfully extracted from chili fibres by acid hydrolysis. Unusual low lignin content was found for these fibres compared to other annual plants making them highly suitable for the extraction of cellulose and preparation of CNCs. Ensuing rod-like nanoparticles had a diameter of 4-6 nm and length of 90-180 nm, showing an aspect ratio around 26. They were used as the reinforcing phase in commercial cariflex IR latex. The morphological observation of these bio based nanocomposites showed that the CNCs were well dispersed in IR matrix without microscale aggregation. Dynamic mechanical thermal studies showed increased storage modulus indicating good interaction between CNC and IR latex. The tensile strength and modulus values increased with CNC addition, accompanied by a moderate decrease in yield strain.

2.9 REFERENCES

Ahmad, I, Mosadeghzad, Z, Daik, R, Ramli, A. (2008). The effect of alkali treatment and filler size on the properties of sawdust/ UPR composites based on recycled PET wastes. *Journal of Applied Polymer Science*, *109*, 3651-3658.

Alemdar, A., Sain, M. (2008). Isolation and characterization of nanofibres from agricultural residues-wheat straw and soy hulls. *Bioresource Technology*, *99*, 1664-1671.

Angellier, H., Molina-Boisseau, S., Lebrun, L., Dufresne, A. (2005). Processing and structural properties of waxy maize starch nanocrystals reinforced natural rubber. *Macromolecules, 38*, 3783-3792.

Angellier, H., Molina-Boisseau, S., Dufresne, A. (2005). Mechanical properties of waxy maize starch nanocrystals reinforced natural rubber. *Macromolecules, 38*, 9161-9170.

Ashori, A., Jalaluddin, H., Raverty, W.D., Mohd Nor, M.Y. (2006). Chemical and morphological characteristics of Malaysia cultivated kenaf (Hibiscus cannabinus) fibre. *Polymer-Plastics Technology and Engineering*, *45*, 131-134.

Azizi Samir, M.A.S., Alloin, F., Dufresne, A. (2005). Review of recent research into cellulosic whiskers, their properties and their application in nanocomposite field. *Biomacromolecules*, *6*, 612-626.

Bendahou, A., Habibi, Y., Kaddami, H., Dufresne, A. (2009). Physico-chemical characterization of palm from *Phoenix Dactylifera* – L, preparation of cellulose whiskers and natural rubber–based nanocomposites. *Journal of Biobased Matererials and Bioenergy, 3*, 81-90.

Bendahou, A., Kaddami, H., Dufresne, A. (2010). Investigation on the effect of cellulosic nanoparticles' morphology on the properties of natural rubber based nanocomposites. *European Polymer Journal, 46*, 609-620.

Bendahou, A., Kaddami, H., Espuche, E., Gouanvé, F., Dufresne, A. (2011). Synergism effect of montmorillonite and cellulose whiskers on the mechanical and barrier properties of natural rubber. *Macromoleculat Materials and Engineering, 296*, 760-769.

Bettaieb, F., Khiari, R., Dufresne, A., Mhenni, M.F., Belgacem, M.N. (2015). Mechanical and thermal properties of *Posidonia oceanica* cellulose nanocrystal reinforced polymer. *Carbohydrate Polymers, 123*, 99-104.

Blackley, D.C. (1997). Polymer Latices, Science and Technology. Volume 3: Applications of Latices, 2nd edition, Chapman and Hall, London, p. 156.

Bledzki, A.K., Gassan, J. (1999). Composites reinforced with cellulose based fibres. *Progress in Polymer Science, 24*, 221-274.

Bras, J., Hassan, M.L., Bruzesse, C., Hassan, E.A., El-Wakil, N.A., Dufresne, A. (2010). Mechanical, barrier, and biodegradability properties of bagasse cellulose whiskers reinforced natural rubber nanocomposites. *Industrial Crops and Products*, *32*, 627-633.

Bras, J., Viet D., Bruzzese C., Dufresne A. (2011). Correlation between stiffness of sheets prepared from cellulose whiskers and nanoparticles dimensions. *Carbohydrate Polymers*, *84*, 211-215.

Buschle-Diller G, Zeronian SH (1992). Enhancing the reactivity and strength of cotton fibers. *Journal of Applied Polymer Science*, *45*, 967-979.

de Mesquita, J.P., Donnici, C.L., Pereira, F.V. (2010). Biobased nanocomposites from layer-by-layer assembly of cellulose nanowhiskers with chitosan. *Biomacromolecules*, *11*, 473-480.

Dufresne, A. (2008). Polysaccharide nanocrystals reinforced nanocomposites. *Canadian Journal of Chemistry*, *86*, 484-494.

Dufresne, A. (2012). *Nanocellulose: From Nature to High- Performance Tailored Materials*, Berlin/Boston: de Gruyter.

Fahma, F., Iwamoto, S., Hori, N., Iwata, T., Takemura, A. (2011). Effect of pre-acid-hydrolysis treatment on morphology and properties of cellulose nanowhiskers from coconut husk. *Cellulose, 18*, 443-450.

Filho, P.A., Badr, O. (2004). Biomass resources for energy in North-Eastern Brazil. *Applied Energy*, *77*, 51-67.

Gopalan Nair, K., Dufresne, A. (2003a). Crab shells chitin whiskers reinforced natural rubber nanocomposites. 1. Processing and swelling behavior. *Biomacromolecules, 4*, 657-665.

Gopalan Nair, K., Dufresne, A. (2003b). Crab shells chitin whiskers reinforced natural rubber nanocomposites. 1. Mechanical behavior. *Biomacromolecules, 4*, 666-674.

Hornsby, P.R., Hinrichsen, E., Tarverdi, K. (1997). Preparation and properties of polypropylene composites reinforced with wheat and flax straw fibers. Part I. Fiber characterization. *Journal of Materials Science*, *32*, 443-449.

Jonoobi, M., Harun, J., Shakeri, A., Misra, M., Oksman, K. (2009.) Chemical composition, crystallinity, and thermal degradation of bleached and unbleached kenaf bast (*Hibiscus cannabinus*) pulp and nanofibres. *Bioresources*, *4*, 626-639.

Klemm, D., Heublein, B., Fink, H.-P., Bohn, A. (2005). Cellulose: fascinating biopolymer and sustainable raw material. *Angewandte Chemie International Edition*, *44*, 3358-3393.

LeCorre, D.S., Bras, J. & Dufresne, A. (2012). Influence of starch nanocrystals' botanic origin on morphological and mechanical properties of natural rubber nanocomposites. *Macromolecular Materials and Engineering, 297*, 969-978.

Lin, N., Dufresne, A. (2014). Surface chemistry, morphological analysis and properties of cellulose nanocrystals with gradient sulfation degrees. *Nanoscale*, *6*, 5384-5393.

McLeod, M.J., Eshbaugh, W.H., Guttman, S. I. (1979). A preliminary biochemical systematic study of the genus *Capsicum-Solanaceae. In* J. G. Hawkes, R. N. Lester, and A. D. Skelding, ed, The Biology and Taxonomy of the Solanaceae. Academic Press, NewYork, pp. 701-713.

Mélé, P., Angellier-Coussy, H., Molina-Boisseau, S., Dufresne, A. (2011). Reinforcing mechanism of starch nanocrystals in a non-vulcanized natural rubber matrix. *Biomacromolecules, 12*, 1487-1493.

Moran, J.I., Alvarez, V.A., Cyras, V.P., Vazquez, A.(2008). Extraction of cellulose and preparation of nanocellulose from sisal fibers. *Cellulose*, *15*, 149-159.

Pasquini, D., Teixeira, E.M., Curvelo, A.A.S., Belgacem, M.N., Dufresne, A. (2010). Extraction of starch nanocrystals and cellulose whiskers from cassava bagasse and their applications as reinforcing agent in natural rubber. *Industrial Crops and Products, 32*, 486-490.

Razera, I.A.T., Frollini, E. (2004). Composites based on jute fibers and phenolic matrices: properties of fibers and composites. *Journal of Applied Polymer Science, 91*, 1077-1085.

Roman, M., Gray, D.G. (2005). Parabolic focal conics in self-assembled solid films of cellulose nanocrystals. *Langmuir, 21*, 5555-5561

Roman, M., Winter, W.T. (2004). Effect of sulfate groups from sulfuric acid hydrolysis on the thermal degradation behaviour of bacterial cellulose. *Biomacromolecules*, *5*, 1671-1677.

Sain, M, Panthapulakkal, S. (2006). Bioprocess preparation of wheat straw fibres and their characterization. *Industrial Crops and Products, 2*, 1-8.

Satyanarayana, K.G., Wypych, F. (2007). Characterization of natural fibers. In: Fakirov S, Bhattacharyya D (eds)Handbook of engineering biopolymers: homopolymers, blends and composites. Carl Hanser Verlag, Munchen, pp. 4-47.

Shanmuganathan, K., Capadona, J.R., Rowan, S.J., Weder, C. (2010). Bio-inspired mechanically-adaptive nanocomposites derived from cotton cellulose whiskers. *Journal of Materials Chemistry*, *20*, 180-186.

Shrinath, A., Tschirner, U., Ramaswamy, S. (2003). Economics and feasibility of a greenfield cereal straw market pulp mill. *Pulp Paper Canada*, *104*, 34–37.

Siqueira, G., Abdillahi, H., Bras, J., Dufresne, A. (2010). High reinforcing capability cellulose nanocrystals extracted from *Syngonanthus nitens* (Capim Dourado). *Cellulose*, *17*, 289-298.

Siqueira, G., Tapin-Lingua, S., Bras, J., da Silva Perez, D., Dufresne, A. (2011). Mechanical properties of natural rubber nanocomposites reinforced with cellulosic nanoparticles obtained from enzymatic and acid hydrolysis of sisal fibers. *Cellulose*, *18*, 57-65.

Troedec, M., Sedan, D., Peyratout, C., Bonnet, J., Smith, A., Guinebretiere, R., Gloaguen, V., Krausz, P. (2008). Influence of various chemical treatment on the composition and structure of hemp fibres. *Composites Part A*, *39*, 514-522.

Zuluaga, R., Putaux, J.L., Velez, J., Mondragon, I., Gañán P. (2009). Cellulose microfibrils from banana rachis: effect of alkaline treatments on structural and morphological features. *Carbohydrate Polymers, 76*, 51-59.

Chapter-3

Surface modification of CNC

Ionic compatibilization of cellulose nanocrystals with quaternary ammonium salt and their melt extrusion with polypropylene.

(ACS applied materials and interfaces 2016, 8, 8755-8764)

Chapter-3: Ionic compatibilization of cellulose nanocrystals with quaternary ammonium salt and their melt extrusion with polypropylene.

ENGLISH ABSTRACT

On account to their high mechanical properties along with high reinforcing capacity, cellulose nanocrystals (CNCs) could be the ultimate choice for polymer nanocomposites as filler. Recently, different strategies are reported for the melt extrusion of CNC based polymer nanocomposites since it is a solvent free process and also this technique is more viable for commercial industrialization. However, most thermoplastic polymers are processed at high temperatures and sulfuric acid-prepared CNC limits the processing due to surface sulfate groups degradation. In this study we profitably used these negatively charged groups and quaternary ammonium salt was ionically adsorbed on CNC by a simple aqueous method. The adsorbed CNC was characterized by Fourier transform infrared spectroscopy (FTIR), thermogravimetric analysis (TGA), X-ray diffraction (XRD), and also the hydrophobic nature and surface charge was measured by using contact angle and zeta sizer. The modified CNC (M-CNC) was extruded with polypropylene (PP) at 190°C and the ensuing composites were characterized to investigate their mechanical, thermal and morphological properties using dynamic mechanical analysis (DMA), differential scanning calorimetry (DSC), tensile tests and scanning electron microscopy (SEM). The melt rheology of PP based nanocomposites was also reported.

RESUME FRANÇAIS

Du fait de leurs propriétés mécaniques élevées et de leur grande capacité de renfort, les nanocristaux de cellulose (CNCs) pourraient représenter le choix ultime de charge dans les nanocomposites polymères. Récemment, différentes stratégies ont été décrites pour l'extrusion à l'état fondu de nanocomposites polymères à base de CNC. L'extrusion présente l'intérêt d'être un procédé sans solvant, compatible avec une utilisation à grande échelle et notamment à l'échelle industrielle. Cependant, la plupart des polymères thermoplastiques sont mis en forme à des températures élevées alors que les CNC, préparés par hydrolyse acide, contiennent en surface des groupements sulfates, sensibles à la dégradation thermique. Dans cette étude, nous avons justement mis à profit ces groupements sulfates, chargés négativement, pour les faire réagir avec un sel d'ammonium quaternaire, en milieu aqueux, en tirant parti de l'absorption ionique à la surface des CNC. Les CNC adsorbés ont été caractérisés par spectroscopie infrarouge à transformée de Fourier (FTIR), analyse thermogravimétrique (TGA) et diffraction des rayons X (XRD). Le caractère hydrophobe des surfaces obtenues a été évalué par des mesures d'angle de contact et par mesure de potentiel zeta. Les CNC ainsi modifiés ont ensuite été incorporé à une matrice polypropylène (PP) et le mélange a été extrudé à 190 ° C. Les composites obtenus sont ensuite caractérisés par leurs propriétés mécaniques, thermiques et morphologiques en réalisant des essais de traction, en utilisant l'analyse mécanique dynamique (DMA), la calorimétrie différentielle à balayage (DSC) et la microscopie électronique à balayage (SEM). Le comportement en écoulement de ces composites a également été caractérisé par des mesures de rhéométrie.

3.1 INTRODUCTION

The use of nanomaterials as reinforcing phase into polymers to form nanocomposites has attracted attention because these materials generally allow to increase the mechanical properties even at low filler content.[1] Nano reinforcing materials, such as hydroxyapatite,[2] nano clays,[3-7] carbon nanotubes[8-11] and reduced graphene oxide[12] have been broadly studied. However, most of them are not biodegradable,[1] and during the last decade the interest for nanomaterials issued from renewable resources has been increased. Cellulose nanocrystals (CNCs) extracted from natural plant fiber by strong acid hydrolysis are probably the most interesting nanomaterials for strengthening the properties of nanocomposites.[13-15]

However, the recent industrial-scale production of CNC as a commercial grade needed most feasible process for industries like melt extrusion, which is the most common process to produce thermoplastic polymer composites, is a highly viable and solvent-free process but relatively infrequent for the fabrication of polymer nanocomposites with CNC as reinforcing phase, since CNC have some major difficulties like instability at higher temperatures. Mainly the hydrophilic behavior of CNC are forming microscale aggregates on subsequent drying and their incompatibility with hydrophobic polymer matrices causes to form excess hydrogen bonds among the nanocrystals. Importantly the CNC prepared by acid hydrolysis with sulfuric acid is not stable at high temperature.[16, 17] altogether these problems are limiting the melt extrusion process for the polymer nanocomposites based on CNC. Whereas the solvent casting method was used in majority even if not well-suited for industries.[18]

The surface functionalization of CNC is a possible solution to evade the micro scale aggregation after drying as well in hydrophobic matrices.[19-21] towards the development of various applications, different approaches have been attempted to increase the dispersion in nonpolar matrices.[22] The surface functionalization of CNC reported by using radical

polymerization.[23-26] few studies reported on the surface grafting like alkyne, azide and amine groups [27-29] and further these functional groups allow for derivatization or click chemistry. The covalent bond can be attained by isocynate reaction. [30, 31] acid halides[23,25,26] and acid anhydrides.[32] the chemical bonding approaches are required huge amounts of organic solvents and it is deadly process to exchange organic solvents from aqueous medium more over it is not viable process for commercial industries. Moreover this strategy is hardly possible for industry since it involves an organic solvent process.[33]

The main aim of this study was to progress the green process such as aqueous based surface modification using quaternary salts through strong electrostatic interactions. Few studies have been previously reported on surfactant modification of CNC, despite of different purpose.[34-37] Recently, investigation of CNC Pickering emulsions charged with surfactant was described.[38] The preparation of surfactant-modified CNC reinforced polylactic acid (PLA) nanocomposites was also reported but it was shown that the surfactant had a negative effect such as polymer chain degradation of the PLA.[39]

In the present study a comprehensive investigation of surfactant-coated CNC reinforced polypropylene composites prepared by melt extrusion was addressed. This type of material could find potential applications as automotive parts, sailing dinghies, packaging, etc. In order to strengthen the interactions between CNC and adsorbed molecules, the sulfate groups borne on CNCs were profitably used. Quaternary ammonium cations bearing long alkyl groups were used to modify the surface by a chemical-free method which is more compatible for industrial applications. The dispersibility of modified CNCs in organic solvents was studied and their surface charge was measured. They were also characterized using atomic force microscopy (AFM), Fourier transform infrared spectroscopy (FTIR), X-ray diffraction (XRD) and thermogravimetric analysis (TGA). The hydrophobic nature of M-CNC was

demonstrated by using contact angle. The modified CNCs prepared by this water-based method were used for melt extrusion with high molecular weight polypropylene matrix and the thermal, mechanical, morphological and rheological properties of ensuing nanocomposites were investigated.

3.2 Experimental Methodology

3.2.1 Materials

Sodium hydroxide (sigma Aldrich) and hexadecyl trimethyl ammonium bromide (Sigma Aldrich) was used. Commercial grade cellulose nanocrystals (CNCs) were procured from university of Maine, USA, as 11.5 wt% suspension. Elemental analysis showed that the sulfur content was 1.1 wt% and the surface half ester groups per 100 bulk glucose units was 5.65 by using the following equation $C_6H_{10}O_5$-$(SO_3)_n$ as described elsewhere.[40] The surface charge density was -36.15 mV (Zetasizer measurement). Polypropylene (PP) with a density 0.960 $g.cm^{-3}$ and a weight average molecular weight 337,000 $g.mol^{-1}$ was used to produce the polymer nanocomposites.

3.2.2 Methods

Zeta Potential Measurements

The surface charge density was measured by using the Malvern Instruments Zetasizer ZEN-2600 zeta sizer.

Atomic force microscopy (AFM)

AFM observations were performed to study the diameter and approximate length of individual nanocrystals using a Nanoscope III (Veeco). CNC samples were previously diluted to a concentration of 0.01 wt% and a drop of the suspension was placed on mica plate which

was allowed to dry at room temperature and each sample was analysed by tapping mode (OTESPA®, Bruker). At least 10 different locations were analyzed to obtain representative measurements. CNC diameter was determined from height profile of height sensor images.

Fourier transform infrared spectroscopy (FTIR)

FTIR analysis was done by means of a Spectrum 65 spectrometer (PerkinElmer) on dried CNC obtained by freeze drying for 24 h, in order to determine the functional groups present in the CNC. The samples were analyzed by attenuated total reflectance (ATR) in which the sample was placed on the evanescent wave on the ATR crystal, through which infrared beam gives the data to the detector.

Thermogravimetric analysis (TGA)

Thermal degradation of the samples was monitored by TGA using a simultaneous thermal analyzer (STA) 6000 (PerkinElmer, USA). The weight loss and dTG curves were obtained for a 20 mg sample at a heating rate of 10°C.min^{-1} in the temperature range of 30-950°C under oxidizing atmosphere (air).

X-ray diffraction (XRD)

Wide angle XRD analysis was performed on dried CNC/M-CNC and were stored at well controlled humidity. The CNC/M-CNC were deposited in a 2.5mm cell and measurements were performed with a diffractometer (X' Pert PROMPD®, PAN analytical) attached to detector. The operating conditions of the refractometer were: copper Kα radiation (λ = 1.5418 Å), 2θ (Bragg angle) between 2 and 56°, step size 0.067°, counting time 90 s. Each sample was measured once.

Contact angle measurements

The hydrophobic nature of CNC/M-CNC was measured by using the contact angle and all these measurements were done at room temperature.

Nanocomposite processing

Extrusion was used to prepare PP nanocomposite films reinforced with various filler contents. The polymer matrix (PP) and freeze-dried CNC were first mixed and introduced in the mixing chamber of a twin-screw DSM Micro 15 compounder. Around 15 g of material was used and the mixing conditions were 190°C at 150 rpm for 8 min. The outlet of the extruder was attached to the 0.6mm slit die with one centimeter length. PP nanocomposites were prepared with modified CNC (M-CNC) at 1, 3, 6 and 10 wt%, and unmodified nanocrystals at 3 wt% were used to compare the results.

Visible light transmittance

The transparency of the prepared composites were analysed by using shimadzu uv2401 uv vis spectrometer within the range of 200-800nm. The transmittance spectra were acquired using air as background. The resolution of the spectrophotometer was 1.5 nm and the photometric accuracy was ±0.01 in absorption.

Dynamic mechanical analysis (DMA)

DMA was used to study the viscoelastic behavior of the nanocomposites. DMA experiments were carried out using a RSA3 (TA Instruments, USA) equipment working in the tensile mode. The storage modulus E′ (elastic response) of the materials was measured as a function of temperature as it was deformed under an isochronal oscillatory stress at a controlled temperature in a specified atmosphere. The storage modulus is related to stiffness. Varying

stress with a frequency of 1 Hz was applied when heating the sample from -30 to 100°C with a ramp rate equal to 3°C.min^{-1}. The length of the sample was 10 mm.

Tensile tests

The tensile high-strain mechanical tests were performed using a RSA3 (TA Instruments, USA) with a load cell of 100 N. Sample dimensions were 4-5 mm and 20 mm for width and length, respectively, and the gap between pneumatic jaws at the start of each test was adjusted to 10 mm. Before analysis the samples were stored overnight in desiccators containing silica gel. All experiments were carried out at room temperature (25°C) with a cross-head speed of 3 mm .min^{-1}.

Differential scanning calorimetry (DSC)

The thermal behavior of nanocomposites was studied by DSC. The melting of nanocomposites was investigated with a Perkin-Elmer DSC instrument using aluminum pans. The samples were scanned from -30 to 200°C at a heating rate of 10°C.min^{-1}.

Scanning Electron Microscopy (SEM)

SEM was used to observe the nanocomposite cross section in order to check the possible filler aggregation. Prior to this, the samples were frozen using liquid nitrogen and broken to obtain a clear fracture (the polymer was in the glassy state T << Tg). It was glued to the sample holder for cross section images. The samples were coated with gold in order to prevent the charring of the sample due to the electron bombardment. The SEM images were captured by using FEI (MED) Quanta200.

Melt rheology

The viscoelastic behavior of the nanocomposites was analyzed by a dynamic oscillatory rheometer in the melt state from 0.1 to 100 rad.s^{-1}. A controlled strain rheometer (ARES, Advanced Rheometric Expansion System, and Rheometric Scientific) equipped with 25 mm diameter parallel plate geometry was employed for the rheological tests. Samples were directly loaded and molded between the plates and rheological tests were carried out at 180°C with a gap distance of 1 mm under nitrogen atmosphere.

3.3 RESULTS AND DISCUSSION

In this Section, the surface modification of CNC will be first described and then the structural, functional, surface, and thermal properties for both modified and unmodified CNCs will be reported. Thereafter, the characterization of polypropylene composites reinforced with these cellulosic nanomaterials will be presented.

3.3.1 Modified CNC by using QS

As shown scheme-1 the quaternary salt (QS) hexadecyl trimethyl ammonium bromide was utilized to form electrostatic interactions with sulfonated groups on the surface of CNC. previously reported procedure was used.[41] 5g of CNC were dispersed in aqueous medium and their PH was adjusted to 10 by using NaoH and then CNC mixture was slowly added to the 500mg of quaternary salt at 40 C i.e. the ratio of salt to CNC was 10wt%. The reaction mixture (R.M) was continued stirring at 40°C for 3 h, and the temperature maintained constant since the sulfate groups are sensitive to the alkali conditions at high temperatures and then the reaction mixture was stirred at room temperature and the RM was dialyzed in order to remove the unabsorbed QS and also NaBr formed during reaction. The RM was

freeze dried before extrusion with PP. Unmodified CNC and CNC modified with quaternary ammonium salt will be denoted as CNC and M-CNC, respectively.

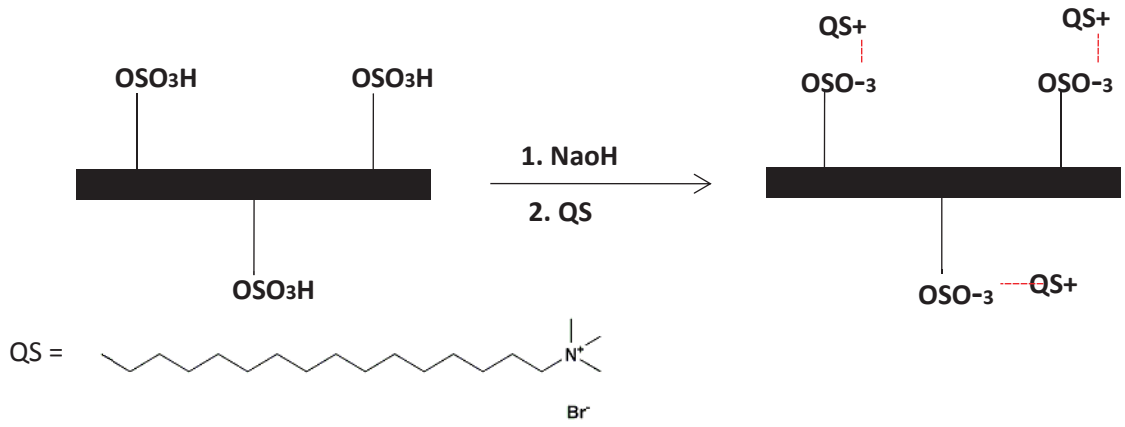

Scheme 1. Reaction of cellulose nanocrystals with quaternary ammonium salt.

3.3.2 Surface charge measurements

The surface charge of modified and unmodified CNC was measured and ζ-potential values were determined. The surface charge of unmodified CNC was -36.15mV due to the negatively charged sulfate groups induced by the sulfuric acid treatment.[17] After surface modification the CNC showed a +6.09 mV ζ-potential value since the surface charge was neutralized by QS and positive charge is due to the non-adsorbed quaternary salt.

3.3.3 Dispersion of modified CNC in organic solvents

A simple and valuable experiment to evidence the successfulness of the surface modification was conducted through wettability tests. The dialyzed final suspension of M-CNC was freeze-dried and redispersed in different organic solvents like toluene, chloroform and ethyl acetate (1 wt%) using an ultrasonic treatment for 1 min. Photographs of these suspensions can be seen in Figure 1. Figure 1a shows unmodified CNC in a solvent system composed of water and chloroform. These two liquids are immiscible and the upper phase corresponds to water (density = 1 g.cm^{-3}) whereas the lower phase corresponds to chloroform (density = 1.49

g.cm^{-3}). It is clearly observed that unmodified CNC displays a higher affinity for polar solvents such as water and migrates to the aqueous phase due to their hydrophilic nature. Figure 1b shows that on the contrary M-CNC migrates to the chloroform phase. Figure 1c shows M-CNC in toluene, ethyl acetate and chloroform (from left to right). A good dispersion is observed suggesting the lower polar nature of the nanocrystal surface after chemical modification. Similar results were obtained in previous work.[33, 42]

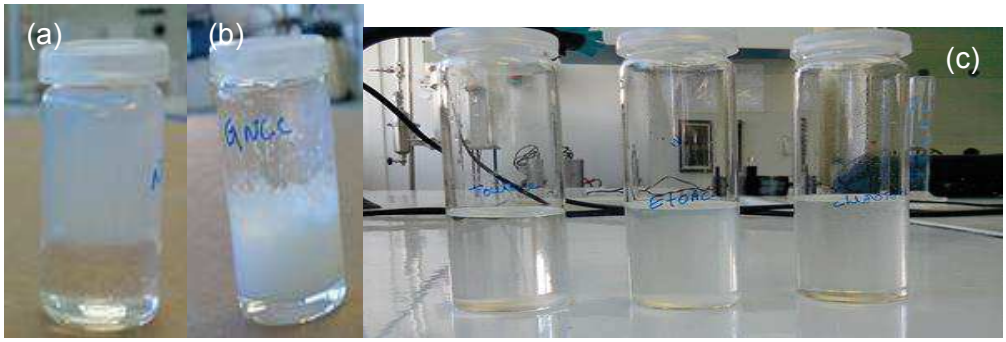

Figure 1. Wettability tests: (a) unmodified CNC and (b) CNC modified with quaternary ammonium salt (M-CNC) in a solvent system composed of chloroform (lower phase) and water (upper phase), and (c) M-CNC dispersed in toluene, ethyl acetate and chloroform (from left to right).

3.3.4 Atomic force microscopy

The structural morphology of modified and unmodified CNC was investigated by means of AFM. The CNCs used in this study were of commercial grade and produced from wood pulp. Figure 2a shows an AFM image of these CNCs. The length and diameter of the nanorods are in the range of 24-195 nm and 2-9 nm, respectively. The modified CNCs can be seen in Figure 2c. The length and diameter of the M-CNC increased by 3-5 nm and 10 nm, respectively. This is ascribed to the surface adsorption of the quaternary salt which size is around 2-8 nm as can be seen in figure 2b. These values are consistent with surfactant layer of 15 Å thickness reported when coating CNC with phosphoric ester of poly(ethylene oxide) (9) nonyl phenyl.[35]

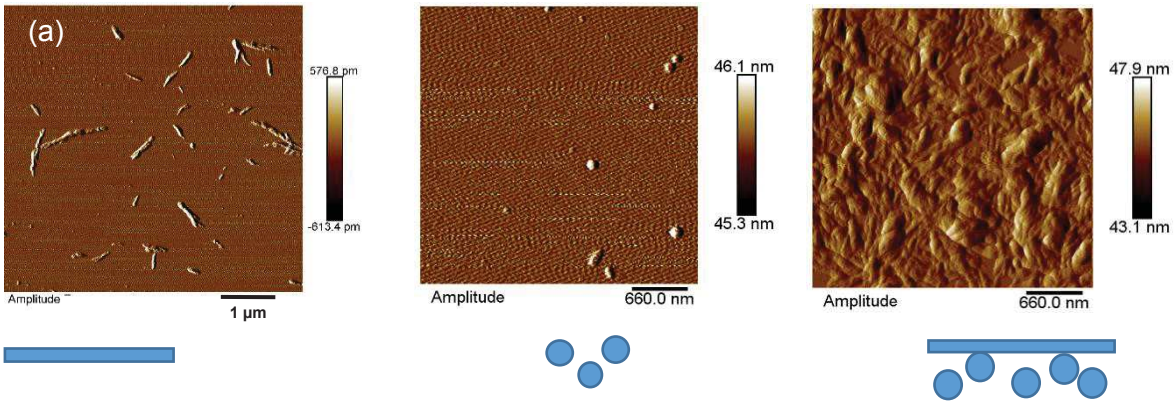

Figure 2. AFM images for (a) unmodified CNC, (b) quaternary salt, and (c) modified CNC.

3.3.5 FT-IR

FTIR spectroscopy was used to check the functional properties of both neat and modified CNC. Figure 3 shows FTIR spectra obtained for neat CNC and M-CNC. Before the chemical treatment CNC displays several bands characteristic of cellulose at 3350 cm^{-1} (O–H), 2868 and 2970 cm^{-1} (C–H from –CH2–). For M-CNC a substantial increase of the bands at 2868 and 2970 cm^{-1} corresponding to asymmetric and symmetric –CH2 – stretches from fatty chain was observed.[43] The signal associated with the vibration of adsorbed water at 1650 cm^{-1} strongly decreased after modification, probably because of the hydrophobic behavior of the modified material and a new band at 1480 cm^{-1}, [33] corresponding to the trimethyl groups of the quaternary ammonium can be identified for the modified CNC sample.

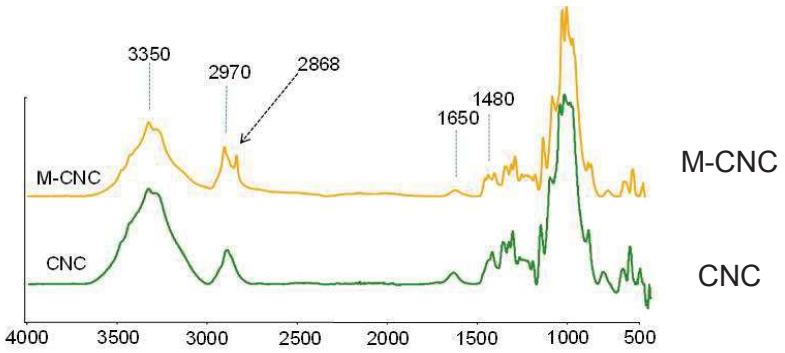

Figure 3. FTIR spectra for unmodified CNC and CNC modified with quaternary ammonium salt bearing long alkyl chain (M-CNC).

3.3.6 TGA

The thermal stability of CNC and modified CNC was analyzed by using TGA. Initially small loss of weight was observed for CNC which is due to the moisture presence in CNC. There after continuous weight loss was noted from 200-600°C this can be easily predict that is because of sulfate groups acquired from sulfuric hydrolysis.[16,17] The weight loss around 200°C is related to more accessible sulfate groups in amorphous cellulose regions. The weight loss around 400-600°C is corresponding to the breakdown of crystalline regions of unsulphated cellulose. The thermal stability is always depends on the number sulfated groups attained from acid hydrolysis.[44]

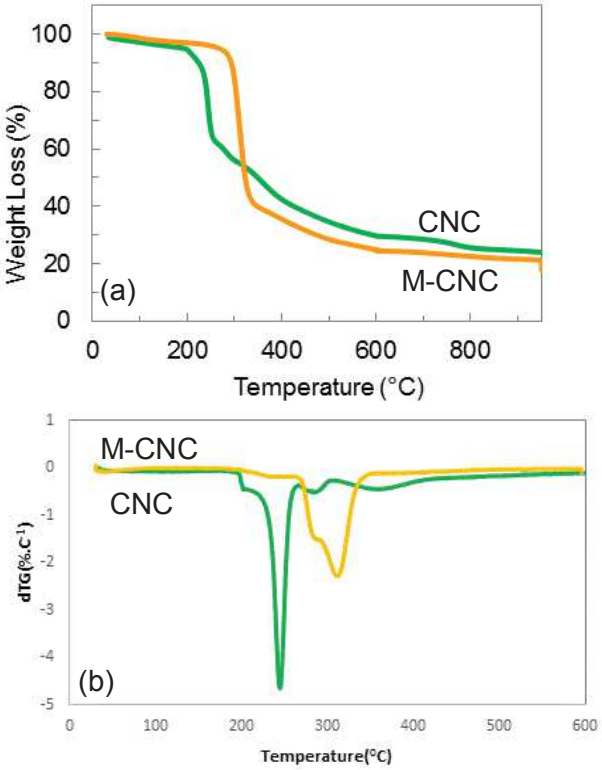

Figure 4. (a) TGA spectra, and (b) dTG curves for unmodified CNC and CNC modified with quaternary ammonium salt bearing long alkyl chain (M-CNC).

For M-CNC, the thermal degradation behavior is significantly different and the temperature values associated to different relative weight loss values for neat and modified CNC have been reported (see Table 1). The low temperatures weight loss is less pronounced for M-CNC compared to CNC, this is because of the hydrophobic nature of the material. Moreover, the degradation temperature is increased highly compared to the neat CNC and this might be due to the strong electrostatic adsorption of the QS on the surface of CNC and the long aliphatic chains of QS were covered the sulfated groups present on CNC. It should improve the thermal stability and it will help to process the PP-nanocomposites by using M-CNC. Also, it is interesting to see that the char residue is lower for M-CNC than for CNC. Indeed, it was shown that the surface of CNC contains the more number of sulfated groups which caused for more charred residue at 350°C.[16]

Table 1. The loss of weight values at different temperature for neat CNC and CNC modified with quaternary ammonium salt (M-CNC).

Sample	Temperature (°C) at different relative weight loss			
	10%	20%	40%	60%
CNC	227	238	271	426
M-CNC	292	303	314	361

The relative dTG curves corresponding to CNC and M-CNC are shown in Figure 4b and they clearly indicate that the main degradation temperature for CNC is lower than for M-CNC. It shows further that the surface of CNC is modified with the quaternary salt.

3.3.7 XRD

The crystalline structure of CNC plays a vital role in their reinforcing effect and it should be well-maintained even after modification. The crystalline structure of CNC and M-CNC were

studied by means of XRD. The diffraction patterns for both modified and neat CNC are shown in Figure 5. The diffraction peaks appearing at 22.6°, 14.8°, 16.4°, and 34.4° were related to the typical cellulose I.[45,46] The intensity of the 16.4° peak was slightly increased (see expanded view in Figure 5) after modification which is due to the surfactant adsorption. It is indicating that surface modification has no impact on the crystalline structure of modified cellulose nanocrystals and that surfactant modification is only on the surface of CNC, as expected.

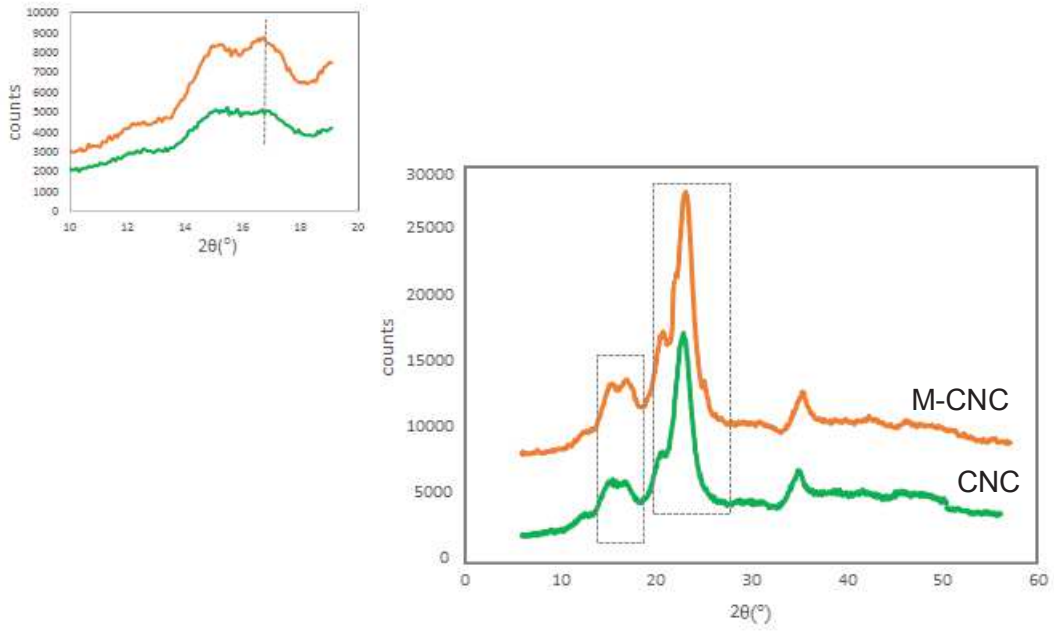

Figure 5. The XRD patterns for unmodified CNC and CNC modified with quaternary ammonium salt bearing long alkyl chain (M-CNC).

3.3.8 Contact angle

Contact angle measurements were done to estimate the hydrophobic nature of modified nanocrystals compared to unmodified CNC. The results are presented in Figure 6. As expected the contact angle value for modified CNC is higher than that for neat CNC. The contact angle of the water drop for unmodified CNC decreased sharply with spreading within

30 s and the contact angle after 20 s was around 20° (±2). Even after several measurements, the same behavior was always observed. This is obviously due to the hydrophilic nature of CNC whereas M-CNC has a significantly higher contact angle around 45° (±3) that remained constant even after 20 and 30 s. This is a clear evidence of the hydrophobic nature induced by the surface modification. The –OH groups are hid by the long fatty chains on the surface of the CNC as described in Scheme 1.

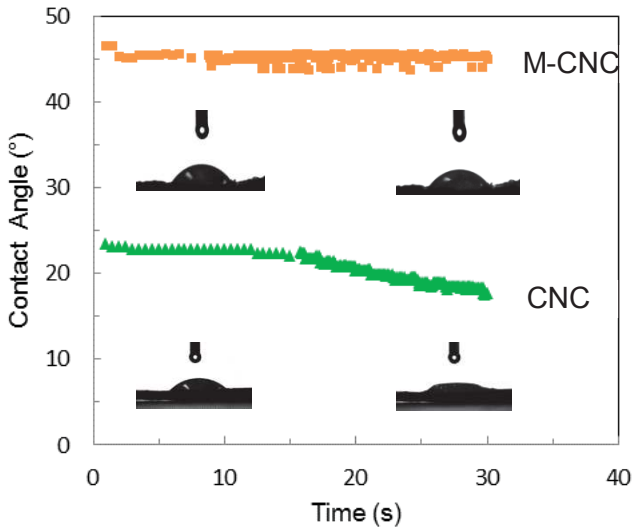

Figure 6. Time-dependence of the contact angle for a water drop on sheet samples (inserted photographs for the water drop on the sheet sample after 5 and 20 s) for unmodified CNC and CNC modified with quaternary ammonium salt bearing long alkyl chain (M-CNC).

3.4 Preparation and characterization of polymer nanocomposites

Nanocomposites were fabricated by melt extrusion using PP as matrix and either unmodified or modified nanocrystals as the reinforcing phase. The aspect of resultant nanocomposite films is shown in Figure 7. The neat PP film is translucent as any low thickness semi crystalline polymeric film. When adding only 3 wt% unmodified CNC, the film becomes evenly darker. This is due to the degradation of the nanofiller. The appearance of nanocomposite films reinforced with up to 10 wt% modified CNC is like neat PP film. This

observation agrees with TGA experiments and this might be due to the protection of the sulfate groups on surface of CNC provided by the electrostatically interacting quaternary ammonium chains. Similar observations were reported when coating CNC with high molecular weight polyoxyethylene (PEO)[18,47] but higher interactions are expected between negatively charged sulfated CNC and quaternary ammonium salt.

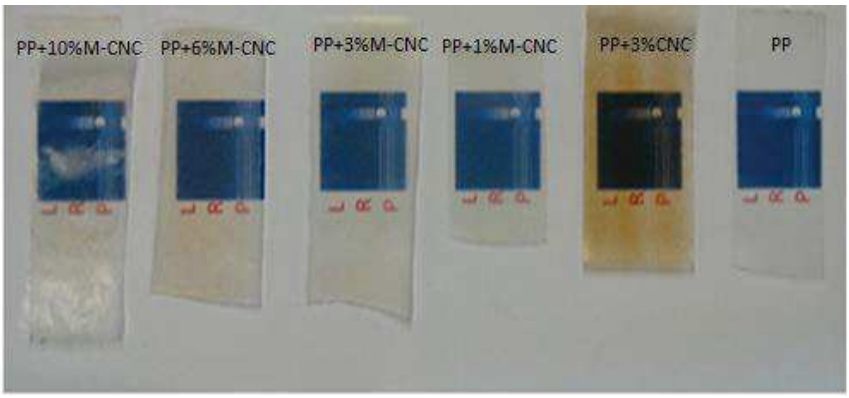

Figure 7. Appearance of extruded PP/CNC and M-CNC nanocomposite films: PP+10%M-CNC, PP+6%M-CNC, PP+3%M-CNC, PP+1%M-CNC, PP+3%CNC and PP (from left to right).

3.4.1 UV spectrophotometer

The light transmittance of CNC and M-CNC extruded polypropylene nanocomposites was analyzed by using UV spectrophotometer, as shown in Figure S1 (Annexure-1). It is observed that when adding CNC and M-CNCs to PP matrix the transmittance decreased, especially for composites containing higher filler contents. The PP matrix shows a high transmittance (65%) as subsequently it is transparent. The lowest transmittance (36.8%) was observed for the PP film reinforced with unmodified CNC (3wt %), due to the degradation of the cellulosic nanomaterial as evidenced in Figure 7. However, this effect was alleviated when using up to 10 wt% modified CNC. The transmittance was around 60%, 57.2%, and 49.5% for PP films reinforced with 1, 3 and 6 wt% M-CNC, respectively. A stronger decrease of the transmittance to 40.5% was observed for the 10 wt % M-CNC reinforced composite probably

due to the filler aggregation. In overall the transmittance of M-CNC reinforced composites are higher than 40%.

3.4.2 DSC

The thermal characterization of CNC/M-CNC reinforced PP nanocomposite films was analyzed by using DSC. The thermograms can be seen in Figure S2 (Annexure-1) and thermal data determined from these thermograms are collected in Table 2. Neat PP displays a melting point around 170°C that drops to 163°C after extrusion. Moreover, an additional peak appears around 122°C for extruded PP. Both events are brought about by the extrusion process and could be related to a decrease of the molecular weight of the polymer upon extrusion due to high shear rates involved during melt processing.[48] This secondary melting peak progressively recedes when adding modified CNC and it is absent for the nanocomposite film reinforced with 3 wt% unmodified CNC. The melting temperature of PP doesn't show any significant change upon CNC loading. On the contrary the degree of crystallinity of the polymeric matrix tends to continuously increase when adding the cellulosic nanomaterial. It is worth noting that for the calculation of the degree of crystallinity, the enthalpy of fusion was normalized to account for the effective PP content. The nucleating effect of CNC has been abundantly reported in literature for different polymer matrices.

Table 2. Melting temperature (Tm), enthalpy of fusion (ΔHm) and degree of crystallinity (χ_c) for neat PP, extruded PP (PPex) and nanocomposites.

Sample	Tm (°C)	ΔHm (J.g^{-1})	χ_c (%)*
PP	170.9	66.03	34.7
PPex	163.6	62.92	33.1
PP + 3% CNC	164.8	78.53	42.6
PP + 1% M-CNC	165.9	73.71	39.2
PP + 3% M-CNC	164.4	80.65	43.8
PP + 6% M-CNC	164.0	81.98	45.9
PP + 10% M-CNC	163.7	83.40	48.8

* $\chi_c = \frac{\Delta H_m}{w \times \Delta H_m^o}$ Where ΔH_m^o= 190 J.g^{-1} is the enthalpy of fusion for 100% crystalline PP[49]and w is the weight fraction of PP matrix in the nanocomposite.

3.4.3 DMA

The mechanical properties of the composites reinforced with CNC/M-CNC were investigated using both dynamic mechanical analysis and tensile tests. The evolution of the logarithm of the storage tensile modulus versus temperature in isochronal conditions at a frequency of 1 Hz is shown in Figure 8. The curves have been normalized at 1 GPa at low temperature to limit the effect of the errors induced by the measurement of the dimensions of the sample. For neat PP, the modulus gradually declines with increasing temperature from -30°C to 100°C. When adding 3 wt% unmodified CNC a substantial increase of the storage modulus is observed over the whole temperature range. Regarding modified CNC, a similar effect is reported and the highest reinforcing effect is induced by 10 wt% M-CNC. However, this reinforcing effect should be, at least partially, attributed to the increase of the degree of crystallinity of the PP matrix evidenced from DSC measurements.

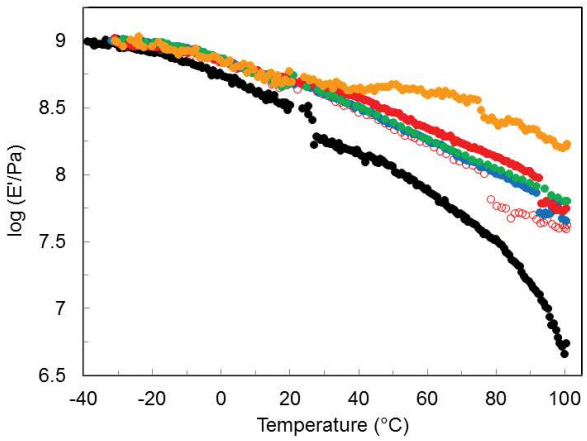

Figure 8. Evolution of the logarithm of the storage modulus as a function of temperature at 1 Hz for neat extruded PP (●) and nanocomposites reinforced with 3 wt% CNC (○), and 1 wt% (●), 3 wt% (●), 6 wt% (●), and 10 wt% M-CNC (●).

3.4.4 Tensile test

The nonlinear mechanical behavior of CNC/M-CNC reinforced PP nanocomposites was characterized at room temperature. Typical stress-strain curves are shown in Figure 9 and the tensile data are reported in Table 3. Compared to the neat PP film, the modulus slightly increases whereas the yield stress slightly decreases for nanocomposites films but the variation remains within the standard deviation. This can be an indication of weak interactions at the filler-matrix interface even in the case of compatibilized CNC. A more significant decrease of the yield strain is observed when adding cellulose nanomaterial but the most important change is observed for the strain at break. It decreases when adding 3 wt% unmodified CNC, but significantly increases for M-CNC, except for 10 wt%. The expected inhomogeneous distribution of unmodified CNC in the PP matrix caused brittle fracture of the composite as already reported for tunicin CNC[50,51] and cellulose nanofibrils[52] reinforced PP. The much higher strain at break values reported for M-CNC reinforced nanocomposites, even surpassing the strain at break for the neat PP matrix, is a good indication of the homogeneous dispersion of the nanofiller within the PP matrix. Such

behavior was already reported for tunicin CNC coated with phosphoric ester of polyoxyethylene (9) nonylphenyl ether[50] and cellulose nanofibrils coated with of polyoxyethylene (10) nonylphenyl ether [52] reinforced PP. The large plastic deformation of the material was attributed to the hindering of inter-nanoparticle interactions and possible plasticizing effect of the surfactant.[52] The sharp decrease of the strain at break for the nanocomposite reinforced with 10 wt% M-CNC could be probably ascribed to aggregation occurring for such nanofiller contents.

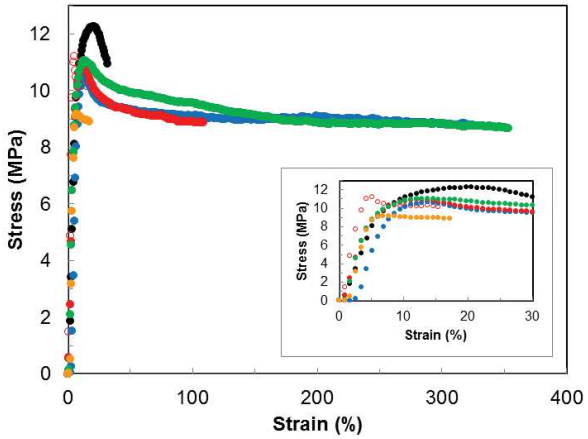

Figure 9. Typical stress-strain curves for neat extruded PP (●) and nanocomposites reinforced with 3 wt% CNC (○), and 1 wt% (●), 3 wt% (●), 6 wt% (●), and 10 wt% M-CNC (●). The insert is an expanded view of stress vs. strain curves for the low strain region.

Table 3. Young's modulus (E), yield stress (σ_y), yield strain (ε_y), and strain at break (ε_b) for neat extruded PP and nanocomposites.

Sample	E (MPa)	σ_y (MPa)	ε_y (%)	ε_b (%)
PP	181±67	12.3±2.1	19.7±3.4	39.4±6.2
PP + 3%CNC	321±47	10.3±1.1	13.7±1.3	15.4±3.7
PP + 1%M-CNC	200±19	10.6±1.5	13.7±1.9	326±18
PP + 3%M-CNC	231±39	11.0±2.1	12.8±2.1	109±28
PP + 6%M-CNC	231±55	11.1±1.3	13.7±1.6	353±23
PP + 10%M-CNC	279±55	9.16±1.05	7.70±0.88	12.0±6.8

3.4.5 SEM

SEM is commonly used for a more extensive morphological inspection even if individual nanocrystals are not visible because of the nanoscale dimension of the reinforcing phase. This technique help to understand the homogeneity of the composite, presence of voids, micro-scale dispersion level of the CNC within the continuous matrix, presence of aggregates, sedimentation and possible orientation of the nanorods. When observing the surface of the films (Figure S3 in annexure-1), differences were observed between the nanocomposites reinforced with modified or non-modified CNC. The PP matrix (Figure S3a) shows a smooth surface whereas the nanocomposite reinforced with 3 wt% neat CNC (Figure S35b in annexure-1) displays a rougher surface and CNC aggregates are observed (circled in red). Improved dispersion is observed for M-CNC up to 6 wt% (Figure S3c-e in annexure-1) and nanocrystals seem to be homogeneously dispersed in the matrix. However, for the 10 wt% M-CNC reinforced PP composite film (Figure S3f in annexure-1) microscale nanoparticle aggregation is reported.

The cryo-fractured cross section of the nanocomposite films was also investigated using SEM (Figure 10). By comparing Figure 10a (neat PP matrix) and Figure 10b (PP reinforced with 3 wt% unmodified CNC), the presence of the filler is evidenced through the observation of white dots probably corresponding to CNC aggregates. Moreover, some holes can be observed (circled in red) attributed to pulled-out CNC aggregates. Figures 10c-e (PP reinforced with up to 6 wt% CNC modified with quaternary ammonium salt) show similar appearance as neat PP matrix and absence of holes evidencing a homogeneous dispersion of CNC within the PP matrix. However, for 10 wt% M-CNC (Figure 10f**)** holes due to CNC aggregates are observed again (circled in red).

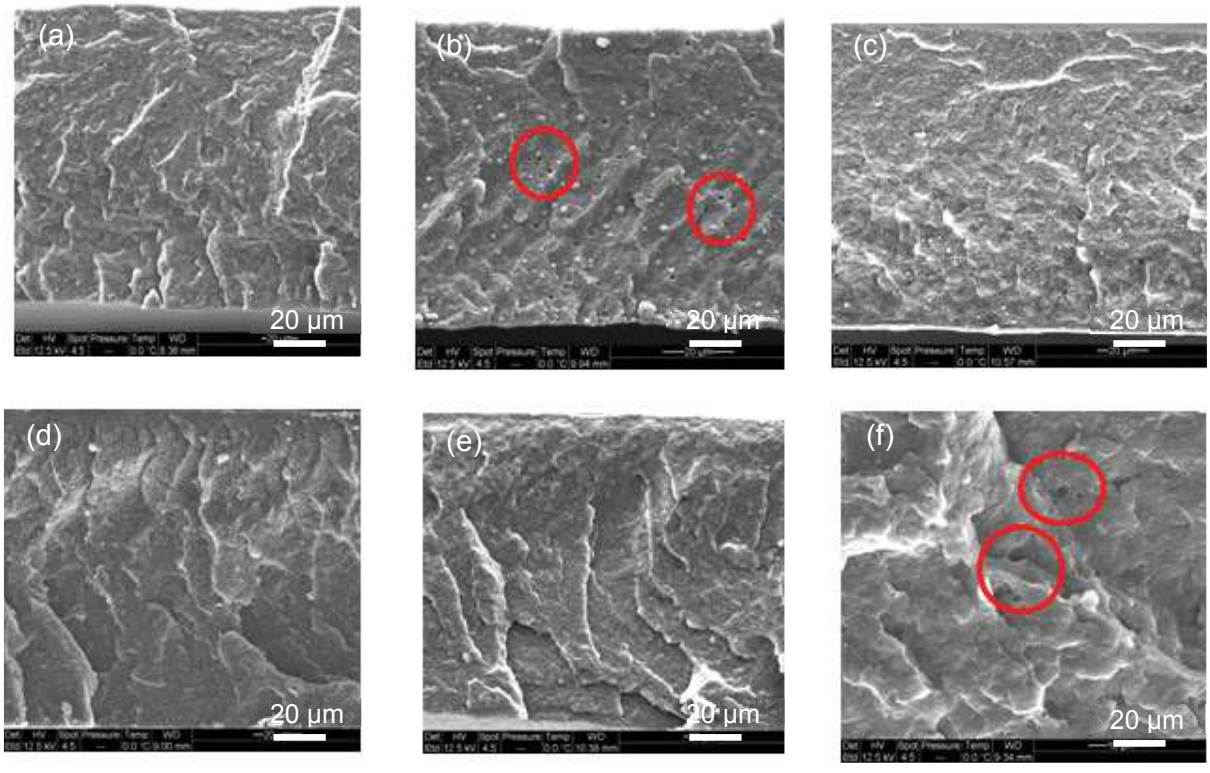

Figure 10. SEM images of the cryo-fractured cross section of the extruded films: neat PP (a), and PP nanocomposites reinforced with 3 wt% unmodified CNC (b), and 1 wt% (c), 3 wt% (d), 6 wt% (e) and 10 wt % (f) CNC modified with quaternary ammonium salt.

3.4.6 Melt rheology

Melt rheology experiments were conducted at 180°C. The evolution of the storage modulus (G'), loss modulus (G'') and complex viscosity (η*) as a function of frequency was measured for CNC/M-CNC reinforced composites and results are shown in Figure 11. By comparing the behavior of freshly melted PP and initially extruded PP (PP_{Ex}), a very slight decrease is observed after extrusion at low shear rates showing that the polymer is practically not degraded by the extrusion process. For nanocomposites, a clear decrease is reported, particularly at low shear rates, as the CNC content increases. The results are contrast to the usual predictions by Einstein[53] and Batchelor,[54] for the relative viscosity increase of a suspension of particles with the volume fraction of suspended particles. This phenomenon has been reported for several nanoparticle-based systems[55-62] and attributed to a dilution effect.

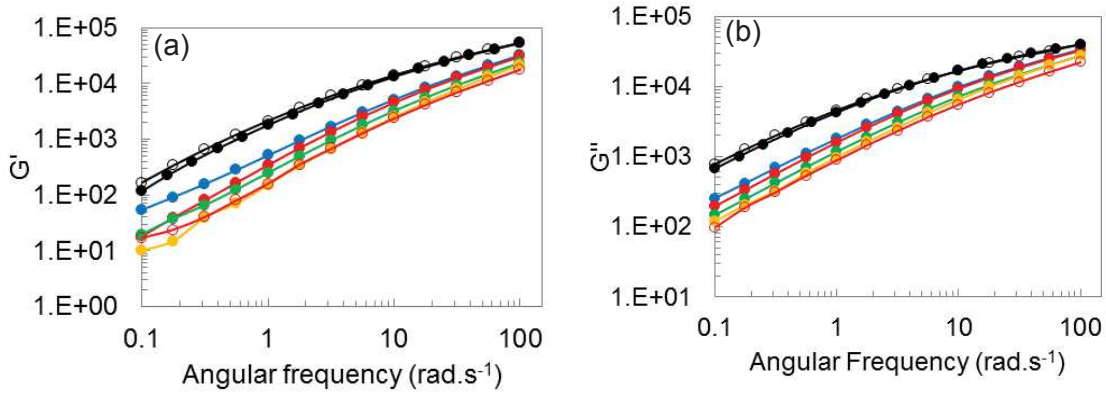

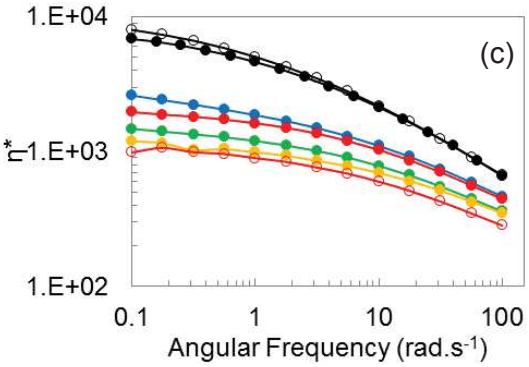

Figure 11. Evolution of (a) the storage modulus (G'), (b) loss modulus (G'') and (c) complex viscosity (η*) as a function of frequency for neat PP (○), neat extruded PP (●) and nanocomposites reinforced with 3 wt% CNC (○), and 1 wt% (●), 3 wt% (●), 6 wt% (●), and 10 wt% M-CNC (●).

3.5 CONCLUSION

We have reported an environmentally friendly water-based, flexible and easy procedure to modify the surface of CNC. Profitably the surface of the negatively charged CNC with sulfated groups resulting from the sulfuric acid extraction step to establish favorable ionic interactions with quaternary ammonium salt bearing long alkyl chain. Hydrophobization of the CNC surface was verified by FTIR spectroscopy and contact angle measurements, and it was observed that modified CNC displays improved thermal stability compared to neat CNC. Hydrophobized CNC disperses well in different non-polar solvents and hydrophobic polymer matrix such as PP, which is impossible for neat CNC. Both unmodified and modified CNCs act as nucleating agents for the PP matrix, promoting its crystallization. A modest reinforcing effect was evidenced from DMA and tensile tests, but a spectacular improvement of the elongation at break was observed when adding few percent of modified CNC. This large plastic deformation of the material was attributed to the hindering of inter-nanoparticle interactions and possible plasticizing effect of the surfactant. A significant decrease of the melt viscosity was reported when adding CNC and ascribed to a dilution effect.

3.6 REFERENCES

1. Yao, X.; Qi, X.; He, Y.; Tan, D.; Chen, F.; Fu, Q. Simultaneous Reinforcing and Toughening of Polyurethane via Grafting on the Surface of Microfibrillated Cellulose. *ACS Appl. Mater. Interfaces* 2014, *6*, 2497-2507
2. Zhao, C.-X.; Zhang, W.-D. Preparation of Waterborne Polyurethane Nanocomposites: Polymerization from Functionalized Hydroxyapatite. Eur. Polym. J. 2008, 44, 1988-1995.
3. Tien, Y.; Wei, K. Hydrogen Bonding and Mechanical Properties in Segmented Montmorillonite/Polyurethane Nanocomposites of Different Hard Segment Ratios. *Polymer* 2001, *42*, 3213-3221.
4. Johnson III, J.R.; Spikowski, J.; Schiraldi, D.A. Mineralization of Clay/Polymer Aerogels: A Bioinspired Approach to Composite Reinforcement. *ACS Appl. Mater. Interfaces* 2009, *1*, 1305-1309.
5. Liff, S.M.; Kumar, N.; McKinley, G.H. High-performance Elastomeric Nanocomposites via Solvent-exchange Processing. Nat. Mater. 2007, 6, 76-83.
6. Qian, Y.; Linsay, C.I.; Macosko, A. Synthesis and Properties of Vermiculite-Reinforced Polyurethane Nanocomposites. *ACS Appl. Mater. Interfaces* 2011, *3*, 3709-3717.
7. Zhou, C.-H.; Shen, Z.-F.; Liu, L.-H.; Liu, S.-M. Preparation and Functionality of Clay-containing Films. *J. Mater. Chem.* 2011, *21*, 15132-15153.
8. Huang, Y.-C.; Lin, J.-H.; Tseng, I.; Lo, A.-Y.; Lo, T.-Y.; Yu, H.-P.; Tsai, M.-H.; Whang, W.-T.; Hsu, K.-Y. An In Situ Fabrication Process for Highly Electrical Conductive Polyimide/MWCNT Composite Films using 2,6-diaminoanthraquinone. *Compos. Sci. Technol.* 2013, *87*, 174-181.
9. Guo, H.; Minus, M.L.; Jagannathan, S.; Kumar, S. Polyacrylonitrile/Carbon Nanotube Composite Films. *ACS Appl. Mater. Interfaces* 2010, *2*, 1331-1342.

10. Kim, J.; Hong, S.M.; Kwak, S.; Seo, Y. Physical Properties of Nanocomposites Prepared by *In Situ* Polymerization of High-density Polyethylene on Multiwalled Carbon Nanotubes. *Phys. Chem. Chem. Phys.* 2009, *11*, 10851-10859.

11. Xia, H.; Song, M. Preparation and Characterization of Polyurethane–carbon Nanotube Composites. *Soft Matter* 2005, *1*,386-394.

12. Wang, X.; Hu, Y.; Song, L.; Yang, H.; Xing, W.; Lu, H. *In Situ* Polymerization of Graphene Nanosheets and Polyurethane with Enhanced Mechanical and Thermal Properties. *J. Mater. Chem.* 2011, *21*, 4222-4227.

13. Eichhorn, S.J.; Dufresne, A.; Aranguren, M.; Marcovich, N.E.; Capadona, J.R.; Rowan, S.R.; Weder, C.; Thielemans, W.; Roman, M.; Renneckar, S.; Gindl, W.; Veigel, S.; Keckes, J.; Yano, H.; Abe, K.; Nogi, N.; Nakagaito, A.N.; Mangalam, A.; Simonsen, J.; Benight, A.S.; Bismarck, A.; Berglund, L.A.; Peijs, T. Review: Current International Research into Cellulose Nanofibres and Nanocomposites. *J. Mater. Sci.* **2010**, *45*, 1-33.

14. Moon, R.J.; Martini, A.; Nairn, J.; Simonsen, J.; Youngblood, Cellulose Nanomaterials Review: Structure, Properties and Nanocomposites. J. *Chem. Soc. Rev.* **2011**, *40*, 3941-3994.

15. Lin, N.; Dufresne, A. Physical and/or Chemical Compatibilization of Extruded Cellulose Nanocrystal Reinforced Polystyrene Nanocomposites. *Macromolecules* **2013**, *46*, 5570-5583.

16. Roman, M.; Winter, W.T. Effect of Sulfate Groups from Sulfuric Acid Hydrolysis on the Thermal Degradation Behavior of Bacterial Cellulose**.** *Biomacromolecules* **2004**, *5*, 1671-1677.

17. Lin, N.; Dufresne, A. Surface Chemistry, Morphological Analysis and Properties of Cellulose Nanocrystals with Gradiented Sulfation Degrees. *Nanoscale* 2014, *6*, 5384-5393.

18. Ben Azouz, K.; Ramires, E.C.; Van den Fonteyne, W.; El Kissi, N.; Dufresne. A. Simple Method for the Melt Extrusion of a Cellulose Nanocrystal Reinforced Hydrophobic Polymer. *ACS Macro Lett.* 2012, *1*, 236-240.

19. de Menezes, A.J.; Siqueira, G.; Curvelo, A.A.S.; Dufresne, A. Extrusion and Characterization of Functionalize d Cellulose Whiskers Reinforced Polyethylene Nanocomposites. *Polymer* 2009, *50*, 4552-4563.

20. Goffin, A.-L.; Raquez, J.-M.; Duquesne, E.; Siqueira, G.; Habibi, Y.; Dufresne, A.; Dubois, Ph. Poly(e-caprolactone) Based Nanocomposites Reinforced by Surface-grafted Cellulose Nanowhiskers via Extrusion Processing: Morphology, Rheology, and Thermo-mechanical Properties. *Polymer* 2011, *52*, 1532-1538.

21. Goffin, A.-L.; Raquez, J.-M.; Duquesne, E.; Siqueira, G.; Habibi, Y.; Dufresne, A.; Dubois, Ph. From Interfacial Ring-opening Polymerization to Melt Processing of Cellulose Nanowhisker-filled Polylactide-based Nanocomposites. *Biomacromolecules* 2011, *12*, 2456-2465.

22. Peng, B.L.; Dhar, N.; Liu, H.L.; Tam, K.C. Chemistry and Applications of Nanocrystalline Cellulose and its Derivatives: A Nanotechnology Perspective. *Can. J. Chem. Eng.* 2011, *89*, 1191-1206.

23. Zoppe, J.O.; Habibi, Y.; Rojas, O.J.; Venditti, R.A.; Johansson, L.S.; Efimenko, K.; Österberg, M.; Laine, J. Poly(N-isopropylacrylamide) Brushes Grafted from Cellulose Nanocrystals via Surface-initiated Single-electron Transfer Living Radical Polymerization. *Biomacromolecules* 2010, *11*, 2683-2691.

24. Xu, Q.X.; Yi, J.; Zhang, X.F.; Zhang, H.L. A Novel Amphotropic Polymer Based on Cellulose Nanocrystals Grafted with Azo Polymers. *Eur. Polym. J.* 2008, *44*, 2830-2837.

25. Majoinen, J.; Walther, A.; McKee, J.R.; Kontturi, E.; Aseyev, V.; Malho, J.M.; Ruokolainen, J.; Ikkala, O. Polyelectrolyte Brushes Grafted from Cellulose Nanocrystals

Using Cu-Mediated Surface-initiated Controlled Radical Polymerization. *Biomacromolecules* 2011, *12*, 2997-3006.

26. Morandi, G.; Heath, L.; Thielemans, W. Cellulose Nanocrystals Grafted with Polystyrene Chains through Surface-Initiated Atom Transfer Radical Polymerization (SI-ATRP). *Langmuir* 2009, *25*, 8280-8286.
27. Filpponen, I.; Argyropoulos, D.S. Regular Linking of Cellulose Nanocrystals via Click Chemistry: Synthesis and Formation of Cellulose Nanoplatelet Gels. *Biomacromolecules* 2010, *11*, 1060-1066.
28. Chen, J.; Lin, N.; Huang, J.; Dufresne, A. Highly Alkynyl-functionalization of Cellulose Nanocrystals and Advanced Nanocomposites thereof via Click Chemistry. *Polym. Chem.* 2015, *6*, 4385-4395.
29. Dong, S.P.; Roman, M. Fluorescently Labeled Cellulose Nanocrystals for Bioimaging Applications. *J. Am. Chem. Soc.* 2007, *129*, 13810-13811.
30. Rueda, L.; d'Arlas, B.F.; Zhou, Q.; Berglund, L.A.; Corcuera, M.A.; Mondragon, I.; Eceiza, A. Isocyanate-rich cellulose nanocrystals and their selective insertion in elastomeric polyurethane. *Compos. Sci. Technol.* 2011, *71*, 1953-1960.
31. Siqueira, G.; Bras, J.; Dufresne, A. New Process of Chemical Grafting of Cellulose Nanoparticles with a Long Chain Isocyanate. *Langmuir* 2010, *26*, 402-411.
32. Yuan, H.H.; Nishiyama, Y.; Wada, M.; Kuga, S. Surface Acylation of Cellulose Whiskers by Drying Aqueous Emulsion. *Biomacromolecules* 2006, *7*, 696-700.
33. Salajkova, M.; Berglund, L.A.; Zhou, Q. Hydrophobic Cellulose Nanocrystals Modified with Quaternary Ammonium Salts. *J. Mater. Chem.* 2012, *22*, 19798-19805.
34. Dong, X.M.; Gray, D.G. Effect of Counterions on Ordered Phase Formation in Suspensions of Charged Rodlike Cellulose Crystallites. *Langmuir* 1997, *13*, 2404-2409.

35. Bonini, C.; Heux, L.; Cavaillé, J.Y.; Lindner, P.; Dewhurst, C.; Terech, P. Rodlike Cellulose Whiskers Coated with Surfactant: A Small-Angle Neutron Scattering Characterization. *Langmuir* 2002, *18*, 3311-3314.

36. Abitbol, T.; Marway, H.; Cranston, E.D. Surface Modification of Cellulose Nanocrystals with Cetyltrimethylammonium Bromide. *Nord. Pulp Pap. Res. J.* **2014**, *29*, 46-57.

37. Elazzouzi-Hafraoui, S.; Putaux, J.L.; Heux, L. Self-assembling and Chiral Nematic Properties of Organophilic Cellulose Nanocrystals. *J. Phys. Chem. B* **2009**, *113*, 11069-11075.

38. Hu, Z.; Ballinger, S.; Pelton, R.; Cranston, E.D. Surfactant-enhanced Cellulose Nanocrystal Pickering Emulsions. *J. Colloid Interface Sci.* **2015**, *439*, 139-148.

39. Bondeson, D.; Oksman, K. Dispersion and Characteristics of Surfactant Modified Cellulose Whiskers Nanocomposites. *Compos. Interfaces* **2007**, *14*, 617- 630.

40. Hamad, W.Y.; Hu, T.Q. Structure-Process-Yield Interrelations in Nanocrystalline Cellulose Extraction. *Can. J. Chem. Eng.* **2010**, *88*, 392-402.

41. Wågberg, L.; Decher, G.; Norgren, M.; Lindström, T.; Ankerfors, M.; Axnas, K. The Build-up of Polyelectrolyte Multilayers of Microfibrillated Cellulose and Cationic Polyelectrolytes. *Langmuir* **2008**, *24*, 784-795.

42. Ansari, F.; Salajková M.; Zhou, Q.; Berglund, L.A. Strong Surface Treatment Effects on Reinforcement Efficiency in Biocomposites Based on Cellulose Nanocrystals in Poly(vinyl acetate) Matrix. *Biomacromolecules* **2015**, *16*, 3916-3924.

42. Missoum, K.; Bras, J.; Belgacem, M.N. Organization of Aliphatic Chains Grafted on Nanofibrillated Cellulose and Influence on Final Properties. *Cellulose* **2012**, *19*, 1957-1973.

43. Bettaieb, F.; Khiari, R.; Dufresne, A.; Mhenni, M.F. ; Belgacem, M.N. Mechanical and Thermal Properties of *Posidonia oceanica* Cellulose Nanocrystal Reinforced Polymer. *Carbohydr. Polym.* **2015**, *123*, 99-104.

44. Liu, H.; Liu, D.; Yao, F.; Wu, Q. Fabrication and Properties of Transparent Polymethylmethacrylate/Cellulose Nanocrystals Composites. *Bioresour. Technol.* **2010**, *101*, 5685-5692.

45. Lin, N.; Huang, J.; Chang, P.R.; Feng, J.; Yu, J. Surface Acetylation of Cellulose Nanocrystal and its Reinforcing Function in Poly(lactic acid). *Carbohydr. Polym.* **2011***, 83*, 1834-1842.

46. Pereda, M.; El Kissi, N.; Dufresne, A. Extrusion of Polysaccharide Nanocrystal Reinforced Polymer Nanocomposites through Compatibilization with Poly(ethylene oxide). *ACS Appl. Mater. Interfaces* **2014**, *6*, 9365-9375.

47. Mariano, M.; El Kissi, N.; Dufresne, A. Melt Processing of Cellulose Nanocrystal Reinforced Polycarbonate from a Masterbatch Process. *Eur. Polym. J.* **2015**, *69*, 208-223.

48 Amash, A.; Zugenmaier, P. Morphology and Properties of Isotropic and Oriented Samples of Cellulose Fibre-Polypropylene Composites. *Polymer* **2000**, *41*, 1589-1596.

49. Ljungberg, N.; Bonini, C.; Bortolussi, F.; Boisson, C.; Heux, L.; Cavaillé, J.Y. New Nanocomposite Materials Reinforced with Cellulose Whiskers in Atactic Polypropylene: Effect of Surface and Dispersion Characteristics. *Biomacromolecules* **2005,** *6*, 2732-2739.

50. Ljungberg, N.; Cavaillé, J.Y.; Heux, L. Nanocomposites of Isotactic Polypropylene Reinforced with Rod-like Cellulose Whiskers. *Polymer* **2006,** *47*, 6285-6292.

51. Iwamoto, S.; Yamamoto, S.; Lee, S.H.; Endo, T. Mechanical Properties of Polypropylene Composites Reinforced by Surface-coated Microfibrillated Cellulose. *Composites, Part A* **2014**, *59*, 26-29.

52. Einstein, A. On the Theory of Brownian Movement. *Ann. Phys.* **1906**, *19*, 371-381.

53. Batchelor, G.K. The Effect of Brownian Motion on the Bulk Stress in a Suspension of Spherical Particles. *J. Fluid Mech.* **1977**, *83*, 97-117.

54. Roberts, C.; Cosgrove, T.; Schmidt, R.G.; Gordon, G.V. Diffusion of Poly(dimethylsiloxane) Mixtures with Silicate Nanoparticles. *Macromolecules* **2001**, *34*, 538-543.

55. Lertwimolnun, W.; Vergnes, B. Influence of Compatibilizer and Processing Conditions on the Dispersion of Nanoclay in a Polypropylene Matrix. *Polymer* **2005**, *46*, 3462-3471.

56. Tuteja, A.; Duxbury, P.M.; Mackay, M.E. Multifunctional Nanocomposites with Reduced Viscosity. *Macromolecules* **2007**, *40*, 9427-9434.

57. Schmidt, R.G.; Gordon, G.V.; Dreiss, C.A.; Cosgrove, T.; Krukonis, V.J.; Williams, K.; Wetmore, P.M. A Critical Size Ratio for Viscosity Reduction in Poly(dimethylsiloxane)-Polysilicate Nanocomposites. *Macromolecules* **2010**, *43*, 10143-10151.

58. Nusser, K.; Schneider, G.J.; Pyckhout-Hintzen, W.; Richter, D. Viscosity Decrease and reinforcement in Polymer-Silsesquioxane Composites. *Macromolecules* **2011**, *44*, 7820-7830.

59. Kim, D.; Srivastava, S.; Narayanan, S.; Archer, L.A. Polymer Nanocomposites: Polymer and Particle Dynamics. *Soft Matter* **2012**, *8*, 10813-10818.

60. Tan, H.; Xu, D.; Wan, D.; Wang, Y.; Wang, L.; Zheng, J.; Liu, F.; Ma, L.; Tang, T. Melt Viscosity Behavior of C_{60} Containing Star Polystyrene Composites. *Soft Matter* **2013**, *9*, 6282-6290.

61. Mangal, R.; Srivastava, S.; Archer, L.A. Phase Stability and Dynamics of Entangled Polymer-Nanoparticle Composites. *Nat. Commun.* **2015**, *6*, 7198.

Chapter-4

Physical adsorption of CNC

Surface adsorption of triblock copolymer (PEO-PPO-PEO) on cellulose nanocrystals and their melt extrusion with polyethylene.

(RSC Advances-2016, 6, 66224)

Chapter-4: Surface adsorption of triblock copolymer (PPO-PEO-PPO) on cellulose nanocrystals and their melt extrusion with polyethylene.

ENGLISH ABSTRACT

Cellulose nanocrystals (CNC) have gained a lot of interest in recent years in the field of composites due to their unique mechanical properties and also because cellulose is the most abundant and renewable polymer in nature. In this work, pluronic grade triblock copolymer was adsorbed on the surface of CNC in order to improve the thermal stability and also its dispersion from the dried state. The adsorbed cellulose nanocrystals (A-CNCs) were characterized to check their thermal, functional and structural properties by thermogravimetric analysis (TGA), Fourier transform infrared spectroscopy (FTIR), X-ray diffraction (XRD) and atomic force microscopy (AFM). Interestingly, improved thermal stability was observed and also the dispersion of A-CNC in aqueous medium was much better than for unmodified CNC. The aqueous A-CNC suspensions were characterized by small angle X-ray scattering (SAXS) to evaluate the dispersion of the nanoparticles. The flow properties of A-CNC dispersions were also analysed. Further, A-CNC was used to prepare nanocomposites by melt extrusion using linear low density polyethylene (LLDPE) as matrix. The thermo mechanical and morphological properties of the ensuing nanocomposites were characterized by dynamic mechanical analysis (DMA), differential scanning calorimetry (DSC) and scanning electron microscopy (SEM). The dispersion state of A-CNC within the polymeric matrix was also characterized by SAXS.

RESUME FRANÇAIS

L’étude des nanocristaux de cellulose (CNC) suscite un intérêt croissant ces dernières années dans le domaine des matériaux composites en raison de leurs propriétés mécaniques uniques et aussi parce que la cellulose, matériau renouvelable, est également le polymère le plus abondant dans la nature. Les verrous à leur utilisation à grande échelle sont liés à leur mauvaise stabilité thermique et à la difficulté à les disperser une fois qu’ils ont été séchés. En vue de parer à ces difficultés, nous avons cherché dans cette étude à modifier la surface des CNC par adsorption d’un copolymère tribloc pluronic. Les CNC adsorbés (A-CNCs) ont été caractérisés à travers leurs propriétés thermiques, fonctionnelles et structurelles par analyse thermogravimétrique (TGA), spectroscopie infrarouge par transformée de Fourier (FTIR), diffraction des rayons X (XRD) et par microscopie à force atomique (AFM). Les résultats montrent effectivement une meilleure stabilité thermique et une meilleure dispersion en milieu aqueux par rapport au cas où des CNC non adsorbés sont utilisés. Les suspensions aqueuses de A-CNC ont été caractérisées par diffusion de rayons X aux petits angles (SAXS) pour évaluer la dispersion des nanoparticules. Leurs propriétés en écoulement ont également été analysées par rhéométrie. En outre, les A-CNC ont été mélangés à un polyéthylène basse densité linéaire (LLDPE) et des nanocomposites ont été préparés par extrusion à chaud. Les propriétés mécaniques et thermiques des films composites ont été déterminées par analyse mécanique dynamique (DMA) et par calorimétrie différentielle à balayage (DSC). La morphologie a quant à elle été observée par microscopie électronique à balayage (SEM). L'état de dispersion des A-CNC dans la matrice polymère a été caractérisé par SAXS.

4.1 Introduction

Cellulose nanocrystal (CNC) has a great interest in nanocomposite field due to its remarkable properties including high surface area, low density, and mechanical strength, as well as inherent abundance, renewability, and biodegradability of cellulose.[1] The numerous hydroxyl groups on the surface of CNC enable for physical adsorption or various chemical modifications including esterification, etherification, oxidation, silylation, and polymer grafting.[2–5] Physically adsorbed nanocrystals are extensively used as nanofiller to enhance various properties through the development of composites.[6, 7]

In recent years the bulk production of CNC increased due to the vast interest of researchers and industries promoting its application in the composite field,[8] but also for advanced functional nanomaterials.[9] However, the processing of CNC based nanocomposites is mainly limited to two methods, viz. 1) solvent casting, and 2) melt processing. The casting/evaporation technique using polymer solution or polymer dispersion (latex) in liquid medium is commonly used in most studies for composites reinforced with CNC.[10, 11] It results in a good dispersion of the nanofiller within the polymeric matrix after evaporation of the liquid medium. However, it involves a huge quantity of liquid to avoid viscosity issues and the dispersion of CNC in low polarity solvents is challenging due to its hydrophilic nature. Especially this process is not viable for industrial applications.

On the contrary, melt extrusion appears as an economical and industrially feasible process since it can be applied to bulk production and it is also a non-solvent method (green process). However, in most research studies, this conventional method was not used frequently for the preparation of CNC based polymer nanocomposites. This is attributed to issues such as low thermal stability of CNC due to sulphate groups present at its surface and resulting from the sulphuric acid hydrolysis step,[12] and inherent incompatibility between cellulose and most synthetic polymers. [8, 13-15] Indeed, the hydrophilic nature of cellulose causes aggregation of

the nanoparticles after drying and limits the dispersion of CNC in a nonpolar matrix because of inter particle hydrogen bonding.

Different strategies were conducted to prepare nanocomposites by melt extrusion or injection moulding with CNC. They mainly involved chemical grafting, which was found to strongly improve the compatibility and dispersion state with hydrophobic matrices.[16-20] However, it is not an inexpensive process for industry. Finally, adsorption of macromolecules and surface modification with surfactant were also tried in order to compatibilize CNC with the polymer matrix.[21-26]

Earlier, PEO chains-coated cellulose nanocrystal (A-CNC) was proposed as a simple method and extrusion with LDPE was successfully reported.[21,27] Similarly, in the present study triblock (PEO-PPO-PEO) copolymer having two hydrophilic ends attached to hydrophobic polypropylene oxide (PPO) was used to coat CNC. This process should subsequently improve the thermal stability of CNC as well as its dispersion and compatibility with a hydrophobic polymer matrix. As reported elsewhere,[28] the PEO blocks of triblock (PEO-PPO-PEO) copolymer has high affinity with cellulosic surfaces while the PPO block displays higher affinity with hydrophobic polymers such as polyethylene or polypropylene. Indeed, in this study when the triblock copolymer (TBC) was introduced to cellulose only the hydrophilic ends were adsorbed on the cellulose surface leaving the PPO part away. On the other hand, when TBC was brought into contact with a hydrophobic polymer, the PPO part alone was adsorbed. In the present study, TBC was first adsorbed on the surface of CNC in which only the hydrophilic ends were lying on CNC parting the PPO part away as expected. This process should improve the thermal stability of the nanoparticle as well as its subsequent dispersion in a hydrophobic medium. The TBC-coated CNC (A-CNC) was use to reinforce linear low density polyethylene (LLDPE) with which the PPO block (hydrophobic part) can have strong interaction with the anticipation of better mechanical properties. In this work, A-

CNC was characterized in terms of thermal stability, as well as structural and functional properties and the rheological behaviour of its suspension in water was investigated. The thermal and mechanical properties of the prepared nanocomposites were studied. The SAXS technique was also used in order to evaluate the dispersion of CNC in aqueous medium and in the LLDPE composites.

4.2 Experimental methodology

4.2.1 Materials

PEO_{101}-PPO_{56}-PEO_{101} triblock copolymer (Sigma Aldrich) was used (total molecular weight = 12,600 $g.mol^{-1}$). LLDPE- FC1010 with molecular weight of 143,000 $g.mol^{-1}$ and density of 0.914 $g.ml^{-1}$ was chosen as the matrix for the processing of nanocomposites. Commercial cellulose nanocrystal (CNC) was procured from the University of Maine, USA, as 11.5 wt% suspension.

4.2.2 Methods

Atomic force microscopy (AFM)

AFM observations were performed to evaluate the diameter and approximate length of individual nanocrystals using a Nanoscope III (Veeco). CNC and A-CNC aqueous suspensions were previously diluted to a concentration of 0.01 wt% and a drop of the suspension was deposited onto freshly cleaved Mica substrate and dried overnight under ambient conditions. Each sample was characterized in tapping mode with a silicon cantilever (OTESPA®, Bruker). At least 10 different locations were analysed to obtain representative measurements.

Fourier transform infrared spectroscopy (FTIR)

FTIR analysis was carried out using a Spectrum 65 spectrometer (PerkinElmer) on dried CNC and A-CNC obtained by freeze drying, in order to determine the functional groups

present in CNC. The samples were analysed by attenuated total reflectance (ATR) in which the sample was placed on the evanescent wave on the ATR crystal, through which infrared beam gives the data to the detector.

Thermal degradation

The thermal degradation of CNC and A-CNC was monitored by thermogravimetric analysis (TGA) using a simultaneous thermal analyser (STA) 6000 (PerkinElmer). Weight loss and dTG curves were recorded for a 20 mg sample at a heating rate of 10°C.min^{-1} in the temperature range of 30-950 °C under oxidizing atmosphere (air).

Wide angle X-ray diffraction (XRD)

XRD analysis was performed for freeze dried CNC and A-CNC. The samples were placed in a 2.5 mm deep cell and measurements were performed with a diffractometer (X' Pert PROMPD®) equipped with a detector. The operating conditions of the refractometer were: copper Kα radiation (λ = 1.5418 Å), 2θ (Bragg angle) between 2 and 56°, step size 0.067°, and counting time 90 s.

Rheological behaviour

The viscosity of the aqueous suspensions containing cellulose nanoparticles and TBC chains was analysed with the stress-controlled rheometer ARG2 (TA Instruments) equipped with a 2° cone and plate geometry of 60 mm in diameter. All rheological measurements were performed at a temperature of 20°C.

Small angle X-ray scattering (SAXS) experiments

The SAXS experiments were performed on ID2 high brilliance beamline at European Synchrotron Radiation Facility (ESRF, Grenoble, France). Dilute samples of CNC and A-CNC suspensions (0.1 and 0.5 wt%) were analysed under controlled temperature (25±1°C). The samples were introduced in a flow-through capillary cell (diameter 1.7 mm) and were further measured at rest. The wavelength of incident X-rays was λ = 0.995 Å and two sample-

detector distances (SD = 2 m and 10 m) were used. The SAXS measurements covered the following scattering vector range: 2.10^{-2} $nm^{-1} < q < 1$ nm^{-1}, $q = (4\pi/\lambda) \sin(\theta/2)$ where θ is the scattering angle. The scattering intensity distribution as a function of scattering vector was obtained by radial integration of the two dimensional (2D) scattering pattern. All the scattered intensities I(q) presented are in absolute units, and correspond to the scattering of the CNC and A-CNC particles only. The normalized background scattering of capillary cell filled with distilled water was systematically subtracted.

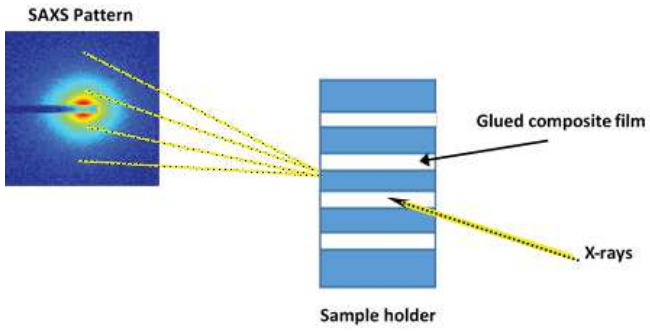

Fig. 1 Sample holder used for LLDPE nanocomposites for the SAXS experiments.

For nanocomposites, the SAXS experiments were performed at SD = 10 m and the films were positioned in front of the X-ray beam with vertical direction corresponding to flow direction during the extrusion process. Figure 1 shows the sample holder used for SAXS experiments. Nanocomposite films were glued horizontally on the sample holder and then the X-ray beam was passed through the sample and results collected by the detector were analysed.

Melt extrusion

A twin-screw DSM Micro 15 compounder was used to prepare the nanocomposites. The polymer matrix pellets (LLDPE) and freeze-dried CNC/A-CNC were mixed (around 15 g total material) and introduced in the mixing chamber of the extruder. Extrusion was performed at 160°C with a mixing speed of 100 rpm for 8 min. The mixture was then extruded through a slit die of 0.6 mm in width and 1 cm in length. Micro-film device was

attached directly to the micro-compounder outlet port. Nanocomposites with A-CNC contents of 1, 3, 6 and 10 wt%, and neat CNC content of 5 wt% were prepared.

Dynamic mechanical analysis (DMA)

DMA was used to study the viscoelastic behaviour of the nanocomposites. DMA experiments were carried out using a RSA3 (TA Instruments) equipment working in the tensile mode. The storage modulus E′ (elastic response) of the material was measured as a function of temperature as it was deformed under an isochronal oscillatory stress at a controlled temperature in a specified atmosphere. The storage modulus is related to the stiffness of the material. Varying stress with a frequency of 1 Hz was applied to the sample while heating from -100 to 100°C with a scanning rate equal to 5°C.min^{-1}. The length of the samples was 10 mm.

Differential scanning calorimetry (DSC)

DSC was used to investigate the thermal behaviour of nanocomposites. The melting temperature of nanocomposites was measured with a Perkin-Elmer DSC instrument using aluminium pans. The samples were scanned from -100 to 130°C at a heating rate of 10°C.min^{-1}.

Scanning electron microscopy (SEM)

SEM was used to characterize the nanocomposite cross section in order to visualize the roughness of the film after reinforcement with CNC/A-CNC and check the possible filler aggregation. Prior to this, the samples were frozen using liquid nitrogen and broken to obtain a clear fracture. It was glued to the sample holder for cross section images. The samples were coated with gold to prevent charging of the sample due to the electron bombardment. The SEM images were captured by using FEI (MED) Quanta200.

4.3 Results and discussion

First, the structural, functional, surface, flow and thermal properties of neat and PEO-PPO-PEO TBC-adsorbed CNC were reported. Thereafter, LLDPE nanocomposites reinforced with A-CNC/CNC were characterized in order to highlight their mechanical behaviour, morphology and dispersion state of the nanofiller.

4.3.1 Surface adsorption on cellulose nanocrystals

The CNC surface was adsorbed with (PEO-PPO-PEO) triblock copolymer. As illustrated in Figure 2, 5 g of PEO-PPO-PEO was dissolved in 100 mL of water (5 wt% solution) and added slowly to the 5 wt% CNC suspension in water. The dispersion was stirred slowly for 2 hours and it was then freeze-dried for one week prior to characterization and extrusion with LLDPE.

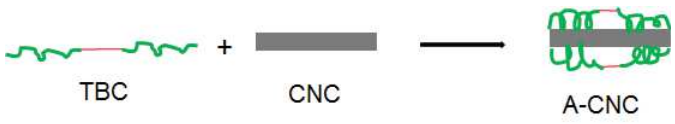

Fig. 2 Schematic illustration of the surface adsorption mechanism of the (PEO-PPO-PEO) triblock copolymer on cellulose nanocrystals.

4.3.2 Atomic force microscopy observation

The morphology of CNC and A-CNC was observed by using AFM and the results are shown in Figure 3. The AFM image of CNC is shown in Figure 3a and the length and diameter of the nanorods were in the range of 24-195 nm and 2-9 nm, respectively. The TBC-adsorbed CNC can be seen in Figure 3b. The triblock copolymer formed a layer on the surface of CNC that can be seen in low magnification image. The high magnification image showed that the individual nanocrystal morphology was different compared to neat CNC. This can be attributed to the adsorption of hydrophilic ends of TBC on CNC. The size of the A-CNC was increased 2-3 nm in width due to the adsorption of TBC.

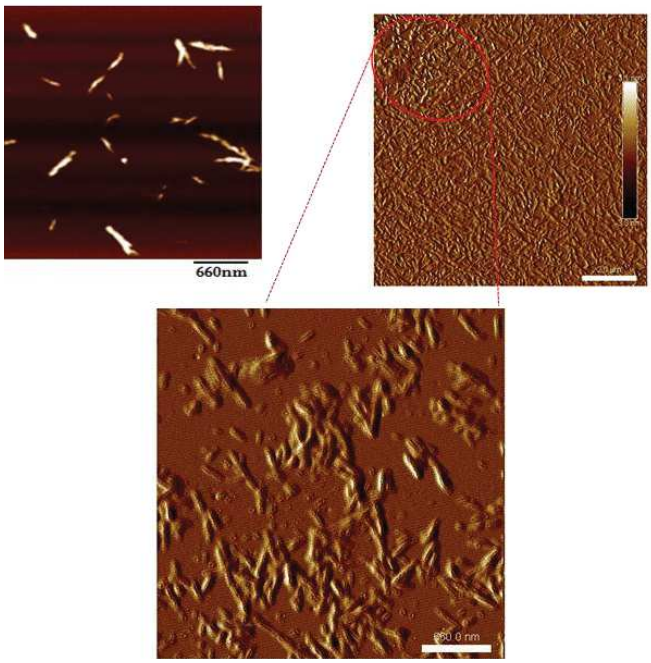

Fig. 3 AFM images for (a) CNC, and (b) A-CNC.

4.3.3 Dispersion of CNC/A-CNC in aqueous medium

Freeze-dried CNC and A-CNC were redispersed in water and the visual appearance of the samples before and after dispersion in water can be seen in Figures 4a and 4b, respectively. It is obvious that CNC cannot redisperse in water after drying due to the strong hydrophilic interactions that are established between the surface hydroxyl groups and aggregates (circled in red) as can be seen in Figure 4b. On the contrary, A-CNC was dispersed uniformly as shown in Figure 4b. It is thus clearly shown that TBC adsorbed on the surface of CNC can swell in water and consequently the remaining CNC can be freely dispersed for naked eye observation.

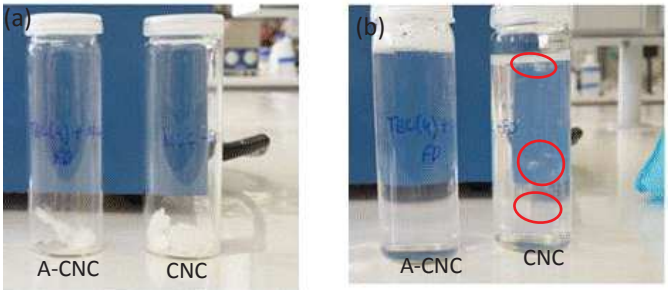

Fig. 4 (a) Freeze-dried and (b) redispersed in water CNC and A-CNC.

4.3.4 Viscosity of CNC/A-CNC in aqueous Medium

The capability of CNC to adsorb PEO-PPO-PEO polymeric chains can be investigated by studying the rheological behaviour of nanocrystal suspensions in the presence of TBC as reported in previous studies.[8,21,27] In the present study, suspensions with a constant TBC concentration of 1 wt% and gradual increase of CNC content from 1 to 9 wt% were prepared and the evolution of their viscosity vs. shear rate was determined. As shown in Figure 5, the TBC solution displays the lowest viscosity. The suspensions with low CNC contents (TBC1%+CNC1% and TBC1%+CNC2%) presented a similar behaviour as the one of neat CNC suspension, which indicates that TBC can be adsorbed on CNC surface. It indicates that the capability of surface adsorption of CNC is around 1-2 g of TBC for 1 g of pristine CNC. This value is lower than for PEO homopolymer with a similar molecular weight,[27] probably because of a different chain conformation of the copolymer at the cellulosic surface. It justifies the 1:1 ratio used for CNC:TBC in the present study. For higher CNC contents, the viscosity increased when increasing the CNC content as expected because free CNC is released in the suspension. Moreover, shear thinning behaviour is observed and this phenomenon is emphasized as the nanoparticle concentration increases.

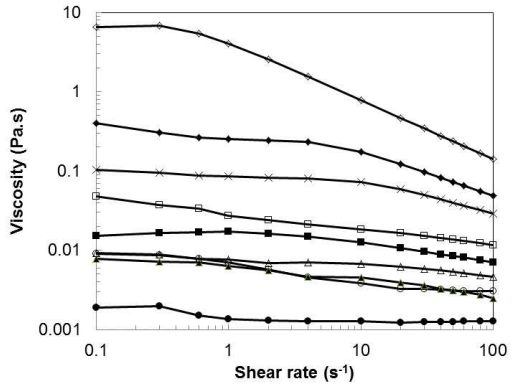

Fig. 5 Evolution of the viscosity as a function of shear rate for aqueous suspensions: (●) TBC1%+CNC0%, (○) CNC 1%, (▲) TBC1%+ CNC1%, (△)TBC1%+CNC2%, (■) TBC1%+CNC3%, (□) TBC1%+ CNC4%, (✕) TBC1%+CNC5%, (♦) TBC1%+CNC7%, (◇) TBC1%+ CNC9%.

4.3.5 SAXS experiments on CNC/A-CNC

Figures 6a and 6b show the radial average experimental curves obtained for neat CNC and A-CNC suspensions, respectively, at concentrations of 0.1 and 0.5 wt%. These curves basically give the scattering information about the elements of the suspension at different magnifications. For higher q values the signal arises from the whole scattering objects and for lower q values it comes from their mutual interactions. The effect of concentration on the structural organization in chiral nematic phase was studied in a previous work.[29] The average separation distance between the CNCs has been determined for a concentration domain ranging from 1.3 to 6.5 vol% which corresponds to 2.08 to 10.4 wt%. The results obtained in the present work correspond to very dilute samples (0.1 and 0.5 wt%) in the isotropic phase. At 0.5 wt% the scattering intensity exhibits a shoulder at q = 0.045 nm^{-1}. We can evaluate an approximate inter-particle distance d = 2□/ q = 140 nm, which is much larger than the diameter of CNC and explains why there is no change in the scattering curve within the analysed low concentration range for the suspension without (Fig. 6 a) or with adsorbed polymer (Fig. 6b).

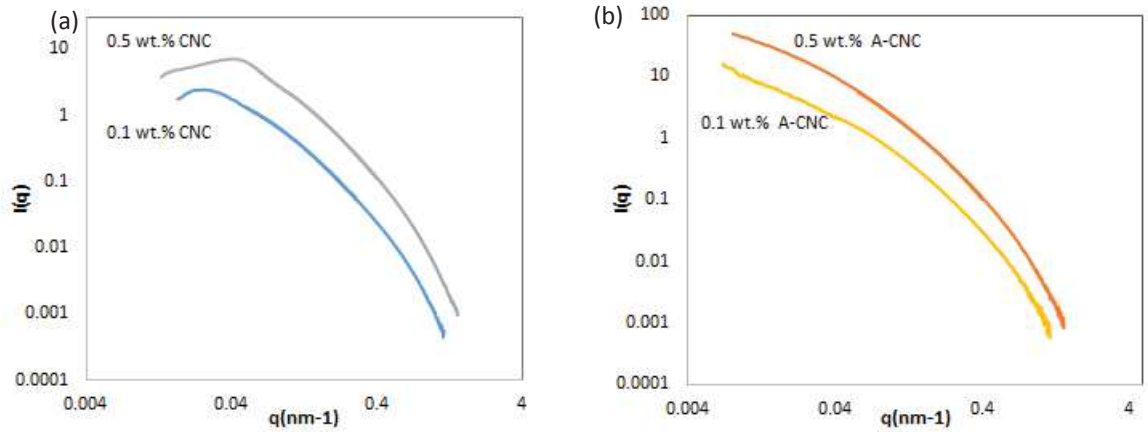

Fig. 6 SAXS characterization of CNC suspensions: scattering intensity as a function of scattering vector for suspensions at concentration of 0.5 and 0.1 wt%: (a) neat CNC, and (b) A-CNC.

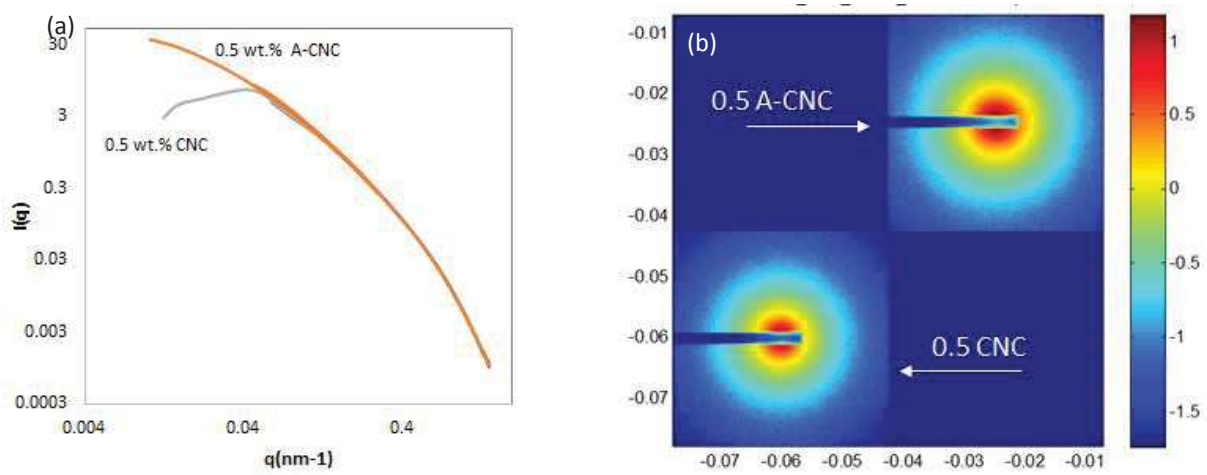

Fig. 7 SAXS characterization of CNC suspensions: (a) scattering intensity as a function of scattering vector for CNC and A-CNC suspensions at concentration of 0.5 wt%, and (b) two-dimensional SAXS pattern for 0.5wt% CNC and A-CNC suspensions at SD = 10 m.

Figure 7a shows a comparison of the radial average experimental curves for the 0.5 wt% CNC suspension before and after TBC adsorption. It is interesting to mention that the scattering intensity is the same for the 0.5 wt% CNC and A-CNC on a wide range of q vectors corresponding to the form factor of the particles, and that a clear change in scattering intensity is detected at lower q vector values below q = 0.045 nm^{-1}. At high scattering vector the scattering intensity is the same before and after adsorption because adsorption is not changing the overall dimensions of the CNC. For lower q vectors (below q = 0.045 nm^{-1}) the A-CNC suspension exhibits an increase in scattering intensity which can be attributed to a change in mutual interactions between the adsorbed cellulose nanocrystals, while no similar effect is detected for neat CNC. Furthermore, the inter-particle distance at q = 0.045 nm^{-1} evaluated for neat CNC is emphasised on the 2D SAXS pattern by the presence of a ring which is no more valid for A-CNC as shown in Figure 7b. The absence of this inter-particle regular distance could be interpreted by the fact that the presence of the copolymer homogeneously dispersed the nanoparticles without regular spacing pertaining to primary aggregates which at higher concentrations give rise to the chiral nematic organization. It is worth noting that this work consists of a preliminary study and future investigation will be conducted at higher concentrations for both neat and adsorbed cellulose nanocrystals.

4.3.6 FTIR experiments

FTIR spectroscopy was used to investigate the functional properties of neat CNC, TBC and A-CNC. The results are shown in Figure 8. Before the adsorption of TBC on CNC, the FTIR spectrum for neat CNC displayed several bands characteristic of cellulose at 3350 cm^{-1} (O–H), 2868 and 2970 cm^{-1} (C–H from –CH2–). The bands at 2970 and 1373 cm^{-1} for TBC correspond to the existence of methyl groups in the PEO-PPO-PEO block copolymer. The antisymmetric C-H stretching vibration of methyl groups in PPO blocks can be seen at 2970 cm^{-1} and 1373 cm^{-1} band confirming the symmetric deformation band of methyl groups.[30,31] Importantly, bands at 1360 and 1108cm^{-1} correspond to the CH2-wagging and C-O-C stretching, respectively, between the PEO and PPO blocks.[30-32]

For A-CNC a substantial increase of the magnitude of the band at 2970 cm^{-1} corresponding to symmetric –CH2 – stretches from copolymer is observed. The signal associated with the vibration of adsorbed water at 1650 cm^{-1} strongly decreased after surface adsorption with TBC. This might be due to the hydrophobic behaviour of the PPO block which is away from the CNC surface as shown in Figure 2. Moreover, the bands appearing at 1360 and 1108 cm^{-1} correspond to TBC. Hence it is evident that the PEO-PPO-PEO block copolymer is present at the surface of CNC.

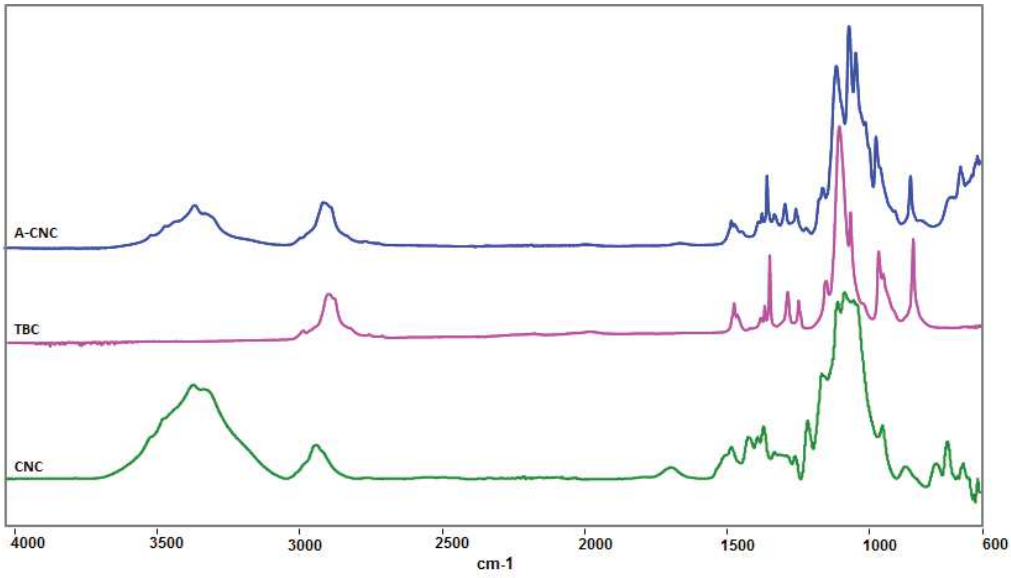

Fig. 8 FTIR spectra for CNC, TBC and A-CNC.

4.3.7 TGA

The thermal degradation behaviour of freeze-dried CNC and A-CNC was investigated by TGA measurements. The results of weight loss and dTG as a function of temperature are reported in Figures 9a and 9b, respectively. Neat CNC displays a slight weight loss from 30 to 130°C. It is attributed to the presence of water due to the hydrophilic character of cellulose. This effect was decreased for the triblock copolymer-adsorbed sample (A-CNC) showing its more hydrophobic nature. It is ascribed to a lower accessibility of -OH groups after TBC surface adsorption. Then, a sharper weight loss is observed in the range 250-300°C for CNC whereas in the case of A-CNC the weight loss is observed over a broader temperature range between 250 and 400°C. The relative dTG curves corresponding to CNC and A-CNC (Fig. 9b) clearly indicate that the main degradation temperature for CNC is slightly lower than for A-CNC. It shows further that the surface of CNC is adsorbed with the triblock copolymer. The thermal decomposition temperatures, associated to weight loss and maximum of derived signal, were determined and results are collected in Table 1.

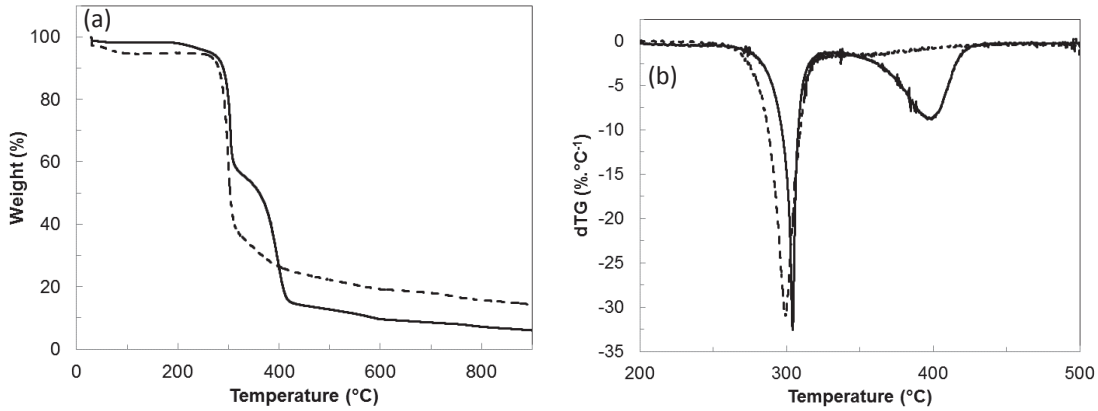

Fig. 9 (a) TGA and (b) dTG curves for CNC (dashed line) and A-CNC (solid line).

Table 1 Temperature values at different relative weight loss for neat CNC and A-CNC.

Sample	Temperature (°C) at different relative weight loss			
	10%	20%	40%	60%
CNC	227	284	298	316
A-CNC	238	289	304	398

4.3.8 X-ray diffraction

The crystallinity of neat CNC and A-CNC was investigated by X-ray diffraction and the patterns are shown in Figure 10. The diffraction peaks for CNC at 22.6°, 14.8°, 16.4°, and 34.4° were assigned to the typical reflection planes of cellulose I.[33] In the case of TBC-adsorbed CNC (A-CNC) new crystalline peaks are observed at 2θ = 19.2°, 26.2° and 26.9° ascribed to PEO chains[8] present in the triblock copolymer. Interestingly the intensity at 16.4° increases after adsorption of TBC confirming that the surface of CNC was adsorbed with PEO-PPO-PEO.

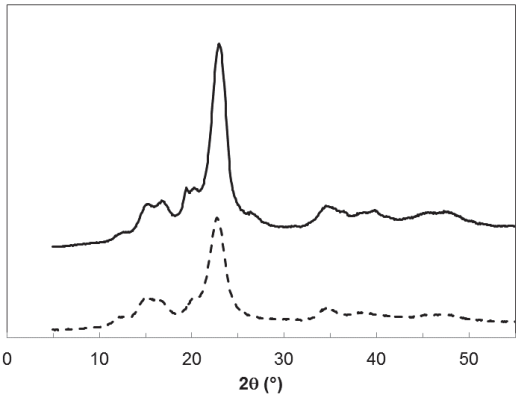

Fig. 10 X-ray diffraction patterns for CNC (dashed line) and A-CNC (solid line).

4.4 CNC/A-CNC reinforced nanocomposites

Neat CNC and TBC-adsorbed CNC reinforced LLDPE nanocomposites were prepared by twin-screw extrusion as detailed in the experimental section. The aspect of resultant nanocomposite films is shown in Figure 11. The neat PE film is translucent as any low thickness semi crystalline polymeric film. When adding only 5 wt% CNC, the film becomes homogeneously darker. This dark colouration after extrusion is a clear indication of the thermal degradation of the cellulosic filler.[21,27] The appearance of the nanocomposite films reinforced with up to 10 wt% A-CNC is similar to that of the neat PE film. This observation agrees with TGA experiments and could be related to the protection of sulphate groups provided by adsorbed TBC.

Fig. 11 Appearance of extruded CNC/LLDPE and A-CNC/LLDPE nanocomposite films.

4.4.1 Thermal properties

The thermal characterization of CNC/A-CNC reinforced LLDPE nanocomposite films was carried out using DSC. From the analysis of DSC traces, the melting temperature (Tm), associated heat of fusion (ΔHm) and degree of crystallinity (χc) were obtained for the unfilled LLDPE film and nanocomposite materials reinforced with either CNC or A-CNC. The resulting experimental data are listed in Table 2.

Table 2 Melting characteristics of LLDPE based nanocomposites reinforced with CNC or A-CNC obtained from DSC measurements: melting temperature (Tm), enthalpy of fusion (ΔHm) and degree of crystallinity (χ_c).

Sample	Tm(°C)	ΔH_m (J/g)	χ_C[a]
LLDPE	118.0	117.4	40.5
LLDPE+1%A-CNC	117.4	121.5	41.9
LLDPE+3%A-CNC	117.5	128.9	44.4
LLDPE+6%A-CNC	119.9	113.9	39.3
LLDPE+10%A-CNC	120.1	117.0	40.3
LLDPE+5%CNC	118.0	99.35	34.3

[a] $\chi_C = \Delta H_m / w\, \Delta H°_m$ where w is the weight fraction of polymeric matrix in the composite and $\Delta H°_m$ = 290 $J.g^{-1}$ (heat of fusion for 100% crystalline LLDPE).

The melting point remained roughly constant between 117 and 120°C upon A-CNC or CNC addition. It indicates that the size of the crystallites was not affected by the filler. On the contrary, the degree of crystallinity of LLDPE was slightly increased for low A-CNC contents (1 and 3 wt%). This effect is classically observed for CNC reinforced semi-crystalline polymers and is generally attributed to a nucleating effect of the cellulosic nanoparticle. For higher A-CNC contents (6 and 10 wt%) the degree of crystallinity of LLDPE crystallinity showed lower values and was similar to that of the neat matrix. It could possibly result from a competitive effect between the nucleating effect of A-CNC and increase of the viscosity of the medium that limits the crystallization of the matrix. Similar behaviour has been reported for CNC reinforced PEO.[34] LLDPE reinforced with 5 wt% neat CNC displays a very low degree of crystallinity compared to neat LLDPE. It seems reasonable to speculate that aggregation and limited filler/matrix interface, as well as thermal degradation of the cellulosic nanofiller, are responsible for this phenomenon.

4.4.2 Mechanical properties

Figure 12 shows the evolution of the logarithm of the storage modulus as a function of temperature for CNC/A-CNC reinforced LLDPE nanocomposites. The behaviour of the neat matrix has been added in the figure for reference. The modulus is roughly constant in the low temperature range but it drops around -40°C due to the anelastic manifestation of the glass transition of the polymeric matrix. For higher temperatures the modulus gradually decreases

because of the progressive melting of the polymer. At the melting temperature of the polymeric matrix, the modulus dropped sharply and the setup fails to measure it due to irreversible chain flow.

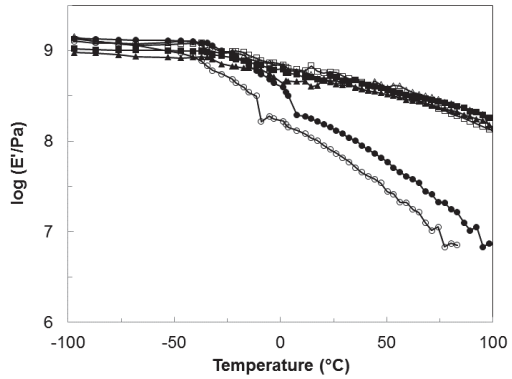

Fig. 12 Evolution of the logarithm of the storage tensile modulus as a function of temperature for the neat and LLDPE nanocomposites: (●) LLDPE, (○) LLDPE+5%CNC, (▲) LLDPE+1%A-CNC, (△) LLDPE+ 3%A-CNC, (■) LLDPE+6%A-CNC, (□) LLDPE+10%A-CNC.

No significant difference is reported between the unfilled LLDPE and nanocomposites in the glassy state of the matrix as expected because of the stiffness of the matrix in this temperature range. At higher temperatures differences are observed and it is clearly seen that the rubbery modulus of the nanocomposite reinforced with 5 wt% neat CNC is lower than that of the matrix. This might be because of the degradation and poor dispersion of CNC. The lower degree of crystallinity of the sample should also, at least partially, participate to this effect. While adding A-CNC, the rubbery modulus significantly increased possibly ascribed to a reinforcing effect of the nanofiller. Improved dispersion of the nanoparticles and favourable interactions with the matrix, but also increased crystallinity of the matrix, are most probably responsible for this effect. It is worth noting that the modulus of the nanocomposite is practically independent of the filler content. It is usually difficult to separate the impact of the CNC-induced crystallization and real reinforcing effect of the nanofiller, but in our case since the degree of crystallinity of the neat matrix and highly filled nanocomposites (6 and 10 wt% A-CNC) are similar (see Table 2), the higher rubbery modulus of the nanocomposites can be unambiguously attributed to a reinforcing effect of the cellulose nanorods. It is worth noting

that this reinforcing effect is much higher than that observed for PE nanocomposites reinforced with CNC coated with PEO homopolymer.[27]

4.4.3 Morphological investigation

The cryo-fractured cross section of the nanocomposite films was investigated by SEM (Figure 13). By comparing Figure 13a (neat LLDPE matrix) and Figure 13b (LLDPE reinforced with 5 wt% CNC), the presence of the nanofiller results in the observation of microscopic holes. These holes most probably correspond to CNC aggregates formed during drying because of hydrogen bonding between individual CNC, that have been degraded during melt processing at 160°C. The cross section of nanocomposites reinforced with A-CNC (Fig. 13 c-f) is similar to that of the neat matrix showing the homogeneous dispersion of the nanofiller within the matrix. These observations corroborate the mechanical properties obtained for these materials.

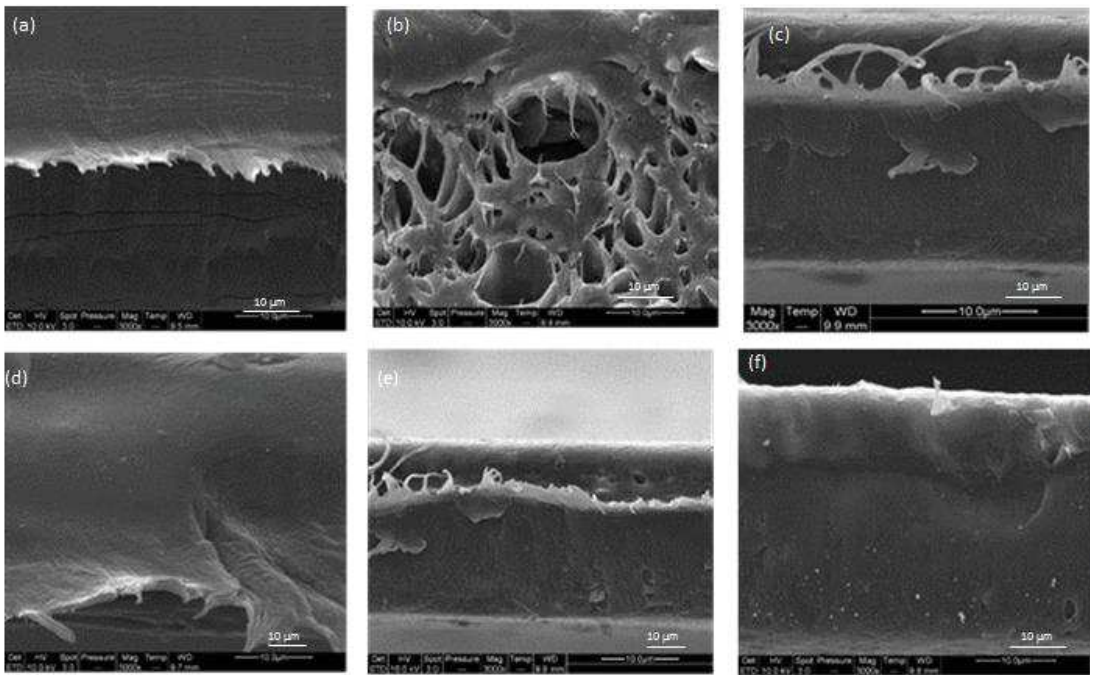

Fig. 13 SEM images of the cryo-fractured cross section for extruded films: (a) neat LLDPE, and LLDPE nanocomposites reinforced with (b) 5 wt% CNC, and (c) 1, (d) 3, (e) 6 and (f) 10 wt % A-CNC.

4.4.4 SAXS characterization

Figure 14 compares the evolution of the scattering intensity as a function of scattering vector for PE+5%CNC and PE+6%A-CNC nanocomposites. A slight variation can be seen between both samples which is due to the slightly different nanofiller content. The inserted images are the scattering patterns corresponding to these samples. Significant difference can be seen between neat CNC and TBC-adsorbed CNC reinforced nanocomposites. The 2D scattering pattern is more anisotropic for PE+6%A-CNC. This can be ascribed to the difference in the dispersion state of CNC in the matrix before and after TBC adsorption. The PE+5%CNC nanocomposite displays poor dispersion, whereas the nanofiller in PE+6%A-CNC has a more uniform dispersion, agreement with SEM observations.

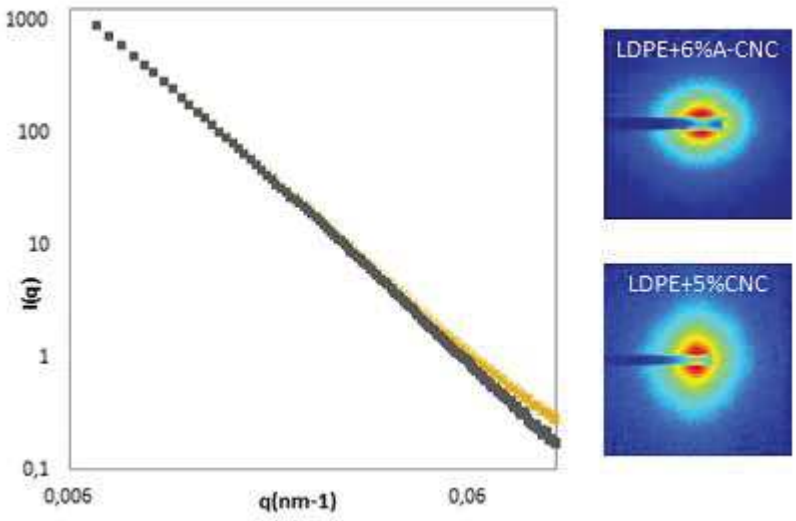

Fig. 14 SAXS characterization of CNC and A-CNC reinforced LDPE nanocomposite films: Scattering intensity as a function of scattering vector for LDPE+6%A-CNC (×), LDPE+5%CNC (♦) and corresponding 2D-SAXS patterns.

Figure 15 shows the 2D-SAXS patterns for A-CNC nanocomposites with different nanofiller contents varying from 1 to 10 wt%. The SAXS patterns exhibit an anisotropic shape with a higher intensity in the horizontal direction which corresponds to a preferential orientation of A-CNC in the flow direction during the extrusion process. For increasing A-CNC content, the anisotropic level is amplified which could be attributed to a higher orientation of the

nanorods or to an increasing quantity of A-CNC nanoparticles orientated in the flow direction during the extrusion process.

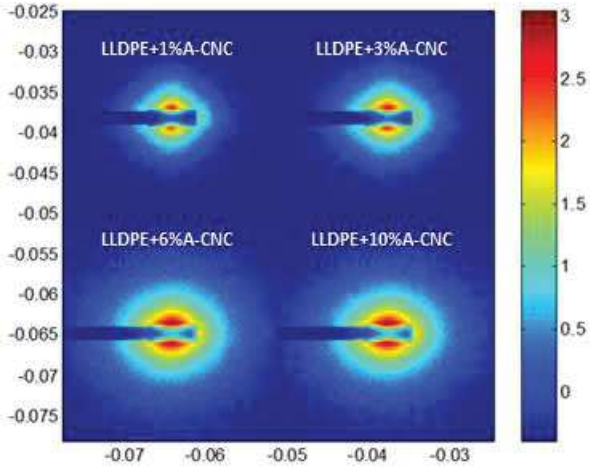

Fig. 15 2D SAXS patterns for LDPE nanocomposites with different A-CNC contents.

4.5 Conclusion

In this study we have developed an efficient and simple water based method to prepare cellulose nanocrystal (CNC) reinforced polyethylene nanocomposites by melt processing. It consists in coating the nanoparticle (ratio 1:1) with a triblock copolymer (TBC) having two hydrophilic ends attached to a hydrophobic central block. The hydrophilic ends were expected to interact with the cellulosic surface leaving the hydrophobic block free to provide compatibility with the polyethylene matrix chains. Coating of CNC with the copolymer was visualized from AFM observations and the rheological behaviour of aqueous dispersions indicates that the surface adsorption capability of CNC is around 1-2 g of TBC for 1 g of pristine CNC. Moreover, this coating allows a much easier and better re-dispersion in water of the nanoparticles after freeze-drying, that was also characterized by SAXS experiments, and improves their thermal stability. After melt extrusion with polyethylene, the visual appearance of films prepared from TBC-coated CNC was clearly indicative of an improved dispersion, that was also evidenced from SEM observations, and limited thermal degradation. It results in significantly improved mechanical properties for the nanocomposites. SAXS experiments show a much more prominent preferential orientation and alignment in the flow direction for TBC-coated CNC compared to neat CNC which is induced by the extrusion step. It further indicates that individual coated nanorods are present in the nanocomposite films.

4.6 References

1 M.A.S. Azizi Samir, F. Alloin and A. Dufresne, Biomacromolecules, 2005, **6**, 612.

2 Y. Habibi, A.L. Lucia and O.J. Rojas, Chem. Rev., 2010, **110**, 3479.

3 D. Klemm, F. Kramer, S. Moritz, T. Lindström, M. Ankerfors, D. Gray and A. Dorris, Angew. Chem. Int. Ed., 2011, **50**, 5438.

4 R.J. Moon, A. Martini, J. Nairn, J. Simonsen and J. Youngblood, Chem. Soc. Rev., 2011, **40**, 3941.

5 N. Lin and A. Dufresne, Biomacromolecules, 2013, **14**, 871.

6 A. Dufresne, Molecules, 2010, **15**, 4111.

7 S.J. Eichhorn, A. Dufresne, M. Aranguren, N.E. Marcovich, J.R. Capadona, S.J. Rowan, C. Weder, W. Thielemans, M. Roman, S. Renneckar, W. Gindl, S. Veigel, J. Keckes, H. Yano, K. Abe, M. Nogi, A.N. Nakagaito, A. Mangalam, J. Simonsen, A.S. Benight, A. Bismarck, L.A. Berglund and T. Peijs, J. Mater. Sci., 2010, **45**, 1.

8 N. Lin and A. Dufresne, Macromolecules, 2013, **46**, 5570.

9 N. Lin, J. Huang and A. Dufresne, Nanoscale, 2012, **4**, 3274.

10 K.L. Dagnon, K. Shanmuganathan, C. Weder and S.J. Rowan., Macromolecules, 2012, **45**, 4707.

11 J.D. Fox, J.R. Capadona, P.D. Marasco and S.J. Rowan, J. Am. Chem. Soc., 2013, **135**, 5167.

12 N. Lin and A. Dufresne, Nanoscale, 2014, **6**, 5384.

13 A. Dufresne, Nanocellulose: From nature to high performance tailored materials, Walter de Gruyter GmbH: Berlin and Boston, MA, 2012.

14 F. Alloin, A. D'Aprea, A. Dufresne, N. El Kissi and F. Bossard, Cellulose, 2011, **18**, 957.

15 W.J. Orts, J. Shey, S.H. Imam, G.M. Glenn, M.E. Guttman and J.F. Revol, J. Polym. Env., 2005, **13**, 301.

16 A.L. Goffin, J.M. Raquez, E. Duquesne, G. Siqueira, Y. Habibi, A. Dufresne and P. Dubois, Biomacromolecules, 2011, **12**, 2456.

17 A.L. Goffin, J.M. Raquez, E. Duquesne, G. Siqueira., Y. Habibi, A. Dufresne and P. Dubois, Polymer, 2011, **52**, 1532.

18 A.J. de Menezes, G. Siqueira, A.A.S. Curvelo and A. Dufresne, Polymer, 2009, **50**, 4552.

19 J.M. Raquez, Y. Murena, A.L. Goffin, Y. Habibi, B. Ruelle, F. DeBuyl and P. Dubois, Compos. Sci. Technol., 2012, **72**, 544.

20 S.H. Xu, J. Gu, Y.F. Luo and D.M. Jia, EXPRESS Polym. Lett., 2012, **6**, 14.

21 K. Ben Azouz, E.C. Ramires, W. van den Fonteyne, N. El Kissi and A. Dufresne, ACS Macro Lett., 2012, **1**, 236.

22 E. Fortunati, I. Armentano, Q. Zhou, A. Iannoni, E. Saino., L. Visai, L.A. Berglund and J.M. Kenny, Carbohydr. Polym., 2012, **87**, 1596.

23 Q. Zhou, H. Brumer and T.T. Teeri, Macromolecules, 2009, **42**, 5430.

24 K. Oksman, A.P. Mathew, D. Bondeson and I. Kvien, Compos. Sci. Technol., 2006, **66**, 2776.

25 D. Bondeson and K. Oksman, Compos. Part A-APPL S, 2007, **38**, 2486.

26 M. Nagalakshmaiah, N. El Kissi and A. Dufresne, ACS Appl. Mater. Interfaces, 2016, **8**, 8755.

27 M. Pereda, N. El Kissi and A. Dufresne, ACS Appl. Mater. Interfaces, 2014, **6**, 9365.

28 Y. Li, H. Liu, J. Song, O.J. Rojas and J.P. Hinestroza, ACS Appl. Mater. Interfaces, 2011, **3**, 2349.

29 C. Schütz, M. Agthe, A.B. Fall, K. Gordeyeva, V. Guccini, M. Salajková, T.S. Plivelic, J.P.F. Lagerwall, G. Salazar-Alvarez and L. Bergström, Langmuir 2015, **31**, 6507.

30 M.A.K.L. Dissanayake and R. Frech, Macromolecules, 1995, **28**, 5312.

31 N. Kimura, J. Umemura and S. Hayashi, J. Colloid Interface Sci., 1996, **182**, 356.

32 S. Yan-lei, W. Jing and L. Hui-zhou, Langmuir, 2002, **18**, 5370.

33 H. Liu, D. Liu, F. Yao and Q. Wu, Bioresource Technol., 2010,**101**, 5685.

34 M.A.S. Azizi Samir, F. Alloin, J.Y. Sanchez and A. Dufresne, Polymer, 2004, **45**, 4149.

Chapter-5

Fabrication of polystyrene nanocomposites reinforced with poly [(styrene)-co-(2-ethylhexylacrylate)]-modified cellulose nanocrystals

(Yet to submit)

5. Fabrication of polystyrene nanocomposites reinforced with poly [(styrene)-co-(2-ethylhexyl acrylate)]-modified cellulose nanocrystals.

ENGLISH ABSTRACT

Cellulose nanocrystals (CNC) play a vital role to improve the mechanical properties of polymer composites since they are unique in mechanical possessions. Due to the low thermal stability of CNC, the preparation of polymer composites by melt-processing is limited. In order to enhance the thermal stability of CNC, they were modified taking advantage of ionic interactions with laboratory-prepared statistical copolymer, *viz.* poly [(styrene)-*co*-(2-ethylhexyl acrylate)]. CNC modified using a water based method were characterized to determine their thermal, functional and structural properties by means of thermogravimetric analysis (TGA), Fourier transform infrared spectroscopy (FTIR), X-ray diffraction (XRD), XPS and atomic force microscopy (AFM). Their hydrophobic nature was investigated by using contact angle measurements. In order to improve the compatibility between CNC and polystyrene matrix, and with the anticipation of high mechanical properties, the modified CNC were incorporated into polystyrene by melt extrusion. The thermomechanical performance of the ensuing composites was examined by means of differential scanning calorimetry and dynamic mechanical analysis (DMA). The morphology of the composites were also studied using scanning electron microscopy (SEM).

RÉSUMÉ FRANÇAIS

Du fait de leurs propriétés mécaniques exceptionnelles, les nanocristaux de cellulose (CNC) jouent un rôle essentiel dans l'optimisation des propriétés de renfort des composites polymères. Cependant, la faible stabilité thermique des CNC limite l'élaboration des composites polymères par des procédés à l'état fondu qui sont de fait une véritable voie de développement à l'échelle industrielle de ce type de matériau. Par conséquent, afin d'améliorer la stabilité thermique des CNC et permettre leur mise en forme à l'état fondu, une modification de leurs propriétés de surface a été envisagée et nous avons utilisé pour cela un copolymère statistique préparé au laboratoire, à savoir le poly [(styrène)-co-(acrylate de 2-éthylhexyle)], capable de développer des interactions ioniques avec les groupements sulfates présents à la surface des CNC du fait de l'hydrolyse acide utilisée pour les préparer. Cette modification intervient en milieu aqueux. Les CNC modifiés ont été caractérisés par leurs propriétés thermiques, structurales et fonctionnelles. Nous avons utilisé pour cela l'analyse thermogravimétrique (TGA), la spectrométrie infrarouge à transformée de Fourier (FTIR), la diffraction des rayons X (XRD) et la microscopie à force atomique (AFM). La nature hydrophobe des surfaces obtenues a été caractérisée par mesure d'angles de contact. Les CNC modifiés ont été incorporé à une matrice polystyrène (PS) et un film composite a été élaboré par extrusion à l'état fondu. Les performances thermomécaniques des composites ainsi obtenus ont été déterminées par calorimétrie différentielle à balayage et analyse mécanique dynamique (DMA). Les propriétés la morphologie ont également été caractérisées. Nous avons réalisé pour cela des essais des observations par microscopie électronique à balayage (SEM).

5.1 Introduction

During the last two decades cellulose nanocrystals (CNC) have been emerging as most promising nanomaterial for both researchers and industries due to their astonishing properties, *e.g.* elastic modulus reaching 150 GPa, high aspect ratio (10−70), high surface area (150 m^2/g) and high crystallinity (95%) (1–5). This in turn expands the production of CNC, which will likely increase by 5 times at least by 2017 (6). Such progress leads to various applications, particularly in the field of composite materials. In this regard, the incorporation of CNC in polymer matrices leads to improvement of the mechanical properties (7).

Most of the research articles reports a solvent casting method for the production of polymer nanocomposites, since it preserves the dispersion state of cellulose nanoparticles in the liquid. However, such approach is limited by the number of polymer matrices that can be used in combination with CNC because of polymer solubility (8). Moreover, solvent casting is not a cost effective process, whereas melt processing is commonly used to process thermoplastic polymers. The latter is industrially and economically viable and also a solvent-free process. However, it limits the optimal preparation of nanocomposites with CNC due to low thermal stability and poor dispersion during drying stage because of the irreversible agglomeration. The huge number of hydroxyl groups at the surface of CNC allows to improve its thermal stability, dispersibility, as well as to provide good compatibility with matrix through surface modification, such as chemical grafting or physical adsorption. Such modification is favourable for further processing of composites by melt extrusion, as previously reported (9-19).

The challenge of melt processing for CNC is to find a suitable treatment to avoid the aforementioned problem and to avoid the issues of inherent incompatibility between cellulose and most polymeric matrices. In a previous work (14), we have demonstrated that physical

adsorption of polyethylene oxide (PEO) chains on the surface of CNCs can improve dispersibility and thermal stability of nanocrystals during the melt processing of low-density polyethylene (LDPE)-based nanocomposites. The improved thermal stability of PEO-adsorbed CNC was ascribed to a protection role of wrapped PEO chains that hide the surface sulphate groups of nanocrystals. In another study (19), surface modification through physical adsorption and/or chemical grafting was performed on CNC, which produced three different types of modified nanocrystals. These three types of CNC were extruded with polystyrene and their reinforcing effect and interfacial mechanisms were investigated.

In this study CNC surface was modified through electrostatic interaction at pH10 with laboratory-synthesized poly[(styrene)-*co*-(2-ethylhexyl acrylate)] prepared by mini emulsion polymerization. These M-CNC which have strong electrostatic interaction with PS co-polymer were extruded with polystyrene. The objective was to obtain good compatibility between the matrix and CNC consequently a reinforcing effect of the incorporated nanofiller.

5.2 Experimental Section

5.2.1 Materials

Styrene (≥99%) and 2-ethylhexyl acrylate (2-EHA, 98%) were purchased from Sigma-Aldrich and were further distilled under vacuum and stored in a cool place (at 4 °C) under nitrogen gas atmosphere. Sodium hydroxide, Luperox A75 (75% of benzoyl peroxide, remainder water), tetra decyl trimethyl ammonium bromide (TTAB, ≥99%), 1-hexadecanol (≥99%) were purchased from Sigma-Aldrich and were used without further purification. Polystyrene (PS) from sigma Aldrich, with density of 1.047 g/mL and molecular weight of 280000 g/mol was chosen as the matrix for the processing of nanocomposites. Commercial 11.5 wt% CNC suspension prepared by sulfuric acid hydrolysis was procured from University of Maine, USA.

5.2.2 Methods

Dynamic light scattering (DLS)

Particle size of PS copolymer particles was examined using dynamic light scattering (DLS) with Vasco particle size analyzer (Cordouan Technologies, France). The measurements were made at 25 °C performing 7 acquisitions for one sample. The data treatment was performed using cumulant method.

Differential scanning calorimetry (DSC)

DSC Q100 (TA Instruments, USA) was used to measure the glass transition temperature of the synthetized latex. The samples around 10 mg were hermetically closed in aluminium pans and were examined in the temperature range from −80 to 150 °C at a scanning rate of 10 °C/min under nitrogen (50 mL/min). The first heating–cooling cycle was carried out to remove the previous thermal history. The glass transition temperature was measured from the second heating scan.

DSC was also used to investigate the thermal behaviour of nanocomposites. The glass transition temperature of nanocomposites was measured with a Perkin-Elmer DSC instrument using aluminium pans. The samples were scanned from 60 to 250°C at a heating rate of 10°C.min^{-1}.

Atomic force microscopy (AFM)

AFM observations were performed to study the diameter and approximate length of individual nanocrystals using a Nanoscope III (Veeco, Canada). CNC and M-CNC samples were previously diluted to a concentration of 0.01wt% and a drop of the suspension was deposited onto freshly cleaved mica substrate and dried overnight under ambient conditions. Each sample was characterized in a tapping mode with a silicon cantilever (OTESPA®, Bruker, USA). Different locations were analysed to obtain representative measurements. Both topographical and phase images were captured and images were subjected to 1st order

polynomial flattening to reduce the effects of bowing and tilt. CNC diameter was determined from height profile of height sensor images.

Rheological behaviour

The viscosity of the aqueous suspensions of cellulose nanoparticles modified with PS copolymer was analysed with the stress-controlled rheometer ARG2 (TA Instruments) equipped with a 2° cone and plate geometry of 60 mm in diameter. All the rheological measurements were performed at a temperature of 20°C.

Fourier transform infrared spectroscopy (FTIR)

FTIR analysis was performed using a Spectrum 65 spectrometer (PerkinElmer, USA) on dried CNC and M-CNC obtained by freeze drying after 24 h, in order to determine the functional groups present in the CNC and M-CNC. The samples were analysed by attenuated total reflectance (ATR) in which the sample was placed on the evanescent wave on the ATR crystal, through which infrared beam gives the data to the detector.

Thermogravimetric analysis (TGA)

Thermal degradation of the CNC and M-CNC was observed by TGA using a Simultaneous Thermal analyser (STA) 6000 (PerkinElmer, USA). Weight loss and heat flow curves were recorded for a 20 mg sample at a heating rate of 10 °C/min in the temperature range of 30–950 °C under oxidizing atmosphere (air).

X-ray diffraction (XRD)

XRD analysis was performed for freeze dried CNC and M-CNC. The samples were placed in a 2.5 mm deep cell and measurements were performed with a diffractometer (X' Pert PROMPD®) equipped with a detector. The operating conditions of the refractometer were: copper Kα radiation (λ = 1.5418 Å), 2θ (Bragg angle) between 2 and 56°, step size 0.067°, and counting time 90 s.

X-ray photoelectron spectroscopy (XPS)

The PS copolymer surface-modified CNC and neat CNC were analysed by XPS. The experiments were carried out using an XR3E2 apparatus (Vacuum Generators, U.K.) equipped with an unmonochromated Mg KR X-ray source (1253.6 eV) and operated at15 kV under a current of 20 mA. Samples were placed in an ultrahigh vacuum chamber (10−8 mbar) with electron collection by a hemispherical analyser at a 90° angle. Signal decomposition was done using Spectrum NT, and the overall spectrum was shifted to ensure that the C−C/C−H contribution to the C 1s signal occurred at 285.0 kV.

Contact Angle Measurements

The hydrophilic/hydrophobic nature of CNC/M-CNC was evaluated at room temperature by measuring the contact angle of a small water drop (ca. 5μL) using an Attension theta contact angle meter. Smooth surfaces were obtained by compacting freeze-dried CNC under a pressure of 10 MPa. Contact angle values were determined from Attension theta Software.

Melt extrusion

A twin-screw DSM Micro 15 compounder was used to prepare the nanocomposites. The polymer matrix pellets (PS) and freeze-dried CNC/M-CNC were mixed (around 15 g total material) and introduced in the mixing chamber of the extruder. Extrusion was performed at 190°C with a mixing speed of 100 rpm for 8 min. The mixture was then extruded through a slit die of 0.6 mm in width and 1 cm in length. Micro-film device was attached directly to the micro-compounder outlet port. Nanocomposites with M-CNC contents of 1, 5 and 10 wt%, and neat CNC content of 5 wt% were prepared.

Dynamic mechanical analysis (DMA)

DMA was used to study the viscoelastic behaviour of the nanocomposites. DMA experiments were carried out using a RSA3 (TA Instruments) equipment working in the tensile mode. The storage modulus E′ (elastic response) of the material was measured as a function of

temperature as it was deformed under an isochronal oscillatory stress at a controlled temperature in a specified atmosphere. The storage modulus is related to the stiffness of the material. Varying stress with a frequency of 1 Hz was applied to the sample while heating from 60 to 120°C with a scanning rate equal to 5°C.min^{-1}. The length of the samples was 10 mm.

Scanning electron microscopy (SEM)

SEM was used to characterize the nanocomposite cross section in order to determine the roughness of films after incorporating the CNC/M-CNC and study the homogeneity of their dispersion. Prior to the analysis, the samples were frozen using liquid nitrogen and broken in order to obtain a clear fracture. The samples were coated with a gold layer in order to prevent the charring of the sample due to the electron bombardment. The SEM images were captured using FEI Quanta 200 SEM (FEI, Netherlands).

Field emission gun scanning electron microscopy (FEG-SEM)

The FEG-SEM was executed using ZEISS Ultra 55 microscope (Zeiss AG, Germany), equipped with In-Lens secondary electron detector at an accelerating voltage of 1–5 kV. The examined latex particles were diluted with distilled water to 0.1 wt.%, deposited on a double-sided adhesive carbon tape and lyophilized using Christ Alpha 2-4 LD plus freeze dryer (Martin Christ, Germany). The samples were sputtered with a gold layer of 3 nm before the analysis.

5.3 Results and discussion

5.3.1 Latex synthesis

Poly [styrene-*co*-(2-ethylhexyl acrylate)] was synthesized *via* mini emulsion polymerization as reported elsewhere (20). Briefly, 0.20 g of TTAB (cationic surfactant) and 0.44 g of 1-hexadecanol (co-stabilizer) were placed in 24.00 g of water and heated at 70 °C for 1 h under mild stirring to prepare a “pre-emulsion”. Then, 8.23 g of styrene and 4.00 g of 2-Ethylhexyl

acrylate were added and the ensuing formulation was emulsified in an ice bath by ultrasound using Branson Sonifier 250 (Emerson Electric, USA) for 5 min at a duty cycle of 70%. A micro tip limit of 4. 1 g of Luperox A75 was added to the obtained nano emulsion and the polymerization reaction was performed under inert nitrogen gas atmosphere, stirring at 150 rpm and heating at 70 °C. The reaction was stopped after 8 h (the time was defined from the monomer conversion analysis, see Fig. 1a) by decreasing the temperature to 25 °C.

5.3.2 Monomer conversion

The degree of monomer conversion was measured using gravimetrical method. Ca. 0.30 mL of the reaction mixture was withdrawn at different times of the polymerization reaction and the exact weight was measured. An exact amount of 1 wt% hydroquinone aqueous solution was added (ca. 0.15 mL) immediately to quench the polymerization reaction. Then, the specimen was dried at ambient temperature until the constant weight in order to evaporate the non-reacted monomers. The degree of monomer conversion was determined as follows:

Conversion (%) = $m_1/m_2 \times 100$

Where m_1 is the weight of the dried specimen with subtracted weight of hydroquinone, surfactant and co-stabilizer; m_2 is the weight of the specimen with subtracted amount of water, hydroquinone, surfactant and co-stabilizer.

5.4 Characterization of PS-copolymer

Figure 1 shows some characterization of the synthesized poly [styrene-*co*-(2-ethylhexyl acrylate)] latex particles. The time evolution of monomer conversion indicates (see Fig. 1a) that almost all the monomer was converted to polymer within 8 h, thus giving information on the necessary time for such reaction conditions. As a result, latex particles with rather wide size distribution were produced in submicron scale (see Fig. 1b). Z-average particle size of 385 nm and a polydispersity index (PDI) of 0.22 were determined from DLS analysis. FEG-SEM (see Fig. 1d) was used to visualize the particles, confirming the results obtained with

DLS. Glass transition temperature of 7 °C was determined from DSC measurements (Fig. 1c), giving the idea about a transition temperature zone from a brittle to rubber-like state.

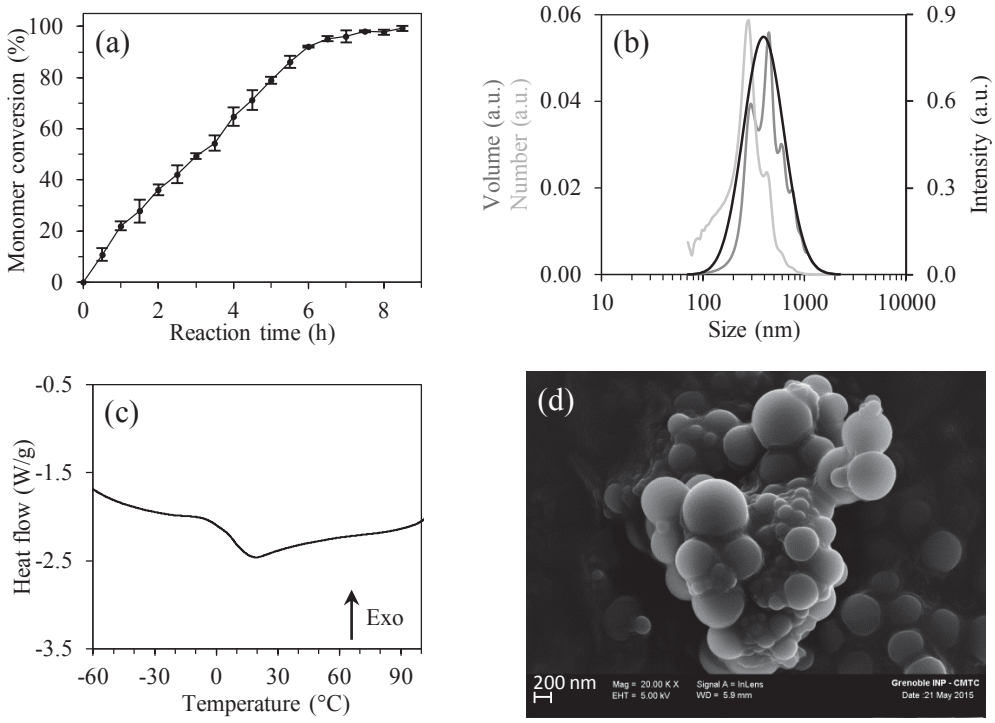

Fig. 1 some properties of the synthetized poly [(styrene)-*co*-(2-ethylhexyl acrylate)]: (**a**) monomer conversion; (**b**) particle size distribution; (**c**) DSC curve and (**d**) FEG-SEM image

5.5 Preparation and characterization of M-CNC

5.5.1 Preparation of M-CNC

As shown in Scheme 1, the polystyrene copolymer synthesized by mini emulsion along with quaternary ammonium salt (QS) tetradecyl trimethyl ammonium bromide was utilized to promote electrostatic interactions with CNC bearing sulfonated groups on their surface. A previously reported procedure was used (21, 22) for this, 3 g of CNC were dispersed in aqueous medium

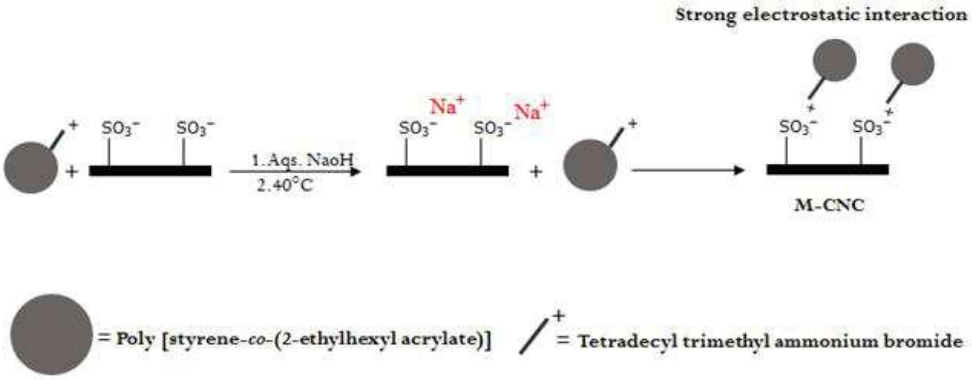

Scheme-1. Illustration reaction of PS-copolymer with cellulose nanocrystals.

(1 wt % in water), and the pH was adjusted to 10 by using NaoH. Then, the CNC dispersion was slowly added to the 300 mg of quaternary salt at 40 °C, i.e. the ratio of salt to CNC was 10 wt %. The mixture was stirred at 40°C for 3 h, under constant temperature. The mixture was freeze-dried to understand the structural, functional, surface, and thermal properties. As illustrated in scheme-1 (right side) the PS copolymer was attached to the CNC by electrostatic interaction with negatively charged sulphated groups on CNC.

5.5.2 Atomic force microscopy

Atomic force microscopy (AFM) was employed to understand the morphology and average size of the modified and adsorbed cellulose nanocrystals. The AFM images of M-CNC are shown in figure 2 at different magnifications. As shown in figure 2 the modified CNC diameter (2-6nm) was increased significantly compared to the neat CNC reported in our previous study (23).

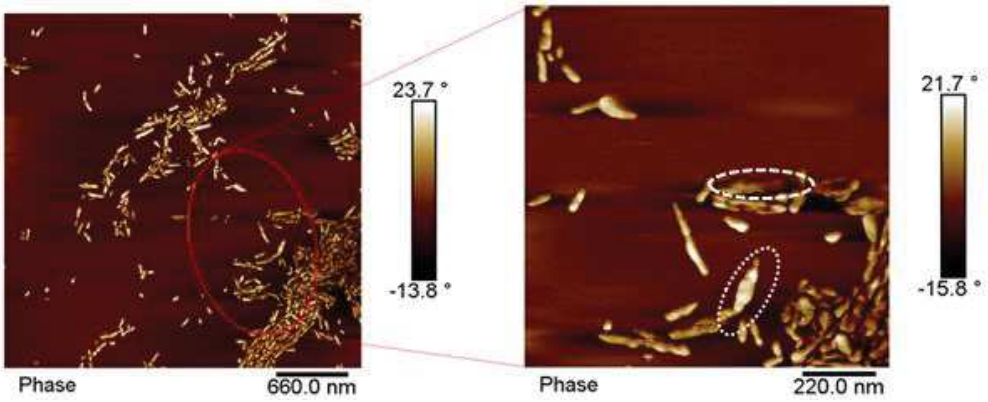

Fig. 2 AFM images of modified cellulose nanocrystals with PS copolymer at different observation scales.

This can be explained by the fact that the PS copolymer formed strong electrostatic interaction with CNC and this can be observed for marked nanocrystals in figure 2 (high magnification). Significantly the dispersion of the nanocrystals was improved due to the electrostatic repulsion between the CNCs.

5.5.3 Viscosity of modified CNC

The viscosity of the modified CNC at 2, 4 and 6wt% was measured as a function of shear rate. The results are shown in figure-3.

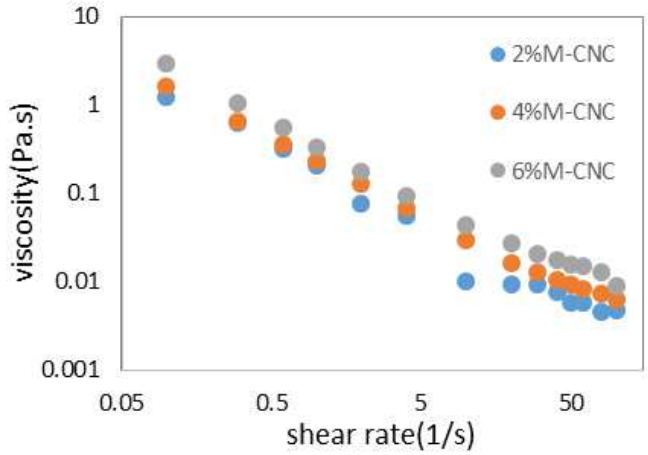

Figure-3. Viscosity vs shear rate for aqueous suspensions of M-CNC

The viscosity was increased while increasing the concentration for M-CNC. Notably, the viscosity was decreased while increasing the shear rate. Certainly this phenomenon can be

attributed to single shear thinning behaviour. This revealed that there was no interaction between the nanocrystals due to the PS copolymer.

5.5.4 Fourier Transform Infrared Spectroscopy (FT-IR)

FT-IR spectroscopy was used to determine the functional properties of the M-CNC and results were compared with PS-copolymer and CNC. The spectra is shown in figure-4.

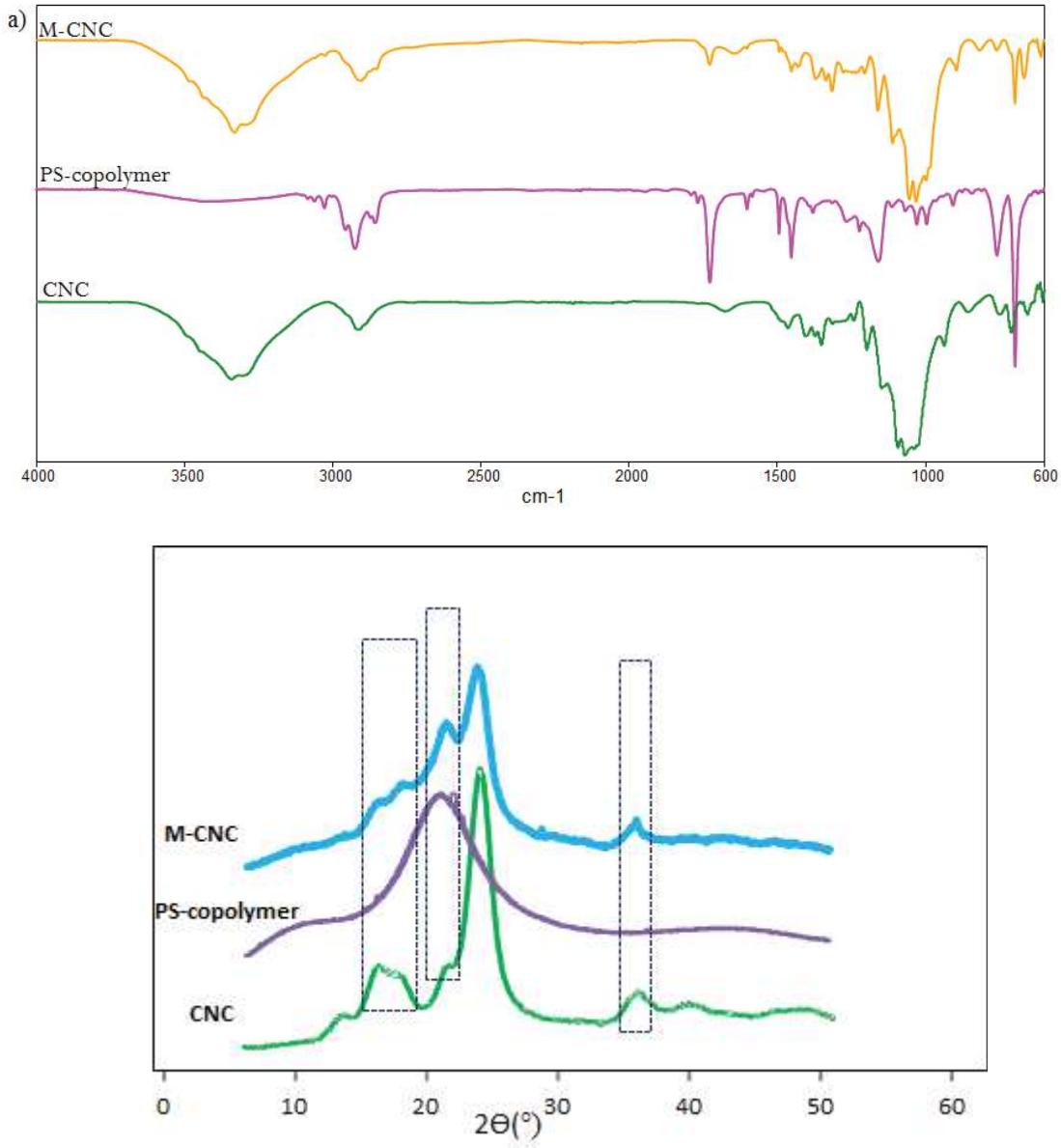

Figure 4. a) FTIR and b) XRD patterns for neat CNC, PS copolymer and M-CNC.

Neat CNC displays several bands characteristic of cellulose at 3350 cm^{-1} (O−H) and 2868 and 2970 cm^{-1} (C−H from−CH2−). The prepared poly [(styrene)-co-(2-ethylhexyl acrylate)]

statistical copolymer spectra shown several significant bands like 3025 and 2921 cm^{-1} (23) corresponding to the aromatic -C-H stretching. Those observed at 1602 and 1494 cm^{-1} are highly characteristic of the aromatic ring itself. More precisely, the 1494 cm^{-1} peak is conforming the substituents of the aromatic ring (24). The peak at 1730 cm^{-1} is matching with the carbonyl stretching vibration of acrylate component and the peaks at 1264 and 1158 cm^{-1} are the stretching vibrations of the saturated ester group (25 and 26). The major bands present in the PS copolymer were present in the modified CNC. It is noteworthy that the peaks at 1730, 1264 and 1158cm^{-1} are saturated in the case of the M-CNC since the adsorbed copolymer content was only 10%.

5.5.5 X-ray diffraction (XRD)

The crystalline patterns for CNC, M-CNC and PS copolymer were obtained by means of XRD and the results are shown in figure 4b. The diffraction peaks appearing at 22.6, 14.8, 16.4, and 34.4° are related to the typical reflection planes of cellulose I (27). A broad amorphous bump at 20.2° was observed for PS copolymer. The diffraction pattern for M-CNC (with peaks at 22.6, 14.8, 16.4 and 34.4°) is similar to CNC. Briefly, this explained that surface modification does not change the crystalline structure of the CNC, as expected. The new signal observed at 20.2° for M-CNC was attributed to the PS copolymer. The intensity of the 16.4° peak was significantly increased after adsorption and surface modification. This was mainly due to the adsorption of PS copolymer. As expected modification with PS-copolymer was only on the surface of cellulose nanocrystals.

5.5.6 Contact angle

The impact of the PS copolymer on surface hydrophobicity of cellulose nanocrystals was determined by using contact angle and the results are reported in figure-5.

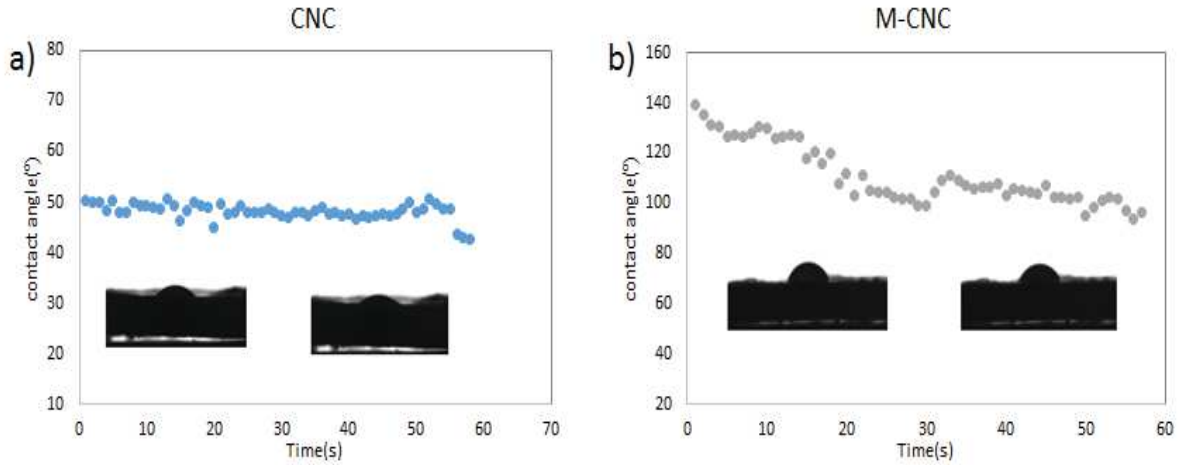

Figure 5 .Evolution of the contact angle for a water drop as a function of time on sheet samples a) CNC, b) M-CNC modified with PS copolymer. (Inserted photographs for the water drop on the sheet sample after 5 and 50 s).

The results show that the contact angle value was significantly higher for modified CNC compared to that of neat CNC. Gradual decrease in the contact angle was observed for CNC and the water droplet was spread with in 50s and the contact angle less than 20° (±2). This was due to the hydrophilic nature of the hydroxyl groups present on the surface of the cellulose. In contrary, the contact angle of the M-CNC was increased to 52° (±4) and 97° (±4) respectively. This can be attributed to the hydrophobic behaviour of the PS copolymer. It is interesting to note that the hydrophobicity of the M-CNC was comparatively higher than that of the neat CNC. This can be because of the strong surface interaction of the PS copolymer in the case of the M-CNC.

5.5.7 Thermo gravimetric analysis (TGA)

The thermal stability of M-CNC was analysed using TGA and the results were compared with neat CNC which can be seen in Figure 6. An initial weight loss was observed at lower temperatures for neat CNC, which was ascribed to the moisture removal. Then, a continuous weight loss was noted from 200 to 450°C. This behaviour was expected because of the sulphate groups induced by the sulfuric hydrolysis treatment (28).

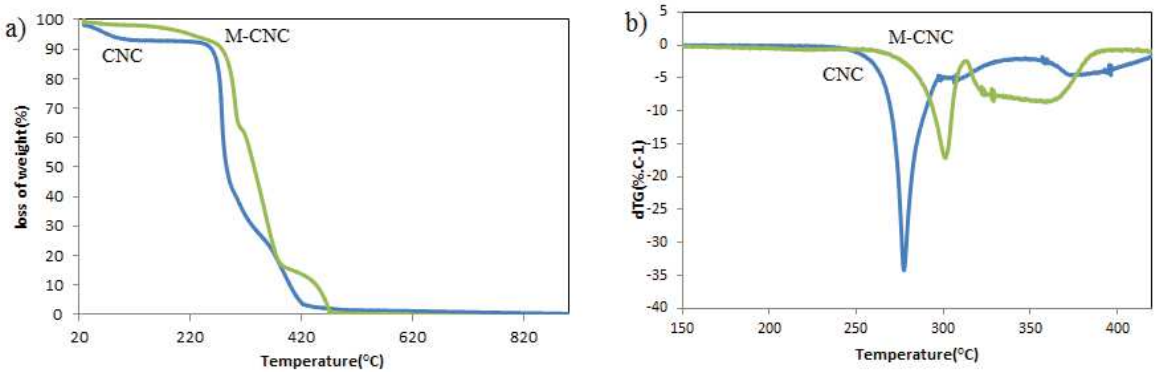

Figure 6. (a) TGA spectra and (b) dTG curves for neat CNC and M-CNC.

The weight loss around 200°C was related to more accessible sulphate groups in amorphous cellulose regions. The weight loss around 270−450°C corresponded to the breakdown of unsulphated crystalline cellulose regions. For M-CNC the thermal degradation behaviour was considerably higher than CNC. The first degradation of M-CNC was observed at 297°C. This can be due to the influence of the PS copolymer on the surface of the CNC. The continuous weight loss was observed from 317 to 490°C.

The relative dTG curves corresponding to CNC, M-CNC are shown in Figure 6b, and they clearly indicate that the main degradation temperature for CNC was lower than the M-CNC. It further shows that the surface of CNC was modified with the PS copolymer.

5.5.8 XPS

The CNC surface modification with PS copolymer was verified by means of XPS characterization. As shown in Figure 1a (Annexure-2), on the general XPS spectra, the new signals can be seen in both neat and modified CNC at 1072 eV which is corresponding to the Na 1s, this might be due to the presence of the sodium on surface of CNC and their traces were continued in the modified CNC as well. For both CNC and M-CNC the more significant peaks was observed at 285, 286.5, 287.5±0.1 and 289eV corresponding to C-C/C-H, C-O, C=O/O-C-O and O-C=O respectively. The peak at 285eV and 286.5eV was observed more

intense for modified CNC compared to neat CNC. This can attributed to increase in the number of C-C/C-H and C-O bonds, which is because of the PS-copolymer adsorption on the surface of CNC. This can be seen in Figure 1b (Annexure-2). However, the significant difference can be seen between the CNC and M-CNC in terms of C/O ratio and the results were reported in table-1. The N 1s peak was not observed for the M-CNC since there is no covalent bond between the surfactant and the CNC.

Table-1 the C/O ratios of CNC and M-CNC

Sample Name	Area of the peak for oxygen(A_O)	Area of the peak for carbon(A_C)	C/O ratio
CNC	346169	24085	0.21
M-CNC	236377	38470	0.50

C/O= (A_C /S_C* S_O/A_O) Atomic Sensitivity Factors S_C=0.205, A_O=0.63

The C/O ratio results reveal that CNC has the PS copolymer adsorption on the surface, as C/O ratio is double to the M-CNC in comparison with neat CNC.

5.6 Preparation and characterization of PS Nanocomposites

In this section neat CNC and M-CNC were extruded with a PS matrix at 190°C for 8 min in order to prepare the nanocomposites. Further these nanocomposites were characterized in order to understand the morphological and mechanical properties by means of SEM, DMA, DSC and tensile test.

5.6.1 Differential Scanning Calorimetry

The extruded composites were characterized to understand the thermal properties by means of DSC. The glass transition temperature (T_g) of polystyrene and its composites was determined and the results are shown in figure-7. As shown in DSC thermograms in Figure 7 the PS glass transition temperature was slightly decreased while introducing the neat CNC. This was due to the inherent incompatibility between the hydrophilic CNC and hydrophobic

polymer (19). The thermograms corresponding to the modified CNC reinforced PS composites and it shows a slight gradual decrease of T_g , though it is not significant. This can be attributed to the weak interfacial interactions between the nanofiller and the matrix. It indicated that the simple addition of neat CNC and modified CNC to PS matrix could not allow the homogeneous dispersion.

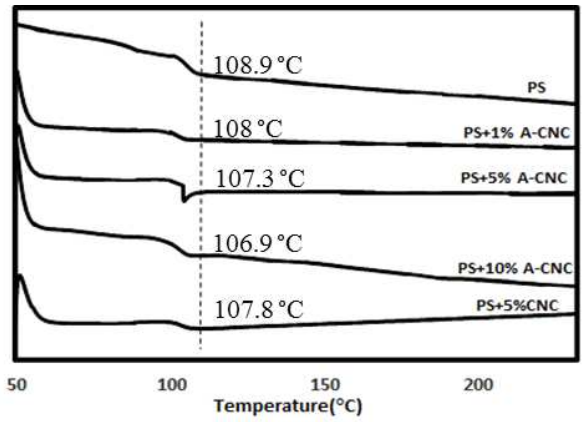

Figure-7.DSC thermograms for M-CNC−PS nanocomposites and results compared with neat CNC and PS

5.6.2 Scanning electron microscopy

The microstructure of extruded nanocomposites was observed by using SEM and the results are shown in Figure 8. Initially the composites were cryo fractured and their cross-section was observed to understand the morphology. When compared to the neat PS matrix (fig.8a), some holes can be seen in figure 8b owing to pulled-out CNC aggregates. Whereas in the case of the M-CNC (8 c, d and e) reinforced composites at 1, 5 and 10wt% no aggregation was noted. However, there was no homogeneity between the filler and matrix and the microphase separation existed in these nanocomposites from 8c-e. It can be explained due to unfavourable interactions between modified CNC and PS chains in the nanocomposites.

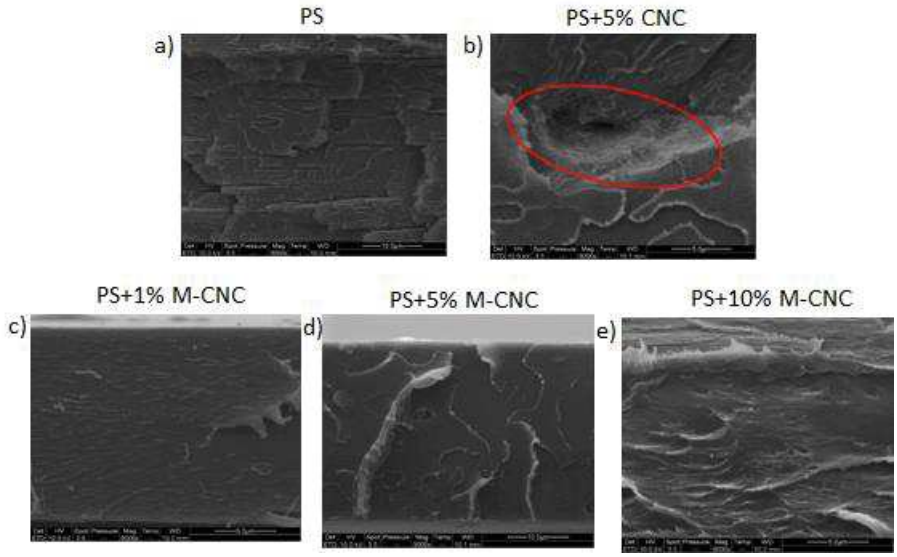

Figure 8.SEM images of the cryo-fractured cross section of the extruded films: neat PS (a), and PS nanocomposites reinforced with 5 wt % neat CNC (b), and PS+1%M-CNC (c), PS+5% M-CNC (d), PS+10% M-CNC (e).

5.6.3 Dynamical mechanical analysis

The mechanical properties of nanocomposites reinforced with CNC/M-CNC were investigated in linear range. The evolution of the logarithm of the storage tensile modulus (log E′) as a function of temperature in isochronal conditions at 1 Hz frequency was shown in Figure 9 (the curves have been normalized at 1 GPa). For neat PS, the storage modulus was remained linear up to glass transition temperature (T_g). The modulus was gradually decreasing while increasing the temperature from 100 to 120°C. When adding 5 wt % neat CNC the modulus was dropped completely. For composites reinforced with M-CNC no significant improvement in the modulus was observed compared to the neat matrix. This can be ascribed to the incompatibility between the polystyrene and the filler.

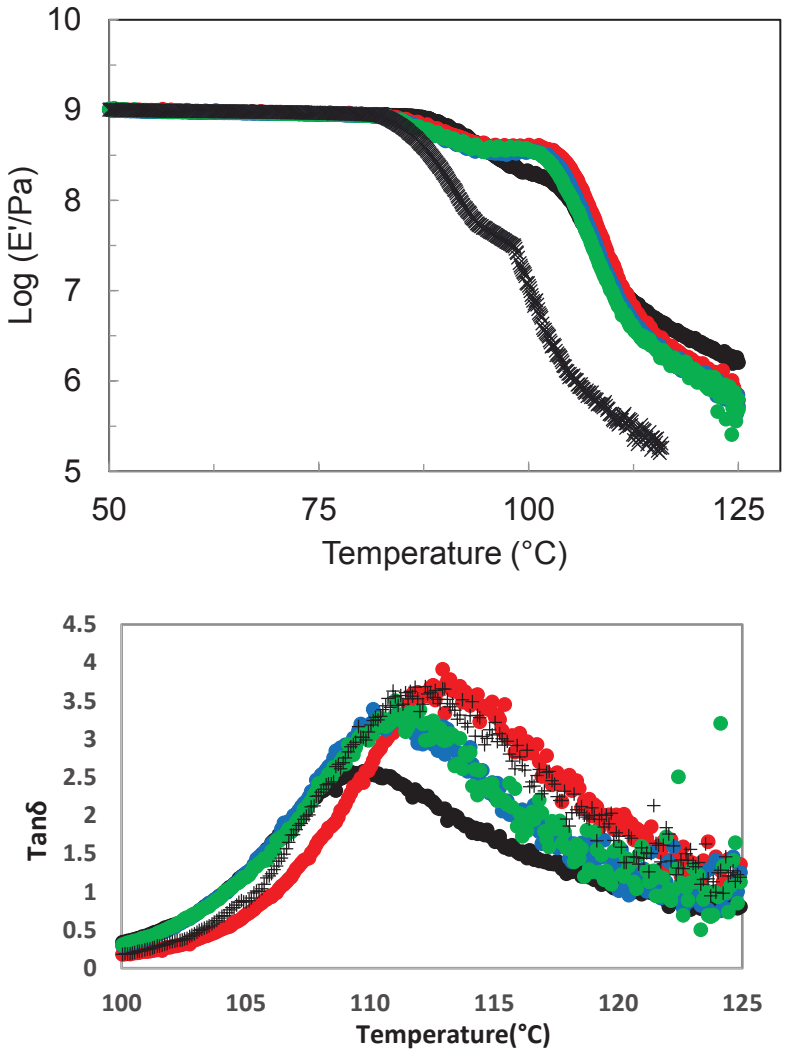

Figure 9.Evolution of a) log E′ and b) tangent of the loss angle tanδ as a function of temperature for PS(●), PS+1%M-CNC (●), PS+5%M-CNC (●), PS+10%M-CNC (●) and PS+5%CNC (⊕) reinforced composites.

Addition of CNC/M-CNC to the PS matrix induced a variation of the tangent of the loss angle, tanδ, as a function of temperature for composites with different filler contents. Results are shown in 9b. Tanδ exhibited a maximum around 109°C for the neat PS matrix which is in agreement with DSC results. This peak shifted to 111-112°C for both CNC and M-CNC reinforced composites in all over the filler content and the magnitude of the peak is increased. It can be attributed to the higher modulus drop for composites.

5.7 Conclusion

The laboratory-prepared and well characterized poly[(styrene)-co-(2-ethylhexyl acrylate)] copolymer was used to modify the surface of cellulose nanocrystals surface by a simple aqueous method. The surface modification was evidenced by FTIR and X-ray photoelectron spectroscopies. X-ray diffraction analysis showed that the initial crystalline structure was preserved. The AFM results showed the influence of the PS copolymer on the surface of the CNC. The hydrophobic nature of the adsorbed and modified CNC was determined by contact angle measurements and it was shown that the surface chemical modification allowed enhancing the nonpolar nature of neat cellulose nanocrystals. It was observed that the modified CNC displays improved thermal stability compared to that of neat CNC. The modified CNC was used to reinforce PS matrix by a solvent free melt extrusion process. The thermomechanical properties of processed nanocomposites were studied by DSC and DMA. There was no further improvement in mechanical properties in spite of improved compatibility between the matrix and the filler. This might be due to the incompatibility between the filler and the matrix.

5.8 References

1. Cavaille, J.Y., Ruiz, M.M., Dufresne, A., Gerard, J.F., Graillat, C., 2000. Processing andCharacterization of new thermoset nanocomposites based on cellulose whiskers. Compos. Interfaces 7 (2), 117–131.

2. Klemm, D., Kramer, F., Moritz, S., Lindström, T., Ankerfors, M., Gray, D., & Dorris, A. (2011). Nanocelluloses: A new family of nature-based materials. Angewandte Chemie International Edition, 50(24), 5438-5466.

3. Habibi, Y., Lucia, L. A., & Rojas, O. J. (2010). Cellulose nanocrystals: chemistry, self-assembly, and applications. Chemical reviews, 110(6), 3479-3500.

4. Moon, R. J., Martini, A., Nairn, J., Simonsen, J., & Youngblood, J. (2011). Cellulose nanomaterials review: structure, properties and nanocomposites. Chemical Society Reviews, 40(7), 3941-3994.

5. Lin, N., Huang, J., & Dufresne, A. (2012). Preparation, properties and applications of polysaccharide nanocrystals in advanced functional nanomaterials: a review. Nanoscale, 4(11), 3274-3294.

6. Boufi, S., Kaddami, H., & Dufresne, A. (2014). Mechanical performance and transparency of nanocellulose reinforced polymer nanocomposites. Macromolecular Materials and Engineering, 299(5), 560-568.

7. Arias, A., Heuzey, M. C., Huneault, M. A., Ausias, G., & Bendahou, A. (2015). Enhanced dispersion of cellulose nanocrystals in melt-processed polylactide-based nanocomposites. Cellulose, 22(1), 483-498.

8. Mariano, Marcos, Nadia El Kissi, and Alain Dufresne. "Cellulose nanocrystals and related nanocomposites: Review of some properties and challenges." Journal of Polymer Science Part B: Polymer Physics 52.12 (2014): 791-806.

9. Goffin, A. L., Raquez, J. M., Duquesne, E., Siqueira, G., Habibi, Y., Dufresne, A., & Dubois, P. (2011). From interfacial ring-opening polymerization to melt processing of cellulose nanowhisker-filled polylactide-based nanocomposites. Biomacromolecules, 12(7), 2456-2465.

10. Goffin, A. L., Raquez, J. M., Duquesne, E., Siqueira, G., Habibi, Y., Dufresne, A., & Dubois, P. (2011). Poly (ε-caprolactone) based nanocomposites reinforced by surface-grafted cellulose nanowhiskers via extrusion processing: morphology, rheology, and thermo-mechanical properties. Polymer, 52(7), 1532-1538.

11. de Menezes, A. J., Siqueira, G., Curvelo, A. A., & Dufresne, A. (2009). Extrusion and characterization of functionalized cellulose whiskers reinforced polyethylene nanocomposites. Polymer, 50(19), 4552-4563.

12. Raquez, J. M., Murena, Y., Goffin, A. L., Habibi, Y., Ruelle, B., DeBuyl, F., & Dubois, P. (2012). Surface-modification of cellulose nanowhiskers and their use as nanoreinforcers

into polylactide: a sustainably-integrated approach. Composites Science and Technology, 72(5), 544-549.

13. Xu, S. H., Gu, J., Luo, Y. F., & Jia, D. M. (2012). Effects of partial replacement of silica with surface modified nanocrystalline cellulose on properties of natural rubber nanocomposites. Express Polym Lett, 6(1), 14-25.

14. Ben Azouz, K., Ramires, E. C., Van den Fonteyne, W., El Kissi, N., & Dufresne, A. (2011). Simple method for the melt extrusion of a cellulose nanocrystal reinforced hydrophobic polymer. ACS Macro Letters, 1(1), 236-240.

15. Fortunati, E., Armentano, I., Zhou, Q., Iannoni, A., Saino, E., Visai, L., ... & Kenny, J. M. (2012). Multifunctional bionanocomposite films of poly (lactic acid), cellulose nanocrystals and silver nanoparticles. Carbohydrate polymers, 87(2), 1596-1605.

16. Zhou, Q., Brumer, H., & Teeri, T. T. (2009). Self-Organization of Cellulose Nanocrystals Adsorbed with Xyloglucan Oligosaccharide− Poly (ethylene glycol)− Polystyrene Triblock Copolymer. Macromolecules, 42(15), 5430-5432.

17. Oksman, K., Mathew, A. P., Bondeson, D., & Kvien, I. (2006). Manufacturing process of cellulose whiskers/polylactic acid nanocomposites. Composites science and technology, 66(15), 2776-2784.

18. Bondeson, D., & Oksman, K. (2007). Polylactic acid/cellulose whisker nanocomposites modified by polyvinyl alcohol. Composites Part A: Applied Science and Manufacturing, 38(12), 2486-2492.

19. Lin, Ning, and Alain Dufresne. "Physical and/or chemical compatibilization of extruded cellulose nanocrystal reinforced polystyrene nanocomposites." Macromolecules 46.14 (2013): 5570-5583.

20. Nechyporchuk, O., Pignon, F., Do Rego, A. M. B., & Belgacem, M. N. (2016). Influence of ionic interactions between nanofibrillated cellulose and latex on the ensuing composite properties. Composites Part B: Engineering, 85, 188-195.

21. Wå gberg, L.; Decher, G.; Norgren, M.; Lindström, T.; Ankerfors, M.;Axnas,K. The Build-upof Polyelectrolyte Multilayersof Microfibrillated Cellulose and Cationic Polyelectrolytes. Langmuir 2008, 24, 784−795.

22. Nagalakshmaiah, Malladi, Nadia El Kissi, and Alain Dufresne. "Ionic compatibilization of cellulose nanocrystals with quaternary ammonium salt and their melt extrusion with polypropylene." ACS Applied Materials & Interfaces (2016) 8755-8764.

23. Nagalakshmaiah, Malladi, Nadia El Kissi, and Alain Dufresne. Surface adsorption of triblock copolymer (PEO-PPO-PEO) on cellulose nanocrystals and their melt extrusion with polyethylene. RSC advances (2016) in press.

24. Wu, H., Wu, S., Wu, I. and Chang, F. (2001). Novel determination of the crystallinity of syndiotactic polystyrene using FTIR spectrum. Polymer, 42(10), pp.4719—4725.

25. Kandil, S. H., & El-Gamal, M. A. (1986). Infrared spectroscopic analysis of poly (methyl acrylate-co-styrene). Journal of Polymer Science Part A: Polymer Chemistry, 24(11), 2765-2771.

26. Ebdon, J. R., Kandil, S. H., & Morgan, K. J. (1979). The effects of overall composition and monomer sequence distribution on the infrared carbonyl stretching frequencies of ethylene–vinylacetate and styrene–vinylacetate copolymers. Journal of Polymer Science: Polymer Chemistry Edition, 17(9), 2783-2790.

27. Dreher, W. R., Zhang, P., Urban, M. W., Porzio, R. S., & Zhao, C. L. (2003). Styrene/2-ethylhexyl acrylate/methacrylic acid (Sty/EHA/MAA) coalescence and response-driven mobility of sodium dodecyl sulfate (SDS) in colloidal films. 22. A spectroscopic study. Macromolecules, 36(4), 1228-1234.

28. Lin, N.; Huang, J.; Chang, P. R.; Feng, J.; Yu, J. Surface Acetylation of Cellulose Nanocrystal and its Reinforcing Function in Poly(lactic acid).Carbohydrate Polymers.2011, 83, 1834−1842.

29. Roman, M.; winter, W. T. Effect of Sulfate Groups from Sulfuric Acid Hydrolysis on the Thermal Degradation Behavior of Bacterial Cellulose. Biomacromolecules 2004, 5, 1671−1677.

Chapter-6 General Conclusion

6.1 General conclusion

The main objective of this thesis dissertation was to investigate the best possible way to reinforce a polymer matrix with cellulose nanocrystals by melt compounding. Mainly in this thesis the aim was to resolve issues like 1) irreversible agglomeration and 2) low thermal stability, resulting respectively from hydrophilic nature of cellulose, and the presence of sulphate groups resulting from the preparation of cellulose using acid hydrolysis. These two issues hugely limit the preparation of the nanocomposites by melt extrusion. In the present study authors reported the simplest methods and easily scalable process like surface modification and physical adsorption, in order to overcome the fore mentioned issues. These methods are viable at industrial level to produce polymer nanocomposites.

Chapter-1 was dealing with the literature review of CNC and mainly its preparation at both laboratory and industrial scale, as well as its physical and chemical properties. The recent trends in the field of nanocomposites especially by melt compounding were reported.

In chapter 2, the new potential agriculture biomass was introduced to extract the cellulose nanocrystals and their reinforcement in a commercial latex was studied. In this chapter cellulose nanocrystals were successfully extracted from chili fibres by acid hydrolysis. Unusual low lignin content was found for these fibres compared to other annual plants making them highly suitable for the extraction of cellulose and preparation of CNCs. Ensuing rod-like nanoparticles had a diameter of 4-6 nm and length of 90-180 nm, showing an aspect ratio around 26. They were used as the reinforcing phase in cariflex IR latex. The morphological observation of these bio based nanocomposites showed that the CNCs were well dispersed in IR matrix without microscale aggregation. Dynamic mechanical and thermal studies showed increased storage modulus indicating good interaction between CNC and IR latex. The tensile strength and modulus values increased with CNC addition, accompanied by a moderate decrease in yield strain.

In Chapter 3 we have reported an environmentally friendly water-based, flexible and easy procedure to modify the surface of CNC. Benefit was taken of the negatively charged surface of the CNC with sulphated groups resulting from the sulphuric acid extraction step, to establish favorable ionic interactions with quaternary ammonium salt bearing long alkyl chain. Hydrophobization of the CNC surface was verified by FTIR spectroscopy and contact angle measurements. It was also observed that modified CNC displays improved thermal stability compared to neat CNC. Hydrophobized CNC disperses well in different non-polar solvents and hydrophobic polymer matrix such as PP, which is impossible for neat CNC. Both unmodified and modified CNCs act as nucleating agents for the PP matrix, promoting its crystallization. A modest reinforcing effect was evidenced from DMA and tensile tests, but a spectacular improvement of the elongation at break was observed when adding few percent of modified CNC. This large plastic deformation of the material was attributed to the hindering of inter-nanoparticle interactions and possible plasticizing effect of the surfactant. A significant decrease of the melt viscosity was reported when adding CNC and ascribed to a dilution effect.

Chapter-4 was mainly focused on physical adsorption of triblock copolymer (TBC) on CNC. In this study we have developed an efficient and simple water based method to prepare cellulose nanocrystal (CNC) reinforced polyethylene nanocomposites by melt processing. It consists in coating the nanoparticle (ratio 1:1) with a triblock copolymer (TBC) having two hydrophilic ends attached to a hydrophobic central block. The hydrophilic ends were expected to interact with the cellulosic surface leaving the hydrophobic block free to provide compatibility with the polyethylene matrix chains. Coating of CNC with the copolymer was visualized from AFM observations and the rheological behaviour of aqueous dispersions indicates that the surface adsorption capability of CNC is around 1-2 g of TBC for 1 g of pristine CNC. Moreover, this coating allows a much easier and better re-dispersion in water

of the nanoparticles after freeze-drying, that was also characterized by SAXS experiments, and improves their thermal stability. After melt extrusion with polyethylene, the visual appearance of films prepared from TBC-coated CNC was clearly indicative of an improved dispersion, that was also evidenced from SEM observations, and limited thermal degradation. It results in significantly improved mechanical properties for the nanocomposites. SAXS experiments show a much more prominent preferential orientation and alignment in the flow direction for TBC-coated CNC compared to neat CNC which is induced by the extrusion step. It further indicates that individual coated nanorods are present in the nanocomposite films.

A better mechanical performance can be possible with better compatibility between the filler and matrix. Thus, laboratory-prepared and well characterized poly[(styrene)-co-(2-ethylhexyl acrylate)] was used to modify the surface of the cellulose nanocrystals by simple aqueous method. The surface modification was evidenced by FTIR and X-ray photoelectron spectroscopies. X-ray diffraction analysis showed that the initial crystalline structure was preserved. The AFM results show the influence of the PS copolymer on the surface of the CNC. The hydrophobic nature of the adsorbed and modified CNC was determined by contact angle measurements. It showed that the surface chemical modification allowed enhancing the nonpolar nature of neat cellulose nanocrystals. It was observed that modified CNC displays improved thermal stability compared to that of neat CNC. The modified CNC was used to prepare nanocomposites with PS as matrix by solvent-free melt extrusion process. The thermomechanical properties of processed nanocomposites were studied by DSC and DMA. There was no further improvement in mechanical properties in spite of improved compatibility between the matrix and the filler. This might be due to the incompatibility between the filler and matrix.

In general the reinforcement effect of CNC with different hydrophobic matrices was reported from low (LLDPE) to high processing temperature (PP and PS) polymers by simple and environmental friendly process, which can applied at the industrial scale production.

Additional information:

Annexure-1

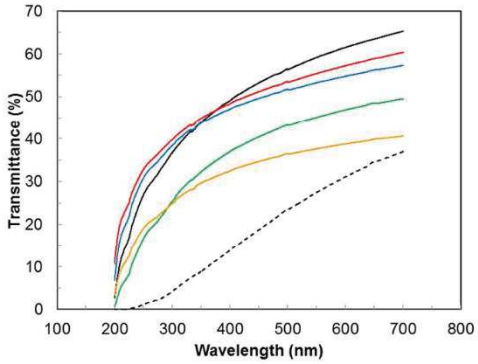

Figure S1. UV transmittance spectra for neat extruded PP (—) and nanocomposites reinforced with 3 wt% CNC (---), and 1 wt% (—), 3 wt% (—), 6 wt% (—), and 10 wt% M-CNC (—).

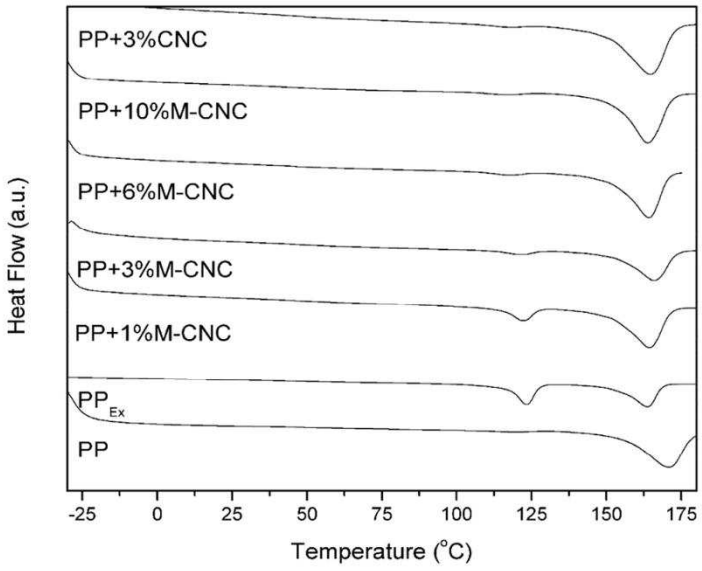

Figure S2. DSC thermograms for neat PP, neat extruded PP (PP_{Ex}) and nanocomposites reinforced with CNC and M-CNC.

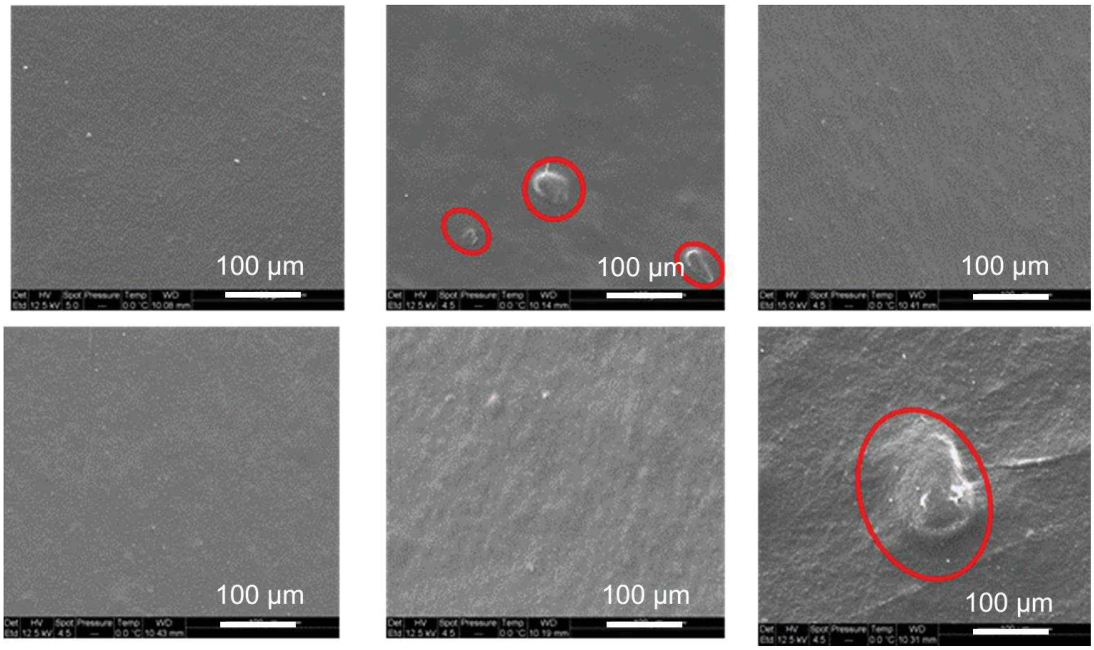

Figure S3. SEM images of the surface of the extruded films: neat PP (a), and PP nanocomposites reinforced with 3 wt% unmodified CNC (b), and 1 wt% (c), 3 wt% (d), 6 wt% (e) and 10 wt % (f) CNC modified with quaternary ammonium salt.

Annexure-2:

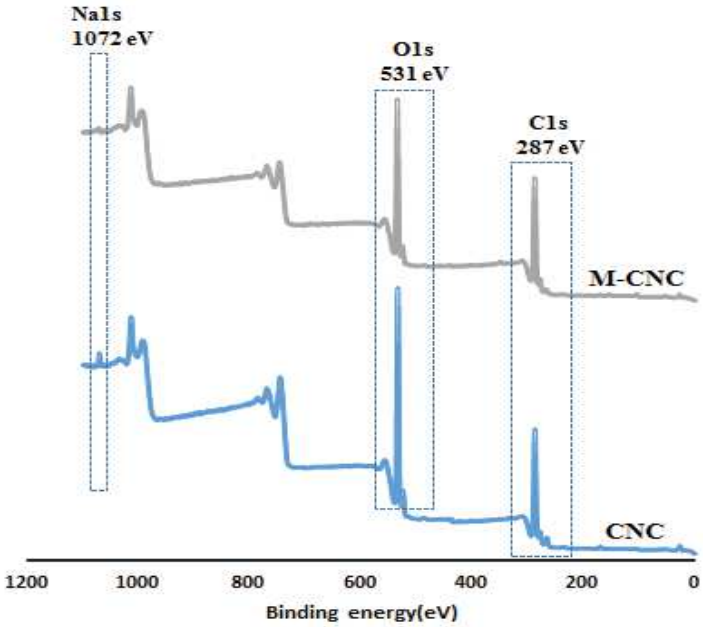

Figure-1 a General XPS spectra for CNC and M-CNC.

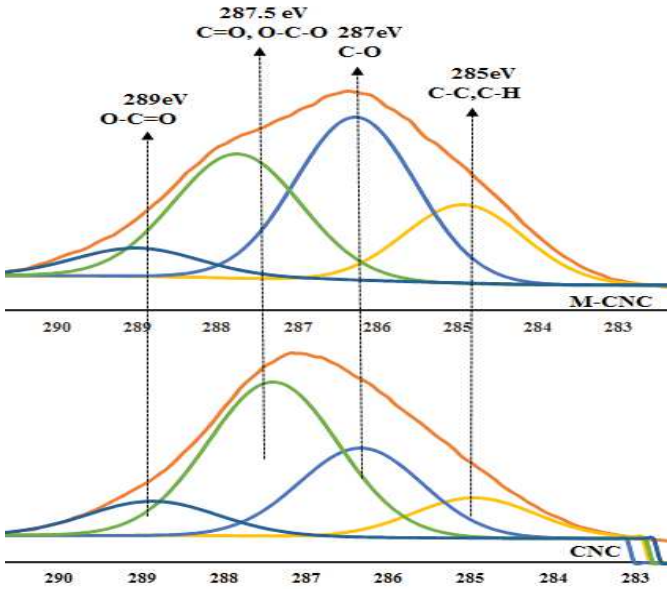

Figure-1b XPS decomposition of the C 1s signal into its constituent contributions for CNC and M-CNC

Abstract

The low thermal stability and irreversible agglomeration issues are limiting the processing of polymer nanocomposites using CNC as the reinforcing phase. In this context, thermally stable and highly dispersed CNC were prepared by green processes (aqueous based methods) like physical adsorption and surface modification. These two different extrudable CNC were used to reinforce hydrophobic polymers. Ensuing polymer nanocomposites had a positive impact on the storage modulus, tensile strength and Young's modulus. Importantly, no evidence of micro aggregates in the matrix was observed in the scanning electron microscopy images contrary to non-treated CNC. Both the surface modification and adsorption are water based methods and are industrially viable solutions.

Résumé

La faible stabilité thermique et les problèmes d'agrégations irréversibles limitent la mise en forme de nanocomposites polymères à renfort cellulosique. Dans ce contexte, des CNC thermiquement stables et fortement dispersés ont été préparés par des procédés verts, basés sur des méthodes en milieu aqueux, telle que l'adsorption physique et la modification de surface. Ces deux types de CNC extrudables ont été utilisés comme renfort dans des polymères réputés hydrophobes. Les composites biosourcés à matrice polymère ainsi réalisés sont caractérisés par une amélioration du module de conservation, de la résistance à la traction et du module d'Young. On constate également sur les images de microscopie électronique à balayage qu'à la différence des observations réalisées avec les CNC non traités, aucun micro-agrégat cellulosique n'est observé dans la matrice polymère. Ces deux méthodes, développées en milieu aqueux, apparaissent ainsi comme des solutions industriellement viables.